Using Functional Assessment and Mapping Tools to Evaluate Headwater Slope Wetlands in Coastal Alabama

by

Kurtis James Fisher

A thesis submitted to the Graduate Faculty of Auburn University
in partial fulfillment of the requirements
for the Degree of Master of Science

Auburn, Alabama

August 03, 2024

Keywords: Headwater wetlands, Wetland functions, Hydrogeomorphic approach, Land use/land cover, Forested wetland mapping, Random Forest, Wetland intrinsic potential, Coastal Alabama.

Approved by:

Christopher J. Anderson: Professor, College of Forestry, Wildlife and Environment, Auburn University. Auburn, AL.

Lana Narine: Assistant Professor, College of Forestry, Wildlife and Environment, Auburn University. Auburn, AL.

Meghan Halabisky: Research Scientist, College of the Environment, School of Environmental and Forest Sciences, University of Washington. Seattle, WA.

Abstract

Headwater slope wetlands are a ubiquitous forested wetland type located at the headwaters of coastal streams in the southeastern U.S. Coastal Plain. There is concern that past and current coastal land use / land cover (LULC) change may reduce the capacity for these wetlands to provide important functions (e.g., habitat, water quality improvement, and flood attenuation). To investigate this, 74 headwater wetlands in coastal Alabama (i.e., Mobile and Baldwin County) were assessed for important functional attributes (forest structure, soils, and hydrology) represented by various ecological measures. These data were compared to LULC data (i.e., % forest, urban and agriculture) from each wetland's catchment over a range of surrounding landscapes typical of the Alabama coast. Wetland attributes were measured using a regionally specific rapid assessment model, the Hydrogeomorphic Approach (HGM) for the functional assessment of headwater slope wetlands in the coastal plain region of Mississippi and Alabama. Significant relationships between wetland shrub cover and agricultural and urban land use suggests LULC change may increase midstories densities. Urban land use was additionally related to increased herbaceous understory coverage and soil dewatering, as well as reductions in soil organic matter content. Despite some significant relationships and notable trends, urban and agriculture were not highly correlated with several other field measurements, suggesting other landscape factors are important for determining the functional capacity of these wetlands.

Headwater wetlands can be difficult to map because of their tendency to transition gradually into uplands on the landscape. For the second part of this study, we evaluated the Wetland Intrinsic Potential (WIP) tool and its use of multi-scale topographic indices, hydrologic proxies, and random forest procedures that contribute to 'cryptic' wetland detection in the Bushy

Creek – Dyas Creek watershed, near Bay Minette, Alabama. An initial model was trained and validated on a spatial subset of the watershed to predict headwater wetland presence, absence, and extent. The model was then applied to the remaining spatial extent of the watershed. Overall accuracy for the secondary validation dataset was 92.3%, with wetland omission and commission errors of 14.0% and 4.5%, respectively. Our statistical analyses indicated WIP reliably discerned wetlands from uplands. These findings can be used to infer the applicability and limitations of this method for wetland mapping along the northern Gulf of Mexico and support future models which explore land use/cover and hydrogeomorphic relationships with wetlands. Ultimately, information gained from this thesis study will assist in wetland monitoring efforts to better assess the environmental services provided by coastal drainages along the Gulf coast.

Acknowledgements

I would like to thank the faculty at Auburn University's College of Forestry, Wildlife, and Environment for meaningful guidance and engagement throughout my coursework and thesis development. The expertise and willingness to share it by Drs. Latif Kalin and Johnathon Valente were vital components that pushed my research forward. During my time at Auburn, I also vied to continue my education in aspects wildlife and forest management. I attribute these learning moments to John Gilbert, Jimmy Stiles, Dr. Will Gulsby, and the Wildlife and Forestry Practicum class of 2023. I am especially grateful to the members of my graduate committee: Drs. Chris Anderson, Lana Narine, and Meghan Halabisky. The mentorship and insights I have gained from each of them are invaluable resources to my career and personal growth. Funding for this project was provided through a grant from the U.S. Department of the Treasury in cooperation with the State of Alabama Department of Conservation and Natural Resources, and the Alabama Center of Excellence at the MESC/Dauphin Island Sea Lab. The opportunity afforded by this grant was an impactful one that has furthered my development as a wetland scientist and natural resource professional.

Many thanks are owed to extension agents throughout coastal Alabama (Joey Koptis, Guilherme Morata, etc.) who facilitated relationships with landowners, and to those landowners (Will Miller, Aaron Bengston, Michael Mullek, the Driskell family, etc.) who provided site access and additional resources to further our network. Our field crew is also appreciative of National Estuarine Research Reserve staff members (Scott Phips, etc.), who hosted and supported us in various ways throughout field seasons. Many thanks to the undergraduate volunteers and researchers in our lab who dedicated time and effort to demanding field surveys:

John-Michael Norris, Hayden Tuite, Mary Ashley Hughes, and Sam McWhorter. I'd like to thank Andrew Balder as a fellow rotating crew member and crew lead, who undoubtedly improved my abilities as a leader and ecologist through his own example and expertise. Never give up on your comedy dream. I'd also like to acknowledge working professionals who volunteered their time and expertise along the way in terms of field work methods (Flynt Barksdale) and geospatial modeling methods (Dr. Gina O'Neill and Connor Racette). Finally, I would like to express gratitude for my friends, family, and mentors who got me to the finish line through their continued support over the years: Dr. Diane Styers, Dr. David Kinner, Dr. Aimee Rockhill, River Jinks, Kayla Baker, Taylor Jones, JP, Filchuck, Steve Starnes, Holly Duggins, etc., and of course, Pippin.

Table of Contents

List of Figures

List of Tables

Chapter I. HEADWATER WETLANDS OF THE EASTERN GULF COASTAL PLAIN: FUNCTIONAL ROLES AND MAPPING CHALLENGES

1. Headwater Wetlands: Functions and Relevance

Although headwaters and their wetlands significantly influence downstream ecosystems, water quantity, and water quality, they remain largely understudied despite being widespread and influential components of the landscape. This need for research is underlined by an uncertainty of federal protections surrounding streams and wetlands that cannot be easily defined as Waters of the United States, particularly those which are ephemeral, intermittent, or non-alluvial (Singh 2015; Sackett v. EPA 2023). Headwater wetlands throughout the coastal plain region are noted for seasonal inundation during the growing season, and varying degrees of baseflow provisions in the nongrowing season (Brinson et al. 2006; Tufford 2011; Rheinhardt et al. 2013). Following the Rapanos v US supreme court decision, wetlands which were not considered 'Waters of the United States' were still subject to federal protections on a case-by-case basis. The grounds for affording these protections were based on the presence of a 'significant nexus' between wetlands and navigable Waters of the United States if one could be identified and aptly justified by regulators (Rapanos v. US 2006). This allowed for site-level interpretations of hydrologic connectivity between wetlands and streams. In 2023, 'significant nexus' was defined more concretely and summarized by Justice Samuel Alito who stated after the ruling of Sacket vs. EPA, "the CWA extends to only those 'wetlands with a continuous surface connection to bodies that are "Waters of the United States" in their own right,' so that they are 'indistinguishable' from those waters" (Sackett v. EPA 2023).

This definition largely ignores hydrologic principles that connect wetlands with each other and streams through various pathways. This is especially true for headwater slope wetlands which serve to mediate processes between uplands and perennial streams. In the northeastern U.S., Alexander et al. (2007) found that 65% of nitrogen fluxes in second order streams, and 40% of those in fourth order and above were sourced from first order streams, which typically lack continuous surface water flows. This is the result of short-lived surface water runoff events and more continuous groundwater fluxes that sustain ephemeral streams. The benefits of groundwater connections with navigable waters are immensely important, as a significant amount of denitrification occurs in these areas compared with hyporheic zones in open channels (Ranalli and Macalady 2010). Headwater wetlands of the coastal plain region are well connected with streams through shallow subsurface hydrology, and the presence or absence of such wetlands have various effects on downstream waters. In-stream conditions of mainstem streams that include waters of the United States are considerably affected by the conditions of their tributaries, as water quality and quantity are first controlled by erosion and drainage processes in headwater catchments that determine oxygen, nutrient, and food resource availability for downstream communities (Gomi et al. 2002).

Headwater streams and wetlands often have specific hydrologic conditions relating to their connections to surrounding uplands. Where reference hydrology in headwaters is altered and rates of surface and groundwater discharge are accelerated, surface runoff responses to storms become more rapid, and baseflows less constant (Gomi et al. 2002; Groffman et al. 2003; Meyer et al. 2005). Retention and biogeochemical cycling of particulate matter and nutrients are further reduced with increased drainage, thereby contributing to excess nutrient fluxes and sedimentation in mainstem streams and rivers (Groffman et al. 2002, 2003). The impact of

headwater stream and wetland degradation on mainstem streams is well documented, yet considerations of these important landscape connections are not well represented in the wetland mitigation processes (BenDor and Brozović 2007; Hoeltje and Cole 2007). Where reference vegetative structure and function are present, headwater slope wetlands perform a variety of ecosystem services due to their unique geomorphic positions, hydrologic regimes, and soil characteristics. Alterations to reference hydrology and structural components represent potential losses to headwater wetland function and area that may impact ecosystem services at multiple scales.

The southeastern region of the U.S. is abundant with forested wetlands. Cubbage and Flather (1993) estimated this region to contain over 65% of all forested wetlands located on nonfederal lands throughout the U.S. High densities of headwater networks occur throughout the coastal plain region of the southeast and commonly contain forested slope wetlands, hereafter referred to as headwater slope wetlands (Noble et al. 2007, 2011). While headwater slope wetlands are well documented across the entirety of the coastal plain region, the following section focuses on those within the eastern gulf coastal plain. These are common palustrine wetlands located at the toe slopes of flatwood pine forests which normally exhibit a transitional drainage pattern between unconcentrated flows from uplands to concentrated flows in streams (Noble et al. 2007; Tufford 2011). Such areas represent important hydrogeochemical and physical buffers between uplands and streams that ensure stable baseflows, sediment and nutrient retention, and flow dispersion via low sloping and hummocky microtopography (Jones et al. 1996; Jones et al. 2006; Noble et al. 2007, 2011; Tufford 2011; Rezaeianzadeh 2015).

Although underlying soils are predominantly sand/sandy loams without restrictive layers above depths of 2 m (Noble et al. 2007), the combined effects of geomorphic position, soil

texture, slope, and hydraulic gradient between uplands and wetlands induce shallow water tables near the soil surface (Winter 1988). Water tables are exceptionally stable in headwater slope wetlands compared to those in riverine wetlands throughout the U.S. and lower coastal plain region (Monk 1968; Winter 1988; Cole et al. 2002). These low flow and gradual-sloped wetlands also produce stabilized rates of discharge throughout the year, often sustaining flows year-round and even in drought years (Tufford 2011; Rezaeianzadeh 2015).

These are also critical zones for nutrient cycling and water quality regulation, due to their gradual slope and flow environments that facilitate the retention of particulate and soluble materials (Noble et al. 2007; Ramesh et al. 2020). Here, carbon storage is promoted by a hummocky microtopography, where detritus accumulates to produce duff and humus layers. Nutrient retention and cycling are facilitated by consistently high-water tables during wet periods and by organic matter accumulation that retains moisture and reduces soil evaporation during dry periods. Biologically mediated carbon storage is furthered by fine root mass associations with hummock mounds and slow rates of root decay (Fritz et al. 2006; Li et al. 2020).

During high flow periods, materials are flushed from headwater wetlands to streams. This seasonal control ensures the movement of materials at times and concentrations in which downstream communities can adequately respond to them, which thus constitute limiting factors to population growth. The environmental parameters in which benthic and lotic populations operate within, in turn determine predator-prey interactions throughout the food web, affecting both ecologically imperiled and commercially important riverine, estuarine, and oceanic species (Colvin et al. 2019). Fritz and Feminella (2011) found that colonization of buried substrates in coastal Alabama headwater wetlands was controlled by hydroperiod, where terrestrial invertebrate occupancy rose in dry periods and aquatic invertebrate colonization in wet periods.

While this phenomenon is well known in the latitudinal plain of perennial streams (Adis and Junk 2002), coastal headwater wetlands additionally sustain ecological flows in the longitudinal plain between communities of intermittent and perennial streams (Fritz and Feminella 2011).

Headwater wetlands additionally provide critical habitats for amphibian populations that rely on small, fragmented aquatic environments during reproductive periods, such as ephemeral pools (Gibbs 1993; Alix et al. 2014). Shallow water tables contribute to breeding habitats during wet periods, and the persistence of small pools in micro-depressions during dry periods provide continued spawning habitats. During these drying periods, a lack of surface water connection with perennial streams provides a refuge from predatory fish, along with the persistence of terrestrial invertebrate food sources, which both contribute to recruitment success (Gibbs 1993; Noble et al. 2007). While forested wetlands are highly selected habitats by many avian and mammalian species, insufficient research has been conducted in headwater wetlands of this region to determine trends in occupancy and selection. As these are infrequently flooded freshwater wetlands with forested canopies, wading birds and raptors are not associated with these habitats. Landscape permeability is often limited in these areas by shrub/sapling strata, which are not generally considered to be well suited for large mammal movement. While beavers are known to utilize small streams during breeding seasons, these habitats are not well documented for use by semi-aquatic mammals either. Headwater wetlands are expected to support breeding bird populations which utilize their associated forest structure and compositions, though more research is needed to determine species-specific relationships.

Ecosystem services provided by headwater wetlands are closely tied to their groundwater hydrology, and include the regulation of nutrient cycling pathways, as well as the provision of base flows, specialized forest communities, and wildlife habitats (Noble et al. 2007).

Degradation of wetland functions occur where land use and land cover (LULC) changes alter wetland hydrology, such as flow concentration and impoundment structures that accelerate or impound drainage to wetlands (Zedler 2003; Zedler and Kercher 2005; Noble et al. 2007; Meyer et al. 2005). Impervious surfaces associated with LULC change are also conducive to overland flows that reduce soil infiltration, groundwater recharge, and water table depths in wetlands and throughout watersheds (Hardison et al. 2009; Meyer et al. 2005; Caldwell et al. 2012).

These hydrologic effects, in turn, limit important wetland biogeochemical pathways including soil denitrification and carbon storage, as anoxic and bioactive portions of the soil stratum are minimized via soil dewatering and organic matter exportation (Groffman et al. 2002; Barksdale et al. 2014). Forested buffers between uplands and wetlands are also reduced as LULC changes occur, as are the benefits of forest structure and soils that moderate surface water accumulation from contributing areas to wetlands (Neary et al. 2009). These losses additionally translate to increased loads of solute pollutants to wetlands and streams, and reduced storage of pollutants in wetlands for biochemical cycling. As nitrogen loads from a given watershed increase along with excess overland flows and reduced time periods to reach peak flows, direct nitrate flushing into streams becomes more frequent (Zedler et al. 2003). Instream and wetland denitrification has also been shown to be far less effective as nitrate loads increase (Phipps and Crumpton 1994; Ranalli and Macalady 2010), and so the need for highly functioning wetlands with forested buffers becomes more evident given the response of inundated soils to produce runoff.

The loss of forested buffers surrounding headwater wetlands also present ecological disturbances associated with altered hydrology and dispersion pathways for exotic species. Exotic shrub abundance in headwater wetlands is positively correlated with LULC changes in

coastal Alabama (Barksdale and Anderson 2014). Evidence of inhibited canopy tree recruitment and L. sinense colonization have also been observed in this region in response to LULC change (Alix et al. 2014; Barksdale et al. 2014; Barksdale and Anderson 2014), forming dense thickets. L. sinense is also associated with accelerated decomposition, denitrification, and reductions of organic matter in forested wetland soils of the coastal plain region by way of altered litter quality and senescence periods (Mitchell et al. 2011). As hydrologic regimes shift due to surrounding LULC, vegetational shifts in headwater wetland forest composition are likely results. *N. biflora* is a common canopy tree species associated with prolonged hydroperiods throughout the gulf coastal plain and is additionally an indicator species of headwater wetland status (Noble et al. 2007; Rheinhardt et al. 2013). Headwater wetlands throughout the region are typically co-dominated by *M. virginiana* and *N. biflora*, though flow obstructions could result in zonation or greater dominance of *N. biflora* over *M. virginiana* as standing water remains for larger portions of the year. Conversely, enhanced drainage typically results in compositional shifts that more closely resemble southern mixed hardwood forests (Monk 1968).

Altered hydrology, vegetative structure, and vegetative composition in turn affect the availability and quality of wildlife habitats. Houlahan and Findlay (2003) found positive relationships between forest cover and amphibian species richness, and between amphibian species richness and proportions of adjacent wetlands. Generalist species are typically less impacted by LULC changes and may benefit where competition from specialists is reduced (Nordberg et al. 2019). Lower detection rates of headwater wetland specialists in agricultural vs forested catchments, and positive relationships between generalist species and LULC change provide evidence that habitat degradation may be occurring in coastal Alabama headwaters that impacts local population dynamics (Alix et al. 2014). The tendency for landscapes to become

increasingly homogenized as LULC changes occur (King et al. 2005) presents additional challenges to species movement and population growth, especially for those with greater limitations on dispersal (Gibbs 1993). As water tables recede due to drainage, fewer ephemeral pools are available for spawning and soil moisture becomes less ideal for amphibian occupancy (Gibbs 1993; Alix et al. 2014). Conversely, impoundments create large open water habitats that may benefit generalists over specialists in headwater wetlands (Nordberg et al. 2019). Sustaining the important ecosystem services and ecological functions associated with headwater wetlands will benefit from continued research that determines important LULC thresholds related to these wetlands.

2. Headwater Wetland Mapping

A well-founded method for guidance on wetland policy making and management, is the use of monitoring and assessment frameworks. This method typically utilizes wetland inventories, where wetland resources are mapped and quantified in terms of area and changes in area over some interval of time (U.S. EPA 2006). Wetland inventories can be used to identify wetland trends, and support or advocate against policies or management practices that are associated with those trends. Wetland mapping begins with wetland determination, which is sometimes difficult, especially where wetland boundaries and/or core areas represent gradational zones between wet and dry areas. As wetland mapping techniques, aerial photograph and satellite image interpretation have improved with advancements in spatial, spectral, and temporal resolutions of imagery datasets. These methods are still limited for accurate detections of indiscrete wetlands that lack clearly visibly boundaries made evident by image color, hue,

texture, etc. Furthermore, such methods lack automation that would contribute to wetland mapping efficiency, reproducibility, and economic viability.

The ability to produce accurate wetland inventories has been a challenge for regions that contain an abundance of 'cryptic' wetlands. Such wetlands may blend into the larger landscape, as 'wet' uplands (i.e., wet forest slopes, etc.), while some uplands may even blend into nearby wetlands. The need to distinguish between wetland and upland land classes serves to better represent natural resources across the landscape as a whole. Furthermore, accurate wetland detection aids in the identification of wetland gains, losses, and trends represented through wetland inventories, which guide and determine the success of wetland policies (U.S. EPA 2006).

Though historically subject to detection limitations with remote sensing methods (Christensen et al. 2023), recent advancements in the quality and accessibility of high-resolution imagery and elevation datasets have spurred interests in cryptic wetland mapping applications. The integration of these datasets with predictive models and machine learning techniques has considerably improved accurate wetland detection rates where metrics used were representative of wetland status. These applications may effectively represent small, forested wetlands that are not easily distinguished from nearby uplands through the use of imagery interpretation, such as headwaters in the coastal plain region of the southeastern U.S. The need for testing such applications in the southeast and coastal plain region in particular, is underlined by a multitude of features associated with wetlands throughout the region.

Two techniques that commonly utilize remotely sensed data and machine learning are automated pixel and object-based classifiers. Satellite and/or aerial imagery are typically used in these processes, but other datasets like digital terrain models (DTM) can be incorporated as well (Halabisky et al. 2011). Training data consist of pixel locations within specified classes, where

band values at the locations of each class contribute to machine learning classifications. While pixel-based classifiers consider pixel band values, object-based classifiers groups pixels into objects where similar band values are closely arranged with each other.

The use of imagery to identify wetlands in automated classifier models is dependent on the wetlands size, homogeneity of cover types, presence of visible standing water, and gradient of data values between uplands and wetlands (Halabisky et al. 2011). The use of imagery with moderate spatial resolutions alongside automated pixel-based classifiers is best suited for larger wetlands with homogenous cover types that contrast from those in surrounding uplands. For example, mapping open water wetlands that contrast an array of vegetated uplands, or emergent wetlands that contrast scrub/shrub uplands could be appropriate applications (Halabisky et al. 2011). Spectral data are central to pixel-based classifiers, though multispectral imagery often lack the necessary spatial resolutions to detect small and/or patchy wetlands (Tiner 1990; Jones et al. 2019). Conversely, where high spatial and adequate spectral resolutions are present in imagery, pixel-based classifiers are less successful at classifying large homogonous wetlands, as significant spectral variation is introduced across large areas (Oruc et al. 2004).

When the detection of wetlands with various spatial configurations and heterogenous cover types is a primary objective, pixel-based classifiers are not a preferred method. Automated object-based classifiers excel where spatial relationships are highly correlated with wetlands of various sizes and cover types. For instance, high spatial resolutions in imagery better characterize wetlands of heterogenous cover types where spatial patterns are persistent, such as beaver pond complexes that contain multiple features in predictable compositions (Fairfax et al. 2023). This method is also useful for methods that use high spatial resolution images where

homogenous cover types represent wetlands, such as reservoirs and geographically isolated wetlands (Halabisky et al. 2011; Jones et al. 2019).

The use of imagery for forested wetland classification is still limited in many applications, as open water may be indetectable through canopies or present throughout the year. Additionally, open water in rarely flooded wetlands may go undetected, dependent on the frequency of image acquisitions (Christensen et al. 2022). Leaf off imagery can provide useful information on forest composition where canopies are easily classified as deciduous, evergreen, or mixed. A primarily deciduous canopy surrounding a large river may suggest the presence of a floodplain forest, as these wetlands are associated with mature hardwoods. Headwater wetlands, however, often lack uniform canopies with strong visual identifiers. Additionally, headwater wetland canopies share visual and spectral characteristics with those in surrounding uplands, as environmental gradients are gradual along with changes in vegetational composition (Lang et al. 2013). Facultative species commonly occur in each, which are closely associated with headwater wetlands and low-lying upland areas (Noble et al. 2007; Rheinhardt et al. 2013). Additionally, many canopy and midstory species in the region show varying degrees of semi-evergreen (*M. virginiana*), semi-deciduous (*N. bifolia*), deciduous persistent, and deciduous characteristics. While leaf-off imagery can work well in many cases to identify wetlands, these may be misleading for headwater wetland identification to both aerial imagery interpreters and object-based classifiers (Lang et al. 2013; Huang et al. 2014).

Landforms made evident through DTMs are consistent landscape features without limited uses in forested areas. Geomorphic positions exert strong influences on slope wetland hydrology (Brinson 1993), which can be made evident through topographic indices. These are geospatial datasets that describe topographic traits and are typically DTM derivatives. These include

variables like planform and profile curvature, which describe slope convergence and shape. These and other indices, such as gradient and topographic position index (TPI), have been implemented into wetland prediction models where landforms are adequate predictors of wetland hydrology (Miller 2003). The use of DTM derivatives to map landforms and wetland features have shown substantial improvements in recent years (Huang et al. 2014), and the combination of DTM derivatives with other meaningful datasets and deep learning frameworks have demonstrated increasing potential to improve wetland prediction accuracy (O'Neill et al. 2020; Christensen et al. 2022).

3. Study Objectives

The proposed combination of spatial and functional data represents a holistic assessment of headwater wetlands in coastal Alabama. Where relationships between mappable landscape features and headwater wetland extent are evident, further potential exists for modeling and mapping wetland functions across various land use scenarios. The identification of these controls through remote sensing methods provides the opportunity for landscape modeling of wetland functions across a gradient of land uses and topographic features. Such models may eventually support regional efforts to identify critical areas for maintaining or improving coastal water quality and implementing broader watershed planning efforts. Our methods-based research objectives outlined in this thesis explore the use of wetland functional assessment and mapping tools to further these goals.

My first research chapter (Chapter 2) addresses land use impacts on headwater wetland functions throughout coastal Alabama. Metrics of headwater wetland function were related to

forested, agricultural, and urban land uses present in headwater catchments. Metrics representing the conditions of wetland hydrology, soils, and vegetation were collected using the Hydrogeomorphic (HGM) Approach to assess the functions of headwater slope wetlands on the Mississippi and Alabama Coastal Plains (Noble et al. 2007). These data were analyzed for relationships with LULC gradients present in across Mobile and Baldwin County (the two coastal counties of Alabama) and are intended to support future applications that model potential impacts to wetland function across various LULC scenarios.

My second research chapter (Chapter 3) explored the use of the Wetland Intrinsic Potential (WIP) tool to improve headwater wetland detection in coastal Alabama. Using this approach, we modeled wetland presence, absence, and extent for a select watershed in coastal Alabama through remotely sensed environmental variables and random forest procedures. Our predictive model is exploratory in nature and seeks to provide guidance on the potential use of such tools and methods for wetland mapping in the eastern gulf coastal plain. Our research is intended to support future models by exploring methods and variables that accurately predict wetlands in our study area and may be applied throughout the coastal plain region. By exploring functional and spatial modeling tools for headwater wetlands, our work addresses the changing landscape in coastal Alabama while providing potential tools for improved wetland monitoring efforts. Our research may be further expanded to provide insights on the synthesis of functional and spatial methods for modeling wetland gains, losses, and trends.

4. Literature Cited

Adis J and Junk WJ. 2002. Terrestrial invertebrates inhabiting lowland river floodplains of Central Amazonia and Central Europe: a review. Freshwater Biology. 47(4): 711-731. https://doi.org/10.1046/j.1365-2427.2002.00892.x

Alexander RB, Boyer EW, Smith RA, Schwarz GE, Moore RB. 2007. The Role of Headwater Streams in Downstream Water Quality. Journal of the American Water Resources Association. 43(1): 41-59. https://doi.org/10.1111/j.1752-1688.2007.00005.x

Alix D, Anderson CJ, Grand J, Guyer C. 2014. Evaluating the Effects of Land Use on Headwater Wetland Amphibian Assemblages in Coastal Alabama. Wetlands. 34(5): 917-926. https://doi.org/10.1007/s13157-014-0553-y

Barksdale FW and Anderson CJ. 2014. The influence of land use on forest structure, species composition, and soil conditions in headwater-slope wetlands of coastal Alabama, USA. International Journal of Biodiversity Science, Ecosystem Services & Management. 11(1): 61-70. https://doi.org/10.1080/21513732.2013.876449

Barksdale FW, Anderson CJ, Kalin L. 2014. The influence of watershed run-off on the hydrology, forest floor litter and soil carbon of headwater wetlands. Ecohydrology. 7(2): 803–814. https://doi.org/10.1002/eco.1404

BenDor T and Brozović N. 2007. Determinants of Spatial and Temporal Patterns in Compensatory Wetland Mitigation. Environmental Management. 40(1): 349–364. https://doi.org/10.1007/s00267-006-0310-y

Brinson MM. 1993. A Hydrogeomorphic Classification for Wetlands. U.S. Army Corps of Engineers, Waterways Experiment Station, Vicksburg, MS, USA. Technical Report WRP-DE-4, U.S. Army Engineer Waterways Experiment Station, Vicksburg, MS.

Brinson MM, Miller KH, Rheinhardt R, Christian R, Meyer G, O'Neal J. 2006. Developing reference data to identify and calibrate indicators of riparian ecosystem condition in rural coastal plain landscapes in North Carolina. Report to the Ecosystem Enhancement Program, North Carolina Department of Environment and Natural Resources. Raleigh, NC, USA. http://www.nceep.net/pages/resources.htm

Cole C, Brooks R, Shaffer P. 2002. Comparison of Hydrology of Wetlands in Pennsylvania and Oregon (USA) as an Indicator of Transferability of Hydrogeomorphic (HGM) Functional Models Between Regions. Environmental Management. 30(2): 265–278. https://doi.org/10.1007/s00267-001-0055-6

Colvin ARS, Sullivan SMP, Shirey PD, Colvin RW, Winemiller KO, Hughes RM, Fausch KD, Infanta DM, Olden JD, Bestgen KR, Danehy RJ, Eby L. 2019. Headwater streams and wetlands are critical for sustaining fish, fisheries, and ecosystem services. American Fisheries Society. 44(2): 49-108. https://doi.org/10.1002/fsh.10237

Caldwell PV, Sun G, McNulty SG, Cohen EC, Myers M. 2012. Impacts of impervious cover, water withdrawals, and climate change on river flows in the conterminous US. Hydrology & Earth System Sciences. 16(8): 2839–2857. https://doi.org/10.5194/hess-16-2839-2012

Christensen JR, Golden HE, Alexander LC, Pickard BR, Fritz KM, Lane CR, Weber MH, Kwok RM, Keefer MN. 2022. Headwater streams and inland wetlands: Status and advancements of geospatial datasets and maps across the United States. Earth-Science Reviews. 235(1): 104230. https://doi.org/10.1016/j.earscirev.2022.104230.

Cubbage F and Flather K. 1993. Forested Wetland Area and Distribution: A Detailed Look at the South. Journal of Forestry. 91(5): 35-40. https://doi.org/10.1093/jof/91.5.35

Fairfax E, Zhu E, Clinton N, Maiman S, Shaikh A, Macfarlane WW, Wheaton JM, Ackerstein D, Corwin E. 2023. EEAGER: A neural network model for finding beaver complexes in satellite and aerial imagery. Journal of Geophysical Research: Biogeosciences. 128(6): e2022JG007196. https://doi.org/10.1029/2022JG007196

Fritz KM, Feminella JW, Colson CG, Lockaby BG, Governo R, Rummer RB. 2006. Biomass and Decay Rates of Roots and Detritus in Sediments of Intermittent Coastal Plain Streams. Hydrobiologia. 556(1): 265-277. https://doi.org/10.1007/s10750-005-1154-9

Fritz KM and Feminella JW. 2011. Invertebrate colonization of leaves and roots within sediments of intermittent Coastal Plain streams across hydrologic phases. Aquatic Sciences. 73(4): 459–469. https://doi.org/10.1007/s00027-011-0192-9

Gibbs JP. 1993. Importance of small wetlands for the persistence of local populations of wetland-associated animals. Wetlands. 13(1): 25–31. https://doi.org/10.1007/BF03160862

Gomi T, Sidle RC, Richardson JS. 2002. Understanding Processes and Downstream Linkages of Headwater Systems: Headwaters differ from downstream reaches by their close coupling to hillslope processes, more temporal and spatial variation, and their need for different means of protection from land use. BioScience. 52(10): 905–916. https://doi.org/10.1641/0006-3568(2002)052[0905:UPADLO]2.0.CO;2

Groffman P, Boulware NJ, Zipperer WC, Pouyat RV, Band LE, Colosimo MF. 2002. Soil Nitrogen Cycle Processes in Urban Riparian Zones. Environmental Science & Technology. 36(21): 4547–52. https://doi.org/10.1021/es020649z

Groffman P, Bain DJ, Band LE, Belt KT, Brush GS, Grove M, Pouyat R, Yesilonis I, Zipperer W. 2003. Down by the Riverside: Urban Riparian Ecology. Frontiers in Ecology and The Environment. 1(6): 315-321. http://dx.doi.org/10.2307/3868092

Halabisky M, Moskal ML, Hall SA. 2011. Object-based classification of semi-arid wetlands. Journal of Applied Remote Sensing. 5(1): 1-13. https://doi.org/10.1117/1.3563569

Hardison EC, O'Driscoll MA, DeLoatch JP, Howard RJ, Brinson MM. 2009. Urban Land Use, Channel Incision, and Water Table Decline Along Coastal Plain Streams, North Carolina. Journal of the American Water Resources Association. 45(4): 1032-1046. https://doi.org/10.1111/j.1752-1688.2009.00345.x

Hoeltje SM and Cole CA. 2007. Losing function through wetland mitigation in central Pennsylvania, USA. Environmental Management. 39(3): 385-402. https://doi.org/10.1007/s00267-006-0212-z

Houlahan JE and Findlay CS. 2003. The effects of adjacent land use on wetland amphibian species richness and community composition. Canadian Journal of Fisheries and Aquatic Sciences. 60(9): 1078-1094. https://doi.org/10.1139/f03-095

Huang C, Peng Y, Lang M, Yeo IY, McCarty G. 2014. Wetland inundation mapping and change monitoring using Landsat and airborne LiDAR data. Remote Sensing of Environment. 141(5): 231-242. https://doi.org/10.1016/j.rse.2013.10.020

Jones RH, Lockaby BG, Somers GL. 1996. Effects of Microtopography and Disturbance on Fine-Root Dynamics in Wetland Forests of Low-Order Stream Floodplains. American Midland Naturalist. 136(1): 57-71. https://doi.org/10.2307/2426631

Jones KL, Poole GC, Meyer JL, Bumback W, Kramer EA. 2006. Quantifying expected ecological response to natural resource legislation: a case study of riparian buffers, aquatic habitat, and trout populations. Ecology and Society. 11(2): 15. http://www.ecologyandsociety.org/vol11/iss2/art15/

Jones T, Marzen L, Mitra C, Barbour M. 2019. Identification and classification of geographically isolated wetlands in North Alabama using geographic object based image analysis (GeOBIA). Geocarto International. 34(7): 769–784. https://doi.org/10.1080/10106049.2018.1438527

King RS, Baker ME, Whigham DF, Weller DE, Jordan TE, Kazyak PF, Hurd MK. 2005. Spatial Considerations for Linking Watershed Land Cover to Ecological Indicators in Streams. Ecological Applications. 15(1): 137-153. https://doi.org/10.1890/04-0481

Lang M, McCarty G, Oesterling R, Yeo IY. 2013. Topographic Metrics for Improved Mapping of Forested Wetlands. Wetlands. 33(1): 141–155. https://doi.org/10.1007/s13157-012-0359-8

Li X, Minick KJ, Luff J. Noormets A, Miao G, Mitra B, Domec JC, Sun G, McNulty S, King JS. 2020. Effects of Microtopography on Absorptive and Transport Fine Root Biomass, Necromass, Production, Mortality and Decomposition in a Coastal Freshwater Forested Wetland, Southeastern USA. Ecosystems. 23(8): 1294–1308. https://doi.org/10.1007/s10021-019-00470-x

Meyer JL, Paul MJ, Taulbee WK. 2005. Stream ecosystem function in urbanizing landscapes. Journal of the North American Benthological Society. 24(3): 602–612. http://dx.doi.org/10.1899/04-021.1

[MEAB] Millennium Ecosystem Assessment Board. 2005. Ecosystems and Human Well-Being: Wetlands and Water Synthesis. World Resources Institute, Washington, DC.

Miller DJ. 2003. Programs for DEM Analysis. Landscape Dynamics and Forest Management, General Technical Report RMRS-GTR-101CD, USDA Forest Service, Rocky Mountain Research Station, Fort Collins, CO, USA.

Mitchell J, Lockaby B, Brantley E. 2011. Influence of Chinese Privet (Ligustrum sinense) on Decomposition and Nutrient Availability in Riparian Forests. Invasive Plant Science and Management. 4(4): 437-447. https://doi.org/10.1614/IPSM-D-11-00020.1

Monk CD. 1968. Successional and Environmental Relationships of the Forest Vegetation of North Central Florida. The American Midland Naturalist. 79(2): 441–57. https://doi.org/10.2307/2423190

Neary DG, Ice GG, Jackson CR. 2009. Linkages Between Forest Soils and Water Quality and Quantity. Forest Ecology and Management. 258(10): 2269-2281. https://doi.org/10.1016/j.foreco.2009.05.027

Noble CV, Wakeley JS, Robert TH, Henderson C. 2007. Regional Guidebook for Applying the Hydrogeomorphic Approach to Assessing the Functions of Headwater Slope Wetlands on the Mississippi and Alabama Coastal Plains. ERDC/EL TR-07-2, U.S. Army Corps of Engineers. Vicksburg, MS.

Noble CV, Murray EO, Klimas CV, Ainslie W. 2011. Regional Guidebook for Applying the Hydrogeomorphic Approach to Assessing the Functions of Headwater Slope Wetlands on the South Carolina Coastal Plain. ERDC/EL TR-11-11, U.S. Army Engineer Research and Development Center. Vicksburg, MS.

Nordberg EJ, Schwarzkopf L. 2019. Reduced competition may allow generalist species to benefit from habitat homogenization. Journal of Applied Ecology. 56(2): 305–318. https://doi.org/10.1111/1365-2664.13299

O'Neil GL, Goodall JL, Behl M, Saby L. 2020. Deep learning Using Physically-Informed Input Data for Wetland Identification. Environmental Modelling and Software. 126(1): 104665. https://doi.org/10.1016/j.envsoft.2020.104665

Oruc M, Marangoz AM, Buyuksalih G. 2004. Comparison of pixel based and object oriented classification approaches using Landsat 7 ETM spectral bands. In: Orhan Altan, Editor. 20th ISPRS Congress Technical Commission IV. Proceedings of the 20th International Society for Photogrammetry and Remote Sensing Congress; July 12-23, 2004; Istanbul, Turkey. ISPRS Archives: 35(B4) p. 1118–1122.

Phillips JD. 1989. Nonpoint source pollution control effectiveness of riparian forests along a coastal plain river. Journal of Hydrology. 110(3-4): 221-237. https://doi.org/10.1016/0022-1694(89)90189-3

Phipps RG and Crumpton WG. 1994. Factors affecting nitrogen loss in experimental wetlands with different hydrologic loads. Ecological Engineering. 3(4): 399-408.

Ramesh R, Kalin L, Hantush M, Anderson CJ. 2020. Challenges Calibrating Hydrology for Groundwater-Fed Wetlands: a Headwater Wetland Case Study. Environmental Modeling & Assessment. 25(6): 355–371. https://doi.org/10.1007/s10666-019-09684-8

Ranalli AJ and Macalady DL. 2010. The importance of the riparian zone and in-stream processes in nitrate attenuation in undisturbed and agricultural watersheds - a review of the scientific literature. Journal of Hydrology. 389(3-4): 406-415. https://doi.org/10.1016/j.jhydrol.2010.05.045

Rapanos v. US. 2006. 547 U.S. 715, 126 S. Ct. 2208, 165 L. Ed. 2d 159.

Rezaeianzadeh M, Kalin L, Hantush MM. 2018. An Integrated Approach for Modeling Wetland Water Level: Application to a Headwater Wetland in Coastal Alabama, USA. Water. 10(7): 879. https://doi.org/10.3390/w10070879

Rheinhardt R, Wilder T, Williams H. 2013. Variation in Forest Canopy Composition of Riparian Networks from Headwaters to Large River Floodplains in the Southeast Coastal Plain, USA. Wetlands. 33(6): 1117–1126. https://doi.org/10.1007/s13157-013-0467-0

Sackett v. EPA. 2023. 143 S. Ct. 1322, 598 U.S. 651, 215 L. Ed. 2d 579.

Singh M. 2015. Isolated Wetlands: Assessing Their Values & Functions. Journal of Aquatic Science. 3(1): 6-13. https://pubs.sciepub.com/jas/3/1/2

Tiner RW. 1990. Use of high-altitude aerial-photography for inventorying forested wetlands in the United States. Forest Ecology and Management. 33-34(10): 593–604. https://doi.org/10.1016/0378-1127(90)90221-V

Tufford D. 2011. Shallow Water Table Response to Seasonal and Interannual Climate Variability. Transactions of the ASABE: American Society of Agricultural and Biological Engineers. 54(6): 2079-2086. https://doi.org/10.13031/2013.40663

[U.S. EPA] U.S. Environmental Protection Agency. 2006. 2006–2011 EPA strategic plan: charting our course. EPA-190-R-06-001. U.S. Environmental Protection Agency, Office of Planning, Analysis, and Accountability, Washington, DC.

Winter TC. 1988. A Conceptual Framework for Assessing Cumulative Impacts on the Hydrology of Nontidal Wetlands. Environmental Management. 12(5): 605-620. https://doi.org/10.1007/BF01867539

Zedler JB. 2003. Wetlands at your service: reducing impacts of agriculture at the watershed scale. Frontiers in Ecological Environments. 1(2): 65–72. https://doi.org/10.1890/1540-9295(2003)001[0065:WAYSRI]2.0.CO;2

Zedler JB and Kercher S. 2005. Wetland Resources: Status, Trends, Ecosystem Services, and Restorability. Annual Review of Environmental Resources. 30(1): 39-74. https://doi.org/10.1146/annurev.eg.30.102405.100001

Chapter II. LAND USE EFFECTS ON HEADWATER WETLAND FUNCTIONS IN COASTAL ALABAMA

Abstract

Headwater slope wetlands are forested wetlands located at the headwaters of coastal rivers and streams. They are a ubiquitous wetland type in the southeastern U.S. Coastal Plain and a critical element to the Gulf coast landscape because they occupy the interface of uplands and drainages, and therefore provide important functions related to water storage, water quality improvement, and wildlife habitats. There are concerns that past and current coastal land use / land cover (LULC) changes may severely reduce the capacity for these wetlands to provide these functions. To investigate this, 42 headwater wetlands in coastal Alabama (i.e., Mobile and Baldwin County) were assessed for important functional attributes (wetland forest structure, soils, and hydrology) represented by various ecological measures over a range of surrounding watershed LULC in 2022-23. Wetland attributes were measured using the Hydrogeomorphic Method (HGM) approach for the functional assessment of headwater wetlands in the coastal plain region of Mississippi and Alabama. These data were added to past HGM assessments (n=32) for a total of 74 wetlands evaluated. Wetland data were collected throughout Baldwin and Mobile County, AL, to determine potential declines in function and condition in response to percent cover of urban and agricultural land use in the watershed. Land class data represented by the National Land Class Dataset were transformed via principal component analysis into LULC gradients, depicted by principal components (Comps.) 1 (agricultural to forested) and 2 (urban to rural) for use in linear regression. Comps. 1 and 2 held significant relationships with shrub cover that suggest agricultural and urban LULC may yield higher midstories densities in headwater

wetlands. Urban LULC was additionally related to increased herbaceous understory coverage and soil dewatering, as well as reductions in soil organic matter content. Neither principal component was highly correlated with any field measurements, though multiple wedge shaped distributions (increasing variability across the land gradient) in our data suggest that ecological functional limits may be present in response variables that limit their use as effective response variables. Our findings also emphasize the need to account for variation introduced by flow concentration and obstruction structures and spatial complexities present in LULC composition. We discuss the implications of continued LULC change along the coast and potential measures to sustain headwater wetland functions under increasingly urban conditions. Ultimately, the information gained from this study will assist watershed managers interested in wetland monitoring efforts that sustain environmental services provided by coastal drainages along the Gulf coast.

Keywords: Land use land cover, headwater slope wetland, forested wetlands, wetland functional assessments, hydrogeomorphic approach, forest structure, coastal Alabama.

1. Introduction

In many parts of the world, watershed headwaters are dominated by wetlands. Headwater wetlands (those wetlands associated with zero- and first-order streams) are critical areas for both water resource quality and quantity due to high levels of connectivity with their surrounding drainage areas. Further, headwaters have a disproportionate impact on downstream waterways and ecosystems due to the significant amount of terrestrial land-water interface from which nutrients and other matter are sequestered and hydrologic baseflows are sustained (Gomi

et al. 2002; Armstrong et al. 2012; Colvin et al. 2019). Headwater wetlands are hotspots for additional ecosystem services that include flood attenuation, biodiversity, wildlife habitat, and carbon storage. Wetland ecosystem services are typically foregone where lands are converted for agricultural production or human settlement. These land uses have historically resulted in the loss of over half of wetlands worldwide (Foley et al. 2005; Zedler and Kercher 2005).

In the United States (U.S.), measures have been taken to minimize impacts to water resources since the passing of the 1972 Clean Water Act and related amendments (Mitsch and Gosselink 2015). Over time, the Clean Water Act included provisions to Section 404, which requires dredge and filling of certain wetlands to undergo a costly and time-consuming mitigation process. Where wetland loss does not occur, many wetlands remain intact but still experience degradation from the indirect effects of land practices which can alter drainage patterns (Groffman et al. 2003; Zedler & Kercher 2005). Sustaining wetland functions has become an increasingly relevant topic surrounding wetland mitigation, as focal objectives for science-driven policies and public perceptions of wetlands have shifted to the protection of ecosystem services and ecological integrity. In unaltered forested (reference) catchments of the southeastern U.S., drainage in response to storm events is tempered by forest vegetation and soils which contribute to shallow subsurface flows (Barnes et al. 1997; Neary et al. 2009). Reductions in wetland functions may occur where watershed drainage properties are altered beyond those observed in these reference conditions for a given wetland community. The loss of canopy and midstory trees in upland forests can translate to reductions in rainfall interception, effective infiltration, and evapotranspiration. Organic rich duff layers in the upland forest soils are also diminished by accelerated decomposition and soil erosion rates when canopies are reduced,

which further the tendency of uplands to produce more surface runoff (Barnes et al. 1997; Mitsch and Gosselink 2015; Neary et al. 2009).

In addition to the loss of forest cover, agricultural and urban LULC are often paired with drainage structures such as stormwater drains and agricultural ditches. These features commonly drain stormwater rapidly and directly into wetlands and streams, thereby accelerating surface discharge and altering wetland hydroperiod (Zedler 2003). As land surfaces become increasingly impervious due to agricultural and (especially) urban LULC, designed stormwater overland flows are promoted that reduce groundwater recharge and water table depth in riparian wetlands (Walsh et al. 2005; Schiff and Benoit 2007; Hardison et al. 2009). Increased agricultural and urban land use in the watershed and the resulting hydrologic alterations that promote surface flows can adversely affect wetland hydrologic regimes, particularly in headwaters that are characterized by hillslope seepage, such as headwater slope wetlands of the eastern Gulf Coastal Plain (Noble et al. 2007, 2011). Because wetlands conditions (i.e., species composition, forest structure, soil conditions, ecosystem productivity) are closely tied to its hydrologic regime, LULC changes in drainage patterns may represent an important stressor to headwater wetlands and the functions dependent of wetland conditions. Such effects are potentially detectable through measurable ecological indicators. For example, soil Munsell chroma >2 indicate non-wetland soils (Soil Science Division Staff 2017) and may indicate the loss of anoxic conditions for soils within wetlands. Similarly, soil Munsell value depicts organic content in mineral soils, with lower values in this range indicating greater proportions of organic matter. Headwater Slope wetlands, which are characterized by highly organic soils, are best depicted by a soil Munsell value ≤2.5 (Noble et al. 2007). For wetlands that exceed these conditions, such deviations may indicate degradation by surrounding LULC change, such as increased surface flows and altered

hydrologic regimes that accelerate decomposition and result in functional losses to carbon storage.

Vegetative and hydrologic indicators are also commonly used to evaluate wetland conditions and determine potential losses to wetland functions such as groundwater storage and wildlife habitat value (Rheinhardt et al. 1999). Noble et al. (2007) characterizes highly functioning forest structures in headwater slope wetlands as having mean canopy tree diameters and densities of respectively, ≥30 cm and between 250-425 stems/ha. Highly dense, small-diameter canopy trees indicate forests with considerable disturbances that may promote shrub and ground vegetation coverage. As reference headwater slope wetlands are characterized as climax communities, considerably altered forest structures may indicate wetland degradation by drainage alterations (Monk 1968). Such disturbances additionally mediate invasive species colonization in wetlands where surrounding LULC lacks adequate forested cover (Zedler and Kercher 2005).

Headwater wetlands throughout the Coastal Plain physiographic region are ubiquitous features on the landscape and have varied topographic and hydrologic conditions. Along the northern Gulf of Mexico coast, these wetlands act as transitional drainage zones between unconcentrated and concentrated flows in uplands and streams. Headwater slope wetlands also represents a biogeochemical and physical transition between uplands and streams and are key areas for carbon and sediment storage as retention is elevated due to low slopes and a lack of flooding (Noble et al. 2007; Barksdale et al. 2014; Ramesh et al. 2020). Coastal Alabama represents a vastly changing landscape due to increasing population growth over the span of several decades. Baldwin County, Alabama has experienced some of the most pronounced growth trends in the southeastern U.S. over the last decade, with a 30.7% population increase

between 2010 and 2021 (U.S. Census Bureau 2020, 2021). Approximately 13.7% of the county experienced land use changes between 2011-2019. Of the affected areas, urban LULC rose by 45.2% and forested LULC decreased by 28.3% from their initial extents (Dewitz and U.S. Geological Survey 2021). Land uses changes are expected to follow this trajectory as populations continue to increase. There is ongoing concern among land planners and resource managers that the continued land use change in Baldwin County and many coastal areas along the Gulf of Mexico will result in severe loss of headwater wetland function and ultimately poorer conditions in downstream water bodies.

Due to the rapidly changing landscape, our research was designed to evaluate the use of readily accessible workflows, datasets, and tools for use in wetland functional impact analyses and modeling. To achieve this goal, we investigated the use of publicly available LULC datasets as predictor variables in linear regression. We aimed to identify predictive relationships with wetland functional measurements that could be extrapolated to new areas under alternative LULC scenarios. This workflow serves to model possible impacts on wetland resources before LULC changes occur to potentially justify management actions. To assess headwater wetland conditions relative to surrounding LULC, we used a rapid assessment tool for the determination of important ecological measurements that are related to wetland functional capacities in headwater slope wetlands of coastal Alabama and Mississippi. Based on the Hydrogeomorphic (HGM) approach (Noble et al. 2007) wetland hydrologic, soil, and vegetative mensuration was established to characterize conditions and used in conjunction with headwater catchment LULC to determine its potential effect on headwater wetlands. Based on previous studies, we expected alterations in wetland conditions (relative to reference condition) across a land use gradient from

forested to agricultural LULC, from forested to urban LULC, and from agricultural to urban LULC.

2. Methods

2.1. Description of Study Area

Within the East Gulf Coastal Plain physiographic region, our study area is defined as the extent of Mobile and Baldwin County, Alabama, USA (Fig. 2.1). The region is characterized by mild winters, hot summers and year-round rain. Mean annual temperatures range between 15 and 21 ºC with rainfall amounts of 168 cm/year (Noble et al. 2007). The region is characterized by relatively flat topography with some areas of steeper relief. Representative slopes vary from near zero in the coastal lowlands to upwards of 20% in alluvial valleys, with mean slope value of 3.27% (Ebersole et al. 2019; Soil Survey Staff 2022). Upland soils are characterized as well-drained, udic and perudic, fine sandy loams with average slopes of 5.7% (Soil Survey Staff 2022). Although this region contains a diverse array of wetland types and communities, our sampling efforts were confined to headwater slope wetlands, consistent with biophysical descriptions given by Noble et al. (2007).

While headwater catchments are relatively small watersheds, those in the coastal plain region have large contributing areas proportional to watershed gradient, so that substantial drainage areas are required for stream initiation (Avcioglu et al. 2017). We expected watershed morphology to vary by sub-physiographic unit, so that larger contributing areas and low gradients would occur more frequently in the coastal lowland region, and smaller contributing areas with steeper topography in the alluvial plain region (Avcioglu et al. 2017; Ebersole et al.

2019). Barksdale & Anderson (2014) characterized headwater catchments in southern Baldwin County, Alabama as having a mean watershed area of 77.9 ha, with 6.1% of that area consisting of headwater wetlands.

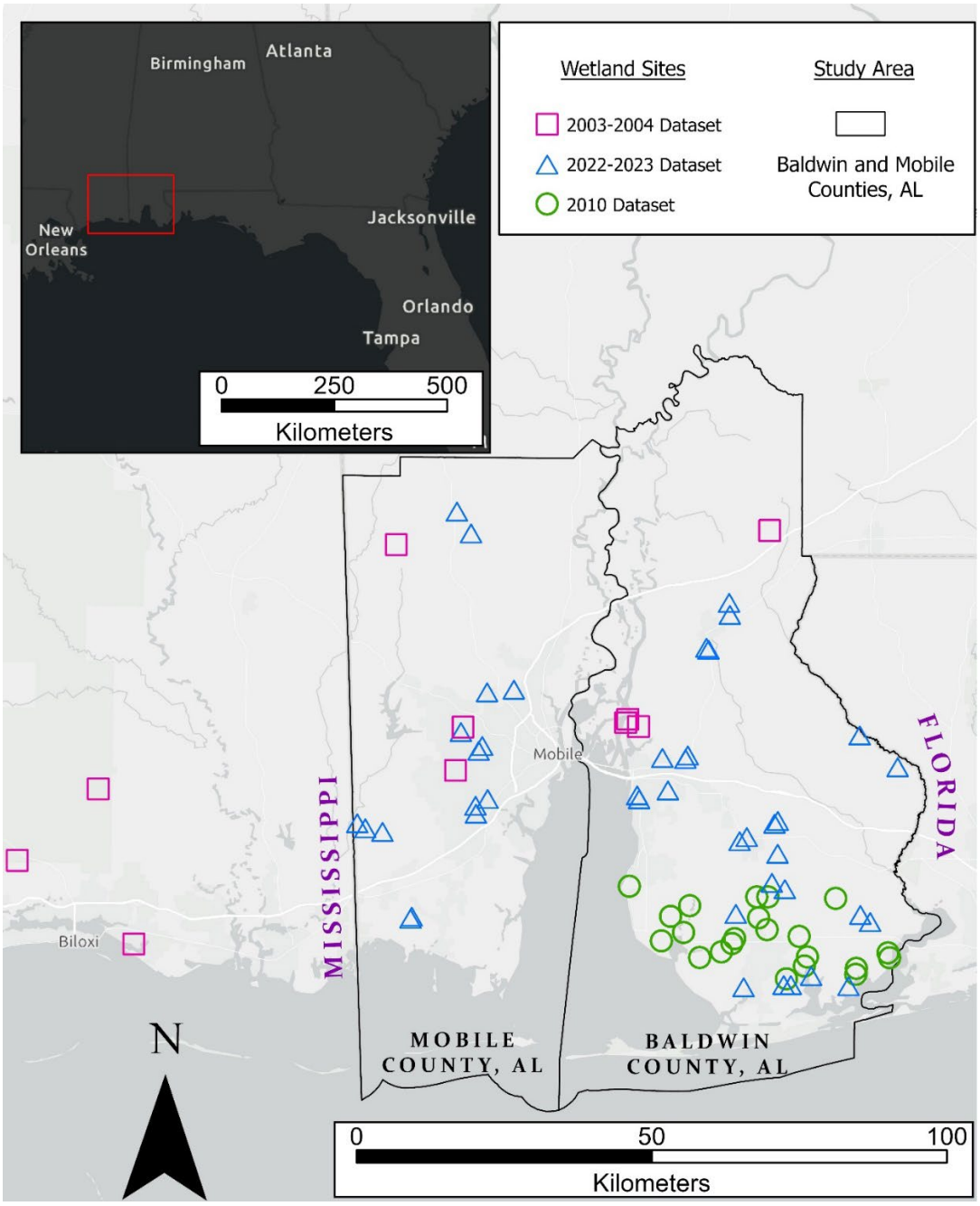

Figure 2.1. *Distribution of wetland sites for all datasets. Sites in the 2003-04 dataset spanned areas of Mobile and Baldwin Counties, AL while sites from the 2010 dataset were constrained to southern Baldwin County, AL. Newly surveyed sites sought to represent previously unrepresented areas of Mobile and Baldwin County, AL.*

Watershed morphology at the headwaters of this region contributes to the predominance of shallow subsurface drainage, in which hillslope and geomorphic position are indicative of wetland type and community composition (Brinson et al. 1993; Gomi et al. 2002). From summit to foot slope, upland communities generally transition from xeric/mesic pine and mixed forests to mesic/hydric mixed forests. At toe-slopes, communities further transition to seepage-dominated bay-tupelo forests in association with headwater slope wetlands and intermittent streams before converging with adjacent drainages to form headwater floodplain wetlands (Monk 1968; Noble et al. 2007; Reinhardt et al. 2013). As tributaries converge further downstream, headwater streams and wetlands give way to mainstem streams and floodplain forests before transitioning into estuarine waterways and wetlands (Reinhardt et al. 2013).

2.2. Spatial Data Sources

Raster and vector datasets encompassing our study area were acquired for various objectives related to image interpretation, watershed/wetland delineations, and LULC information. In the following section, data acquired for different years were used to reflect wetland conditions at the times of wetland surveys and resulting field measurements that were collected. These multi-year datasets apply to dynamic features such as watershed LULC composition and the presence/absence of flow obstruction and/or flow concentration structures that were not present/absent in all years. Wetland boundary features were obtained through The National Wetland Inventory (NWI) (U.S. Fish and Wildlife Service 2022), and streamlines were extracted from the high resolution national release of the National Hydrography Dataset (NHDPlusHR) (U.S. Geological Survey 2022$_a$). One-meter digital terrain model (DTM) tiles which encompassed the study area and corresponded to 2012 acquisition years were accessed

through the National Map database (U.S. Geological Survey 2023). Tiles were mosaicked into a single DTM and subsequently resampled with bilinear interpolation to 5-meter grid size. Additionally, 1-meter hillshade rasters were obtained through the geospatial data gateway (NGCE 2022). Historical topographic maps at scales of 1:24,000 map units were obtained through USGS's topoView data download webpage (U.S. Geological Survey 2022_b).

Aerial imagery orthophoto mosaics were acquired through NRCS/USDA contained within the extent of all counties present in the study area and select sites in Mississippi years for the years 2006, 2011, and 2021 (NGCE 2023) to account for the different field data sets used. These were National Agricultural Imagery Program (NAIP) three-band natural color orthophotos for Baldwin County, AL (2006, 2011, 2021); Mobile County, AL (2006, 2021), Harrison County, MS (2006, 2021), and Jackson County, MS (2006, 2021). Spatial resolutions for 2006 and 2011 Datasets within Alabama were 3-meter and 2-meter for 2006 datasets within Mississippi. All 2021 datasets had spatial resolutions of 0.3-meter. Imagery datasets were used exclusively for visual interpretation. Soil map units and associated runoff curve number ratings were downloaded from the Web Soil Survey (WSS) (Soil Survey Staff 2022), and LULC rasters at spatial resolutions of 30-meter were acquired from the National Land Class Dataset (NLCD) for the years 2004, 2011, and 2019 (Dewitz & U.S. Geological Survey 2021). Each NLCD dataset corresponded to the closest year in which wetland surveys were conducted (2003, 2004, 2010, 2022, 2023).

2.3. Wetland Site Selection Criteria

A total of 74 headwater wetland sites (Fig. 2.1) were included in our analysis, 32 of which were from prior studies that were within or near our study area (Noble et al. 2007; Barksdale and Anderson 2014) and 42 newly surveyed sites. Data collection for all studies was guided by the HGM approach for the determination of wetland functional capacities in headwater slope wetlands of coastal Alabama and Mississippi (Noble et al. 2007). The HGM approach was utilized for newly surveyed wetland sites, in accordance with how those data were collected and reported in prior studies.

Selected sites from Noble et al. (2007) were surveyed between the fall of 2003 and spring of 2004 and are hereon referred to as the 2003-04 dataset (n = 10). Seven sites from the 2003-04 dataset are located within our study area, with three occurring throughout Jackson and Harrison Counties, Mississippi. Selected sites from Barksdale and Anderson (2014) were surveyed during the summer of 2010, and are hereon referred to as the 2010 dataset (n = 22). All sites within the 2010 dataset occur within our study area and are largely concentrated in southern Baldwin County, Alabama. Field sampling efforts as part of this study occurred between the summer of 2022 and spring of 2023, and are heron referred to as the 2022-23 dataset. Wetland sites in the 2022-23 dataset were first targeted based on land uses in headwater catchments that were underrepresented in prior studies. Our second criterion was to better represent under-surveyed geographical regions within the study area, such as those in northern portions of Mobile County, Alabama.

Land use effects on headwater wetlands were considered using watershed delineations of contributing catchments. For an initial consideration and assessment of the landscape, individually delineating each headwater wetland watershed was impractical at the scale of the

study area. Rather, visual interpretation of NHDplusHR, NWI, DEMs, and aerial imagery datasets was the primary method to establish generalized watershed and wetland boundaries. Target wetland sites were expected to occur in headwater catchments where hillslopes drained to steadily low sloping chutes, occurring above and/or with first order streams, and having a predominance of deciduous forest or mixed forest canopy cover, characteristic of these wetlands. Land use classes in this preliminary assessment were interpreted broadly as agricultural, forested, or urban, based on 2019 NLCD data. The characterization of LULC in the watersheds of prior wetland surveys were assessed similarly with NLCD (2004, 2011) data to guide sampling efforts that would result in a relatively equal distribution of LULC classes across the total dataset.

Where spatial datasets collectively indicated headwater slope wetlands and target watershed LULC, sites were inventoried, validated, and surveyed. The distribution of 2022-23 sites reflects land access permissions and public land availability throughout the study area (Fig. 2.1). Sites that lacked sufficient evidence of wetland hydrology, vegetation, and soils consistent with the biophysical descriptions of headwater slope wetlands per Noble et al. (2007) were not assumed to have formerly fit those descriptions at one time based solely on geomorphic position and were not surveyed. These sites include gullies, wet upland slopes, harvested timberlands, and agricultural fields that appeared in geomorphic positions consistent with headwater slope wetlands. Thus, without a way to readily verify historical occurrence of these non-wetland but geomorphically consistent sites, our analysis represents a conservative approach to site selection with a focus on existing wetlands, rather than including those which may have been degraded to the point of wetland loss.

2.4. Wetland Field Surveys

2.4.1. Site & Plot Establishment

For this study, selected wetland sites were regarded as the extent of the wetland area above the confluence of intermittent first order streams with any other stream. The issue of unmapped intermittent headwater streams in NHD was addressed through imagery interpretation of NAIP, NWI, NHD, USGS topographic maps (1:24,000 map units), and DTM hill shade rasters. Where significant evidence suggested the presence of an unmapped headwater stream, our wetland sites were adjusted to account for true wetland boundaries and watershed outlet points. A minimum of three investigators were present for wetland field surveys. Per HGM protocol, each wetland site was to have a minimum surveyed area of 0.04 ha (400 m^2), achievable by various plot number and size configurations as specified by Noble et al. (2007).

As these wetlands are typically narrow and linear, the most common technique used was a four-plot configuration, spaced in relatively equal distances along the longitudinal length of the wetland, from crown to outlet (Fig. 2.2). Plots were established where slope wetland features were most representative, so that ditches, channels, and hillsides were avoided. Where such features were unavoidable, the longitudinal position of the plot within the wetland was either adjusted or the direction of the plot was pivoted. For each plot, an initial corner was established by an investigator from where another investigator extended a field tape 10 m to the next corner. The process was repeated with each corner measured 90º from the last, until a 0.01 ha (100 m^2) square plot was established near the latitudinal center of the wetland. A third investigator walked the plot boundaries as they were established to ensure that errors were minimized, and the process was repeated at each target plot location.

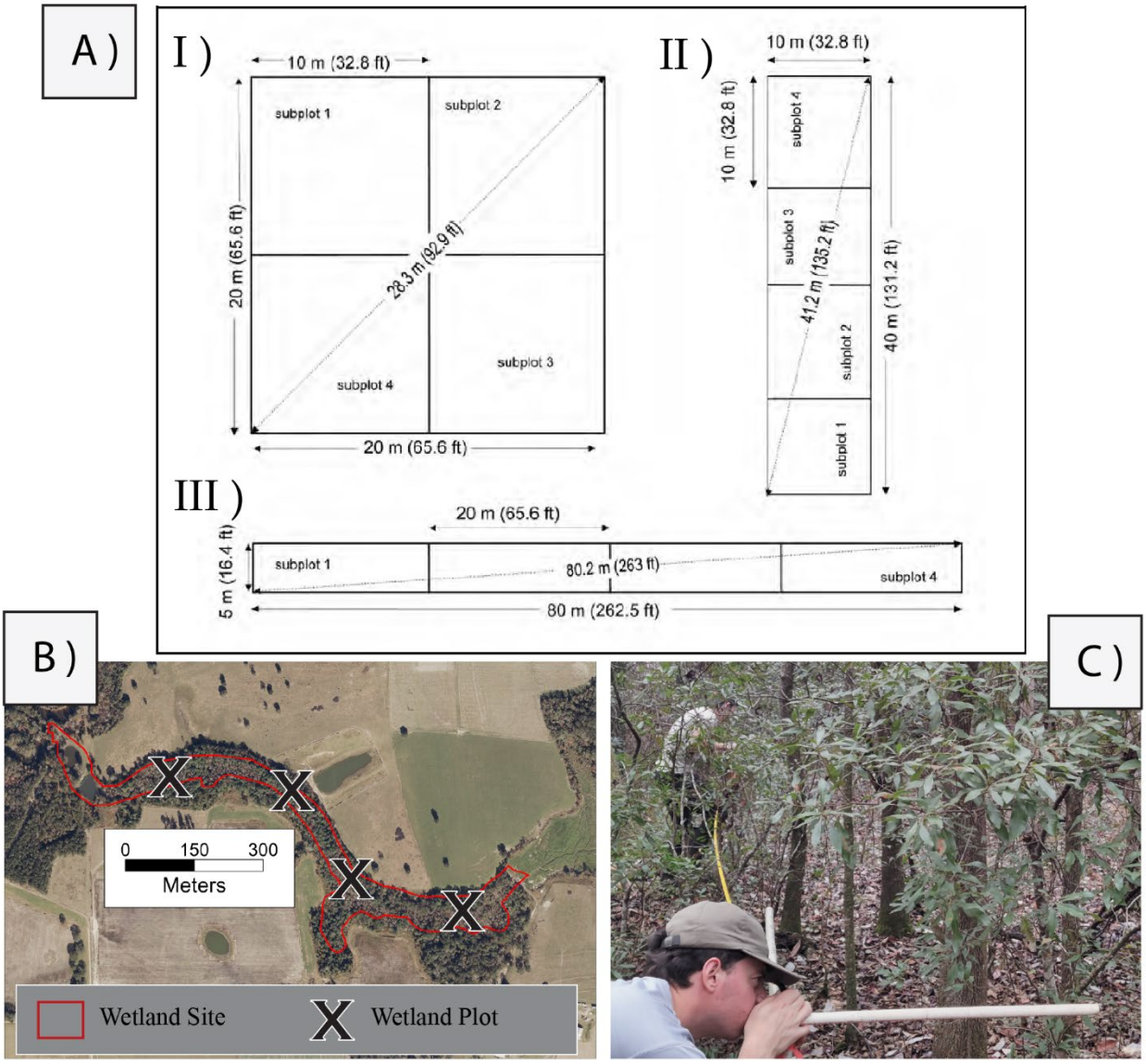

Figure 2.2. *A) Plot configurations described by Noble et al. (2007). I and III were used seldomly, as II was the most appropriate in terms of logistics. B) Four 100 m2 plots were spaced in relatively equal distances across the length of each wetland. C) Plots corners were measured at 90º angles from each previous corner until a 100 m2 square plot was established.*

2.4.2. Vegetative Measurements

At each plot, vegetation data were collected relative to forest stratum, so that canopy tree, shrub/sapling, and herbaceous vegetation strata were measured independently. The canopy tree

stratum was defined as all trees having a diameter at breast height (DBH; measured at 1.37 m above the base of the tree with diameter tape) ≥10 cm, having a portion of crown coverage that was not entirely overtopped. The shrub/sapling stratum was defined as all woody vegetation with a DBH <10 cm, and greater than 1 m in height. The ground vegetation stratum was defined as all nonwoody and herbaceous vegetation, but also included woody vegetation < 1 m in height.

Vegetative cover was determined by visually estimating canopy cover for each stratum individually, as a percentage of the total plot area. Cover estimates included those of canopies and the portions of canopies which were contained within plot boundaries stemming from vegetation that were rooted within the plot. Only the uppermost canopy of each stratum was used in this estimation, so that overtopped canopy cover was not included in the total estimate, and total estimates per strata were limited to values up to 100%. This overtopping rule did not apply between strata, so that the uppermost canopy of each stratum was measured independently of others, as a percentage of the total plot area.

Canopy tree diameters were measured for all trees that fit our criteria of the canopy tree stratum. Each stem was measured to the nearest tenth of an inch, using a diameter tape at DBH. Diameters were later converted to cm and averaged across all plots to determine mean canopy tree diameter per wetland site. Canopy tree stems for all plots were counted, summed, and recorded as stems per total surveyed area (0.04 ha, 400 m^2). This value was later transformed to stems/ha and reported as the representative stem density measurement for each wetland site.

2.4.3. Hydrologic and Soil Measurements

Per HGM protocol, drainage structures which altered reference hydrology were identified in wetlands wherever present. Wetland sites were considered hydrologically altered where flow obstruction (dams, berms, etc.) or concentration (ditches, culverts, etc.) structures were present within wetlands. Where present, the height of the structure was measured from the lowest point of the soil or channel surface to the highest point of the structure in cm. If evidence of additional water level depth was present, such as water marks on the bases of trees, the height of the watermarks extending above the uppermost height of the structure was added to the total measurement. Where structures were detectable with remote sensing methods (combination of NAIP imagery and DTM hillshades) but physically inaccessible, these sites were noted as hydrologically altered, but not estimated for height/water depth through remote sensing methods for consistency in measurements.

Detritus cover was used as a hydrologic proxy to indicate the prevalence of surface flows at a given site. Where detritus cover was low, surface flows were assumed to be more represented in wetland water budgets, and where detritus cover was high, groundwater was assumed to be more represented in wetland water budgets (Noble et al. 2007). Detritus was defined as leaf litter and other partially decayed or decaying plant materials which could be transported in the presence of surface flows. This was a somewhat subjective process as surface flows vary naturally between streams and wetlands. Recorded estimates for each plot were an average of all investigator's estimates (n=3). Detritus cover was measured similarly to vegetative cover, as a visually estimated percentage of the plot area. Detritus was estimated up to a maximum of 100% cover, based on the total areas of which it could potentially occupy (i.e., the areas occupied by tree bases, downed logs, etc., were not subtracted from this total cover value).

The areas of pools, channels, and ditches were considered in this estimate, as these areas would typically be occupied by detritus if surface flows were not present. Estimates were averaged for all plots to determine mean detritus cover per wetland site.

Munsell soil color charts were used for characterizing wetland soils through the interpretation of hue, value, and chroma that most closely resembles the color of a soil sample. Soil color which is low (<3) on the value scale (0-8) indicates high levels of soil organic matter content, while soil color which is low (<2) on the chroma scale (0-8) indicates the dissolution of Fe and Mn oxides due to anaerobic conditions (Mitsch and Gosselink 2015; Soil Science Division Staff 2017). To assess headwater wetland soils, each plot was further subdivided into four 25 m^2 sections from which one soil core was collected from the center of each subplot. Samples were cored to depths of 15.25 cm below the soil surface, where soil conditions were expected to indicate hydric soil status via shallow water tables (Noble et al. 2007). Two investigators rated each soil core for Munsell chroma and value. Ratings which could not be agreed upon were averaged between each investigator's estimate. Recorded estimates were averaged for all cores to determine mean Munsell soil chroma (n = 16) and value (n = 16) ratings per wetland site.

2.5. Watershed Delineations & LULC classification

2.5.1. Watershed Delineation

ArcSWAT is an ESRI extension for use in ArcGIS programs and is commonly used for watershed modeling of various scopes, and additionally contains a simplistic watershed delineator interface (Aloui et al. 2023). DTMs with spatial resolutions of 5m were used in

conjunction with the ArcGIS extension, ArcSWAT (version 2012.10_5.24) for ArcGIS Desktop version 10.5.1 to delineate headwater catchments. NHD streamlines were additionally brought into the ArcSWAT interface as user-specified stream networks from which to build flow direction and accumulation models. NHD streamlines were used in most cases where streams were mapped and accurate. In cases of unmapped streams and inaccurate stream locations, hand-digitized streamlines were used, based on image interpretation of NWI, topographic maps, aerial imagery, and DTM hill shade rasters. Resulting flow direction and accumulation models were used to model stream networks, stream outlets, and catchment boundaries. The outlets of headwater catchments were identified as the confluence of the headwater wetland's flow path or stream with any other stream. Outlet selection was guided by agreement with NHD streams in most cases, and image interpretation for unmapped streams and flow paths where NHD was not in agreeance with aerial imagery. Watersheds were exported as rasters and converted to polygon features in ArcGIS Pro for use in further analyses and data transformations.

Methods described for delineating boundaries thus far represent existing drainage conditions. Per HGM protocol, an additional step was made to assess whether landscape modifications such as berms, roads, dams, and ditches had altered watershed area. Historic watershed boundaries were delineated where evidence of landscape modifications was present in aerial imagery, DTM hillshade rasters, historical topographic maps, and NHDplusHR datasets. Where present, similar steps to those used for existing watershed delineations were used with modified NHDplusHR streamlines that reflected unmodified flow paths. Differences in watershed area between historic and modified watersheds were reported as percent change in drainage area. Historic watersheds are standalone products, specific to the HGM approach. Only

existing watershed boundaries were used to determine wetland boundaries, mean watershed area and slope, LULC cover, and subsequent PCA analysis methods used in the following sections.

2.5.2. Wetland and Initial Contributing Area Delineation

NWI wetland boundaries within ArcSWAT delineated watersheds were used as wetland boundaries in most cases. In cases of wetlands that were not mapped by NWI, wetland boundaries were hand-digitized based on image interpretation of aerial imagery, DTM hillshade rasters, topographic maps, and NHD datasets. The upland areas which drain to wetland boundaries (initial contributing area, ICA) were designated as the difference between watershed and wetland boundaries (Fig. 2.3). This consideration was made to better relate LULC composition in upland areas to environmental measures within wetlands.

2.5.3. Watershed Area, Slope, and LULC Classification

Fifteen LULC classes were present throughout the study area and in selected Mississippi sites for all NLCD datasets. For the purposes of this study, all NLCD classes were reclassified to our four class schemata: open water, urban, forest, and agriculture. Five NLCD classes (Deciduous Forest, Evergreen Forest, Mixed Forest, Shrub/Scrub, Woody Wetlands) representing woody vegetation were combined into a single forest class. Four NLCD classes (Developed: Open Space, Low Intensity, Medium Intensity, High Intensity) representing developed areas were combined into a single urban class, and two NLCD classes (Pasture/Hay, Cultivated Crops) were indicative of agricultural uses and were combined into a single agriculture class. The NLCD classes, emergent wetlands and open water were combined into a

single open water class, as emergent wetlands were most associated with open water conditions in agricultural and stormwater ponds for all watersheds. Barren land was considered most similar to agriculture in terms of surface runoff response, while true grasslands were uncommon in all watersheds and usually the result of misclassified pasturelands by NLCD. Barren land and grasslands were thus reclassified as agriculture.

Mean slope and area metrics were derived from ArcSWAT delineated watersheds in ArcGIS and were additionally calculated for ICAs and wetlands. Percent cover of each LULC class was first determined on a watershed basis in ArcGIS to characterize LULC ratios alongside headwater wetland coverage (Fig. 2.3). LULC ratios within ICAs were then determined, representing the sum of LULC cover in the watershed area without wetland coverage. These proportions were used to generate principal components (Comps.) for use in linear regression as predictor variables (see below), though open water was a negligible proportion in all watersheds and was omitted from the analytical process (Fig. 2.3).

Cover (%) per watershed

		Mean	Min	Max	SE
Headwater Wetland		7	0.9	20.5	1
Initial Contributing Area		93	79.5	99.1	1
LULC	Open Water	0.6	0	5.5	0.1
	Urban	21.8	0	91.6	2.7
	Forest	42.3	1.4	93	3.2
	Agriculture	28.3	0	83	3.2

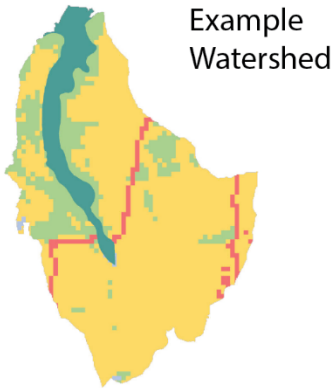

Cover (%) per Initial Contributing Area

LULC	Mean	Min	Max	SE
Open Water	0.6	0	5.9	0.1
Urban	23.5	0	98.5	3
Forest	45.5	1.5	100	3.4
Agriculture	30.4	0	89.3	3.4

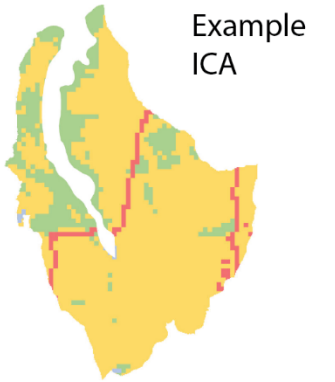

Resulting Principal Components and PCA Loadings

	Comp. 1	Comp. 2	Comp. 3
Proportion of variance in LULC explained by each component (%)	59.63	40.35	0.02

PCA Loadings	Comp.1	Comp. 2	Comp. 3
Urban	NA	0.82	0.57
Forest	0.70	-0.41	0.58
Agriculture	-0.71	-0.40	0.58

Figure 2.3. *Mean, minimum, maximum, and standard errors for LULC cover per total watersheds and initial contributing areas for all wetland sites. LULC per initial contributing areas were used in principal component analysis to build components that represent land use gradients. Comp. 1 represents an agricultural to forested gradient within rural settings, comp. 2 represents a rural to urban gradient, and comp. 3 represents a mixed land use scenario. Comp. 3 explained an exceptionally small amount of variance present in LULC composition for all sites and was omitted from statistical analysis.*

2.6. HGM Functional Assessments

While actual data from wetland measurements were used to statistically relate to watershed LULC, these data were also used to calculate variable index and functional capacity scores per the HGM approach (Noble et al. 2007). Consistent with HGM protocols, additional landscape/watershed metrics were generated in this process with ArcSWAT delineated watersheds, soil series map units, and NLCD datasets in ArcGIS Pro. Variable index scores which were calculated from additional metrics (n = 3) include change in catchment size, upland land use, and habitat connections. Changes in catchment size were calculated as the percent increase/decrease from historic to present watershed area. Upland land use was determined by calculating a weighted average of all runoff curve number values in each wetlands ICA using combined NLCD and WSS hydrologic group map units. Habitat connections were calculated as the percentage of each wetlands perimeter that was connected to suitable habitat, represented by NLCD data. Variable index scores which were calculated from field measurements (i.e., average canopy tree diameter, canopy tree density, ground vegetation cover, sapling/shrub cover, vegetation composition and diversity, soil detritus cover, surface soil organic matter content, and hydrologic alterations).

Per HGM protocol, values for all variable measurements were designated an index score (0–1) using HGM reference data tables that can be used to calculate functional capacity index scores. The compatibility of variable index scores reported in 2003-04 and 2010 datasets were questionable at times, occasionally differing from respective scores of associated measurements. Furthermore, some scores were reported with no measurement, which prevented clear interpretations for variables that could equate to scores < 1 in multiple directions (i.e., canopy tree density > 425 or < 250 stems/ha). Due to these concerns about the application of HGM and

calculations used between the datasets (2003-04, 2010, and 2022-23), we did not use variable and functional capacity index scores to statistically relate to watershed LULC and instead opted to use the field measurements from each period. However, for informational purposes, the results of HGM variable index scores for the 2022-23 dataset are provided in Appendix 1.

2.7. Statistical Analysis

2.7.1. Principal Component Analysis

To account for inherent collinearity associated with ratios of LULC cover as predictor variables in linear regression (King et al. 2005), we created independent variables using LULC composition for all watersheds through principal component analysis (PCA). Principal components that explained the maximum amount of variance between all classes were generated with the princomp function in R statistical software (version 2023.09.01). Three principal components were identified from LULC cover in all ICAs, with the first explaining 59.63% of variance in LULC ratios, 40.35% by the second, and 0.02% by the third (Fig. 2.3).

PCA loadings characterize LULC classes as coefficients, relative to the linear combination of all data which created the component. The absence of a loading for a particular class indicates that it did not contribute to the variance explained by the component, while positive loadings indicate class presence as having contributed to the component, and negative loadings indicate class absence as having contributed to the component. The relative magnitude of each loading is thus how much class presence or absence contributed to the component. Loadings for PCA Comp. 1 were: urban = NA, forest = 0.70, agriculture = - 0.71. The combined weights and directions of Comp. 1 loadings characterize it as a forest-agriculture gradient in rural

settings. PCA Comp. 2 is characterized as an urban-rural gradient, with loadings: urban = 0.82, forest = - .04, agriculture = - 0.40. Comp. 3 represents a mixed land use scenario with loadings: urban = 0.57, forest = 0.58, agriculture = 0.58. Comp. 3 did not explain a considerable amount of variation in LULC cover, nor did it accurately represent LULC composition in any watersheds. Additionally, it could not be used as an interpretable land use gradient from which to attribute the effects of any LULC class on wetland conditions and was omitted from our results.

Loading scores were then generated for each wetland's ICA, representing how closely LULC composition in a given ICA resembled either Comp. 1 or Comp. 2. Loading score interpretations are similar to PCA loadings, whereby positive values indicate similarity to the component, negative values indicate dissimilarity with the component, and the degree of magnitude indicates the level of similarity or dissimilarity. While PCA loadings are constrained to values between -1 and 1, loading scores are relative to the range of a given component which were 130.3 for Comp. 1 and 121.4 for Comp. 2. Each ICA's loading score for a given component was thus independent of the other, so that two datasets of loading scores (Comp. 1, Comp. 2) were created for independent testing in linear regression.

2.7.2. Linear Regression Models

To assess the relationship between LULC cover in headwater catchments and environmental measures in headwater wetlands, simple linear regression models were constructed in R statistical software, using the lm function. Field measurements included in separate linear regression models as dependent variables were 1) average canopy tree diameter, 2) canopy tree density, 3) canopy tree cover, 4) shrub/sapling cover, 5) ground vegetation cover,

6) detritus cover, 7) soil Munsell chroma, and 8) soil Munsell value. Field measurements were modeled as a function of ICA loading scores for both Comp. 1 and Comp. 2, resulting in two models for each response variable and a total of 16 linear regression models. Due to inconsistencies in data collection methods between studies, sample sizes for canopy tree cover (n = 44), shrub/sapling cover (n = 61), herbaceous/ground vegetation cover (n = 55), and soil chroma (n = 63) differed from those in all other models (n=74). To further elucidate LULC patterns on the distribution of wetland conditions, scatterplots with significant linear regression ($p < 0.05$) were indicated and each plot in the scatterplot was identified by relative watershed forest cover patterns based on three groups: ≥85% forest cover, 16-84% forest cover, or ≤15% forest cover.

3. Results

3.1. Physical Characteristics of Watersheds and Wetlands

Where landscape modifications such as berms, dams, roads, and drainage ditches occurred near watershed boundaries, watershed area was noticeably affected. Two sites in the 2003-04 dataset were indicated as modified from historic watershed areas but were not noted for direction of change. These are noted towards total watersheds that were modified from their historical extents (n = 28) but are omitted from subsequent statistical summaries. Of the 72 watersheds in the remaining dataset, 13 experienced reductions and 13 experienced expansions in area from their historic extents. Mean percent change from historic watershed area was an increased 7.5 ± 4.5%.

The maximum watershed area (1566.5 ha) was observed in a headwater catchment with extensive drainage from adjacent catchments through agricultural ditches, representing a 31.8% increase in watershed area from its historic watershed area. The minimum watershed area observed (1.2 ha) occurred in an especially low lying area, where a road may have disconnected it from former contributing areas, though percent change in watershed area could not be effectively determined. Mean watershed area was 161.3 ± 23.9 ha and ICAs represented 93.0 ± 0.1% of this area (Table 2.1), thus having a mean area of 152.9 ± 23.4 ha. Mean slope values for both watersheds and ICAs were 4.6 ± 0.3 %, while mean slope values in wetlands were 5.5 ± 0.4%. On average, wetlands represented the remaining 7.0 ± 0.1% of headwater catchment area, with a mean area of 8.4 ± 1 ha (Table 2.1).

Table 2.1. *Slope and Area metrics for total watersheds, initial contributing areas, and wetlands. Ranges between wetland and watershed areas were considerably high, and often the result of hydrologic alterations that modified drainage area.*

	Area (ha)				Slope (%)			
	Mean	**Min**	**Max**	**SE**	**Mean**	**Min**	**Max**	**SE**
Watershed	161.3	1.2	1566.5	23.9	4.6	1.5	9.6	0.3
Initial Contibuting Area	152.9	1.0	1539.5	23.4	4.6	1.4	10.0	0.3
Headwater Wetland	8.4	0.2	53.3	1.0	5.5	1.3	19.0	0.4

Percent cover of each land class was first determined on a watershed basis to characterize proportions of LULC alongside headwater wetland coverage within a typical headwater catchment. Open water, urban, forested, agricultural, and headwater wetland classes had mean cover values of respectively, 0.6 ± 0.1%, 21.8 ± 2.7%, 42.3 ± 3.2%, 28.3 ± 3.2%, and 7 ± 1%. When only accounting for LULC cover in ICAs, these were 0.06 ± 0.1%, 23.5 ± 3%, 45.5 ± 3.4%, 30.4 ± 3.4% for open water, urban, forested, and agricultural classes, respectively (Fig.

2.3). Based on these data, 16.2% of sites had watershed forest cover >85%, 70.3% of sites had forest cover of 15-84%, and 13.5% had forest cover <15%.

3.2. Wetland Hydrology and Soils

Structures which altered reference wetland hydrology were identified across a variety of LULC compositions in headwater catchments. Common flow obstruction structures encountered were forest roads, small culverts, and low head dams. Recent and past beaver activity was noted in several wetland sites, though intact dams were never observed. Surface water accumulation was noted upslope of flow obstruction structures in nearly all cases. Flow concentration and/or channelization was often observed on the downflow side of these structures where culverts were present. Hydrologically altered wetlands via flow concentration structures were the result of agricultural or stormwater ditches in all cases. Characterizing hydrologic alterations across all sites presented a challenge, as these measurements in 2003-04 and 2010 data repositories were inconsistently reported and occasionally unreliable. Measurements were inconsistent in our own field surveys, as many maximum depths were rarely recorded over 60 cm, and some hydrologic alterations were identified through aerial imagery and DTMs. Thus, our results are limited to the 2022-23 dataset as total sites which were hydrologically altered. These were 23 of the 42 surveyed sites, with nine attributed to flow obstruction structures and 14 to flow concentration structures.

Across all sites, detritus cover ranged from 0-100%, with a mean coverage of 68.3 ± 2.9% (Table 2.2) and lacked significant relationships with either component (Figs. 2.4 and 2.5). Mean detritus cover in sites with ≤15% forest cover was 68.3%, and 78.6% in sites with ≥ 85%

forest cover. Soil chroma and value had significant and positive relationships with Comp. 2, with respective mean values of 2.1 ± 0.1 ($p = 0.012$) and 3.2 ± 0.1 ($p = 0.11$) (Fig. 2.5). While statistically significant, these relationships were weakly correlated, with an r^2 of 0.098 and 0.11 for soil chroma and value, respectively. These trends indicate dewatering and reduced organic matter content in wetland soils as LULC gradients shift from forested to agricultural, and from rural to urban land uses. However, weak correlations coefficients suggest that a considerable amount of variance in soil measurements are not well explained by LULC alone, and that unaccounted variables may influence this relationship. In headwater catchments with ≥ 85% forest cover, mean wetland soil value and chroma were respectively 3.04 and 1.29, and 3.14 and 1.95 for headwater catchments with ≤15% forest cover (Table 2.3). Mean wetland soil chroma in both groups reflect hydric soils (<2) (Soil Science Division Staff 2017), while mean wetland soil values also reflect highly functioning soils (<3.5) in terms of organic content that equate to variable index scores of 0.8 (Noble et al. 2007).

Table 2.2. *Summary statistics for field measurements and linear relationships with principal components.*

Field Measurement	Min	Max	Mean	SE	Comp. 1		Comp. 2	
					P	R^2	P	R^2
Canopy Tree Diameter (cm)	15.49	99.06	43.88	2.33	0.20	0.023	0.96	< 0.01
Canopy Tree Density (stems/ha)	200.00	1750.00	774.66	41.32	0.30	0.015	0.86	< 0.01
Canopy Tree Cover (%)	25.00	88.75	59.34	2.34	0.11	0.059	0.53	< 0.01
Shrub/Sapling Cover (%)	2.50	78.75	34.81	2.46	**< 0.01**	0.14	0.068	0.055
Ground Vegetation Cover (%)	0.75	81.25	27.77	3.07	0.18	0.033	**0.040**	0.077
Detritus Cover (%)	0.00	100.00	68.26	2.92	0.11	0.035	0.77	< 0.01
Munsell Soil Value (0-8)	2.00	5.33	3.23	0.09	0.45	< 0.01	**< 0.01**	0.11
Munsell Soil Chroma (0-8)	1.00	4.31	2.08	0.10	0.26	0.021	**0.012**	< 0.01

Table 2.3 *Summary statistics for field measurements in total wetland sites, as well as those with less than 15% forest cover and greater than 85% forest cover. Mean values between high and low forest cover subsets were generally similar, though maximum values were most noticeably dissimilar for shrub/sapling and ground vegetation cover, consistent with regression results.*

	All Sites (n = 74)			< 15% Forest Cover (n = 10)			> 85% Forest Cover (n = 12)		
Field Measurement	**Min**	**Max**	**Mean**	**Min**	**Max**	**Mean**	**Min**	**Max**	**Mean**
Canopy Tree Diameter (cm)	15.49	99.06	43.88	26.62	62.48	41.72	19.84	99.06	52.27
Canopy Tree Density (stems/ha)	200.00	1750.00	774.66	500.00	1250.00	830.00	250.00	975.00	545.83
Canopy Tree Cover (%)	25.00	88.75	59.34	46.25	51.25	47.97	54.00	59.50	57.17
Shrub/Sapling Cover (%)	2.50	78.75	34.81	28.75	78.75	46.41	2.50	48.50	15.59
Ground Vegetation Cover (%)	0.75	81.25	27.77	11.88	73.75	36.67	4.00	27.50	15.08
Detritus Cover (%)	0.00	100.00	68.26	34.25	100.00	68.30	0.00	100.00	78.56
Munsell Soil Value (0-8)	2.00	5.33	3.23	2.20	4.25	3.14	2.00	4.25	3.04
Munsell Soil Chroma (0-8)	1.00	4.31	2.08	1.00	3.25	1.95	1.00	1.69	1.29

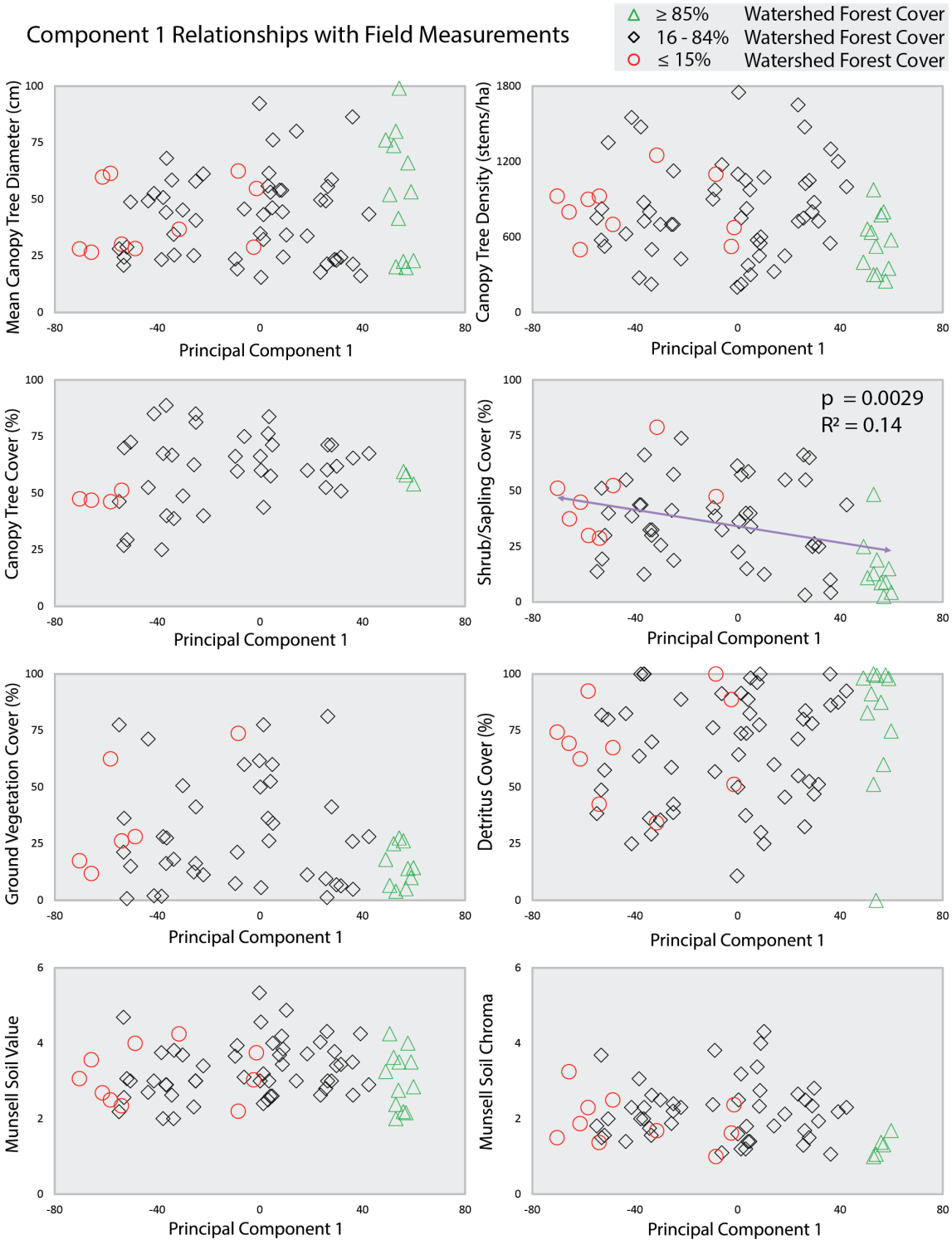

Figure 2.4. *Linear relationships between comp. 1 and field measurements were statistically insignificant in most case, other than shrub/sapling cover. Potential wedge distributions are noted, with increased range and variability as loading scores decrease. Data subsets further depict limited ranges in highly forested watersheds with increasing range and variability in mixed used and agricultural watersheds for canopy tree cover, shrub/sapling cover, ground vegetation cover, and soil Munsell chroma. The opposite is noted for canopy tree diameter, while detritus cover and Munsell soil value show relatively equal distributions across a land use gradient.*

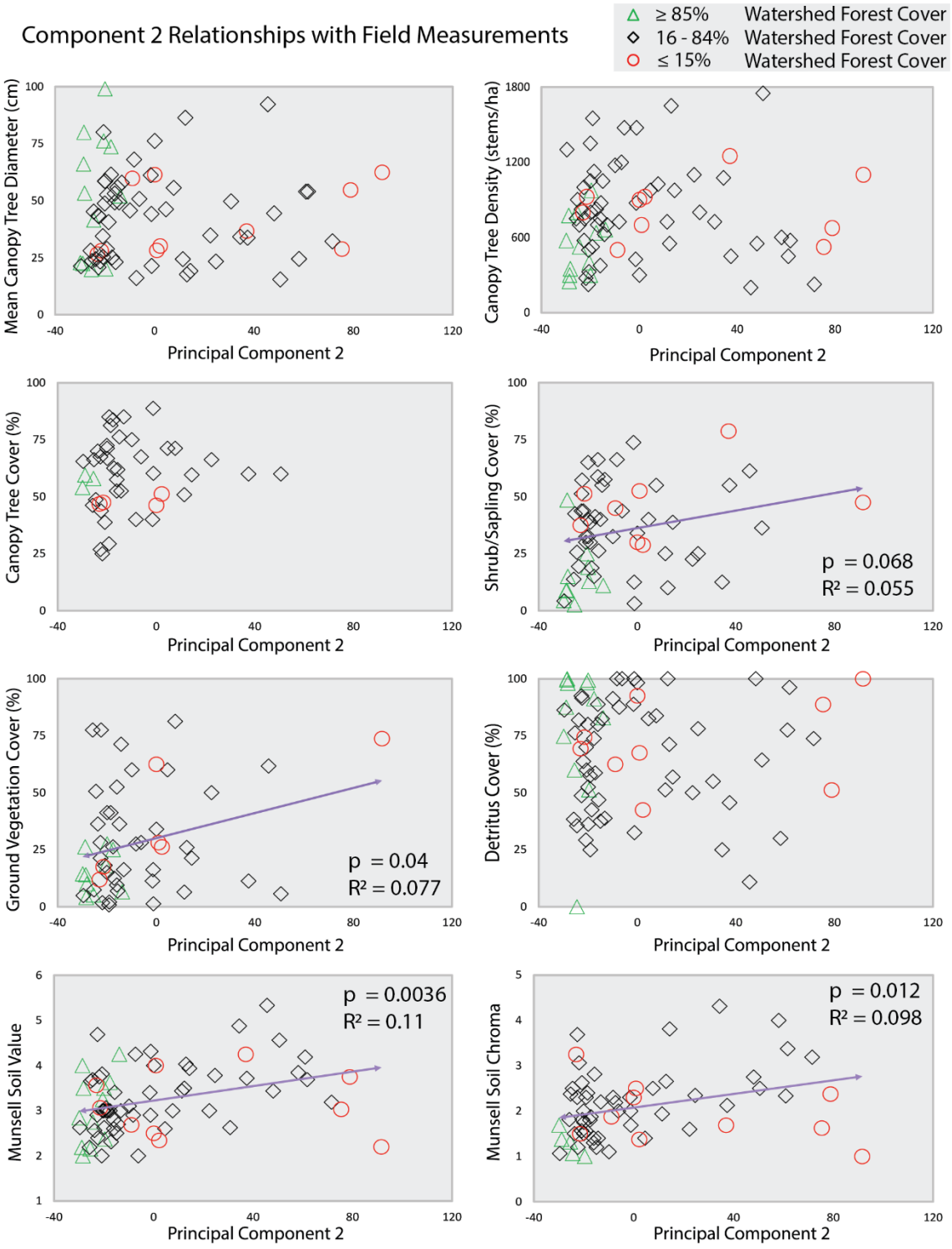

Figure 2.5. *All canopy tree measurements as well as detritus cover lacked significant relationships with Comp. 2. Relationships with all other variables showed varying degrees of statistical significance, though were weakly correlated in all cases. Potential wedge effects are less pronounced than those in comp. 1 regression plots, though variability appears to generally increase in rural watersheds.*

3.3. Wetland Forest Structure

A range of forest structure compositions were observed throughout headwater wetland sites (Table 2.2). Canopy tree strata were largely characterized by sweet bay (*M. virginiana*) dominance, or *M. virginiana* codominance with swamp tupelo (*N. biflora*). Rarely dominant but commonly encountered species included slash pine (*E. elliottii*), tulip poplar (*L. tulipifera*), and water oak (*Q. nigra*). Chinese tallow (*T. sebifera*) occurred seldomly, but occasionally in high densities. Shrub/sapling strata were most often represented by *M. Virginia* and *N. bifolia* regeneration, though were far less dominant in this stratum than in forest canopies. Other commonly occurring species were *L. tulipifera*, *T. sebifera*, red maple (*A. rubrum*), southern bayberry (*M. cerifera*), yaupon (*I. vomitoria*), red bay (*P. borbonia*), and Chinese privet (*L. sinense*). *L. sinense* occurred in variable densities, and sometimes as dense thickets. Although camphor tree (*C. officinarum*) was repeatedly encountered, it was most often a subcanopy tree and thus largely unrepresented in field data. Ground vegetation species varied considerably between sites but were mostly characterized by the presence of switch cane (*A. tecta*), cinnamon fern (*O. cinnamomea*), netted chain fern (*W. areolate*), and various sedges, grasses, and rushes. Japanese stilt grass (*M. vimineum*) and oriental ladies' thumb (*P. longiseta*) were notable invasive exotic species that occasionally dominated small wetland areas.

Mean canopy tree cover, shrub/sapling cover, and ground vegetation cover were respectively 59.3 ± 2.3%, 34.8 ± 2.5%, and 27.8 ± 3.1% (Table 2.2). Shrub/sapling vegetative cover had a significant and negative relationship with Comp. 1 ($p = 0.0029$), which suggests that shrub/sapling cover in headwater wetlands of rural watersheds are less dense where forests are most representative of surrounding LULC and increase with greater proportions of surrounding agriculture (Fig. 2.4). Shrub/sapling cover had a non-significant but positive relationship with

Comp. 2 (*p = 0.068*), which could suggest an increased abundance of shrub/sapling coverage in headwater wetlands of urbanized watersheds. A significant and positive relationship was also found between ground vegetation cover and Comp. 2 (*p = 0.04*) that suggests increased coverage in headwater wetlands of urban watersheds relative to rural ones (Fig. 2.5). These findings also reflect trends observed between Comp. 1 and soil measurements, where weak correlation coefficients between Comp. 1 and shrub/sapling cover ($r^2 = 0.14$), and between Comp. 2 and shrub/sapling cover ($r^2 = 0.055$) / ground vegetation cover ($r^2 = 0.077$) show a considerable amount of unexplained variance by LULC alone. These findings further suggest that additional variables may need to be considered for our purposes.

In highly forested catchments (≥85%), mean canopy tree cover, shrub/sapling cover, and ground vegetation cover were respectively 57.2%, 15.6%, and 15.1% (Table 2.3). These differed from those in catchments containing ≤ 15% forest cover, with respective mean values of canopy tree, shrub/sapling, and ground vegetation cover of 48.0%, 46.4%, and 36.7% (Table 2.3). These findings collectively indicate that surrounding urban and agricultural LULC are associated with denser shrub/sapling and ground vegetation layers in headwater wetlands. Mean canopy tree cover may have had an insufficient sample size (n = 44) and did not exhibit significant relationships with any components. Mean canopy tree diameters were 43.9 ± 2.3 cm, and mean canopy tree densities were 774.7 ± 41.3 stems/ha (Table 2.2). Considerable ranges were observed for canopy tree diameter (16 – 99 cm) and density (200 – 1750 stems/ha) and may have reflected various stages of succession and disturbance. No significant relationships were observed for either metric with any principal components. Field observations suggest that disturbances, such as hydrologic alterations and forest management practices, could have impacted this relationship.

4. Discussion

Our analyses showed that while there were some wetland conditions that were related to LULC gradients established in our study, most significant relationships contained substantial variability (i.e., low r^2 values). While Comp. 1 (forest – agriculture gradient) held few statistically significant relationships with field measurements, a 'wedge-shaped' distribution of the data was evident in numerous scatter plots. These distributions may represent potential ecological limits, whereby measurements in highly forested watersheds (i.e., >85% forest cover) occur in limited, predictable ranges, while measurements in non-forested watersheds vary significantly outside of this range. See Knight et al. (2014) for an example of wedge-shaped distributions of fish species richness in urban streams. Forested wetlands provide an example of this phenomenon through functional responses of forest structure to disturbance. Where reductions in canopy tree cover result in greater photosynthetic opportunities for midstory species, such disturbances result in increased shrub and sapling coverage. Though canopy gaps bolster light availability in understories, ground vegetation expansion is limited by canopies in both over- and midstories. Ground vegetation cover thus exists within a limited range in forested settings and may be additionally limited in such cases as a response variable to LULC changes.

Wedge shaped distributions may also provide insights on ecological responses in non-reference conditions through distributions of ecological indicator values, as expanded ranges could potentially indicate new ecological limits under such conditions. In relation to Comp. 1, field measurements observed in wetland sites of highly forested catchments were generally clustered in relatively small ranges, while the range in sites with less forested cover were typically larger and more variable. Shrub and sapling coverage was clustered between 0 – 25% in highly forested catchments (≥85%) and 25 – 50% in highly non-forested catchments (≤15%).

Canopy tree coverage in highly forested and non-forested wetlands were closely aligned in range. However, sites between 16-84% forest cover that were aligned more closely to agriculture on the Comp. 1 spectrum, showed a much wider spread than those aligned to forested LULC (Fig. 2.4). Maximum values generally increased with decreasing Comp. 1 loading scores and may emphasize an increased threshold for shrub coverage along a forested-agricultural gradient.

Canopy tree diameters in highly forested sites were especially variable, with a range of 70.2 cm compared to 35.9 cm for those in highly non-forested catchments. These data suggest that there are other factors which influence canopy tree sizes in forested settings, such as altered hydrology. Stunted tree growth may be a result of long-term surface water retention in forested catchments with altered hydrology (Halabisky et al. 2023), while reference hydrology in unmodified landscapes support large-diameter trees in mature forests. Some sites may be densely populated with small to medium sized canopy trees following disturbance, regardless of LULC composition. Disturbances in highly forested watersheds may be more frequent than we assumed, possibly through daylighting of wetland forests by adjacent roads and harvests. Forestry-related best management practices in Alabama do not require extended buffers around ephemeral streams for timber harvest, and many sites in forested watersheds were noted for young stands which surrounded them.

Anecdotal evidence may additionally support this possibility, as field observations in wetlands of highly forested catchments suggest that long term ponding from flow obstructions may act as a significant disturbance on community structure and composition. Noticeable shifts in community composition and tree density often occurred along a downflow gradient, as ponding depths increased near wetland outlets which were obstructed by dams or roads (Fig. 2.7). *N. biflora* was noticeably more representative of forest canopies in these areas, though it is

less indicative of headwater wetlands of the Eastern Gulf coastal plain than *M. virginiana* (Rheinhardt et al. 2013). *N. biflora* performs well in periodically and continuously ponded conditions, whereas *M. virginiana* is more often a dominant canopy species, and preferential to infrequent ponding or flooding. Characteristic species of associated with reference hydrology, such as *M. virginiana* and *P. borbonia*, were often observed in greater abundance upslope of these affected areas.

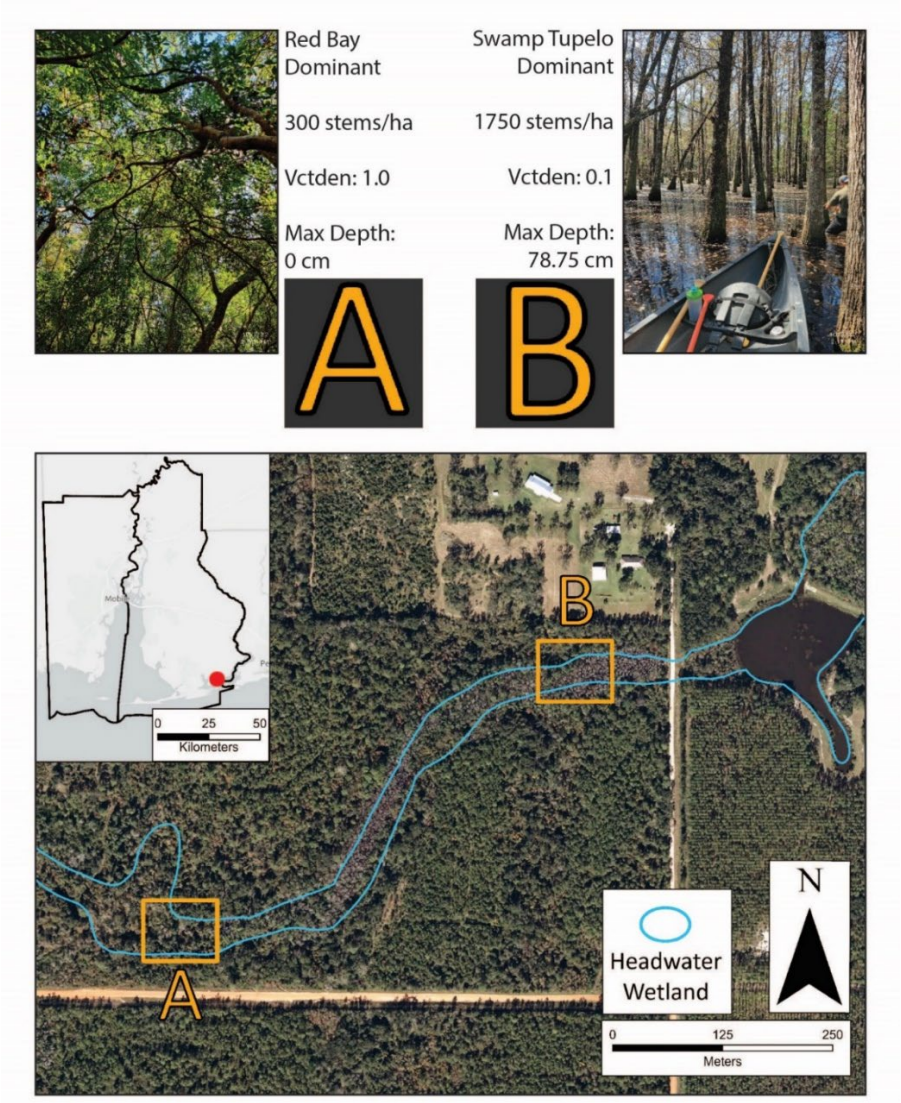

Figure 2.6. *Shifts in community composition and structure were observed anecdotally, between areas which exhibited reference hydrologic conditions and areas which were hydrologically altered. Shrub/sapling strata were noticeably diminished where longstanding water was present, as were species which are most associated with infrequent flooding.*

The lack of predictive relationships between canopy strata and LULC may be partially explained by the length of time in which LULC have been representative of the observed catchments, the degree or presence of hydrologic alterations present, and land use legacies. Wetland degradation may have occurred in currently forested watersheds that were in agricultural production until recently. Our use of LULC at a static point in time is thus limited to the perspective at that time. Furthermore, canopy tree strata are expected to respond slowly to LULC change if advanced regeneration is adequate prior to LULC changes. Shrub/sapling and ground vegetation cover are likely better indicators of recent forest structure responses to LULC changes, which were both significantly related to Comp. 1. Barksdale and Anderson (2014) found that exotic shrub cover was significantly related to agricultural LULC, which represents the 2010 dataset. Exotic grasses and shrubs were observed in high densities of highly agricultural watersheds in the 2022-23 dataset, though this is anecdotal evidence as measurements were not taken to identify the coverage of native vs exotic plants. Field observations along with findings from this previous study suggest that additional research is needed to clarify possible links between invasive species, altered forest structures, and LULC change.

Although soil Munsell color metrics showed statistically significant relationships with Comp. 2, correlation coefficients were nominal for both variables. This may have been the result of various drainage and ponding scenarios in headwater wetlands across all LULC compositions. Within wetlands, various flow patterns were observed between areas of reference wetland hydrology and areas which were noticeably affected by hydrologic alterations, such as ponding above flow obstruction structures and channelized flows below the path of culverts. Wetland soils in watersheds of predominantly agricultural and urban LULC may have experienced greater rates of gleization than expected due to representation of ponded areas above flow obstructions

in our sampling approach. These areas often presented sampling challenges, especially in the case of dams, where open water was present for the remainder of the downflow length of the wetland above the watershed outlet. Thus, Munsell chroma ratings may have represented headwater slope wetlands in the uppermost portions of surveyed areas, while lower portions more closely represented depressional wetlands.

Soil dewatering was expected in wetlands containing ditches and highly incised stream channels, as these features are associated with water table reductions in riparian areas and are good indicators of 'riparian hydrologic drought' in the coastal plain region (Hardison et al. 2009). While urban and agricultural LULC are associated with soil dewatering, accelerated decomposition rates, and elevated transport of organic and mineral substrate through headwater wetlands (Wardrop and Brooks 1998; Walsh et al. 2005), LULC was not attributed to a significant amount of explained variance in soil and hydrology related measurements. Although wetland soils are characterized by Munsell chroma < 2, roughly half of all sites were above this value and were neither highly forested nor highly non-forested. Variation that could not be well explained by principal components in both soil and detritus metrics were likely a result of hydrologic alterations present throughout all represented LULC compositions.

Factors that may have further contributed to unexplained variance include length of time in which LULC have been present on the landscape, ecological disturbances, physiographic variation, and land use legacy effects. While the effects of urban LULC on runoff rates, water table depths, and groundwater storage capacities are well documented (Groffman et al. 2002; Hardison et al. 2009), our approach utilized NLCD as an initial and simplistic predictor. NLCD is potentially too coarse (30-m) to accurately depict these effects at the headwater scale, and our simplified reclassification scheme potentially overrepresented discreet urban features on the

landscape, with varying degrees of imperviousness. A wider gradient of LULC classes is likely needed to demonstrate these effects, such as the full range of NLCD urban classes (open space, low/medium/high intensity) or total impervious area (TIA).

Additionally, the spatial configurations of LULC and flow control structures within watersheds are important determinants of hydroperiod, sedimentation, and material transport that determine functional traits within headwater wetlands (Rheinhardt et al. 1999; King et al. 2005; Schiff and Benoit 2007). Our efforts to characterize LULC impacts on wetland conditions were largely based on the assumption that each class would demonstrate a clear relationship with surface runoff responses. These responses can be complex within watersheds, as wetlands receive variable amounts of drainage contributions from each sub-catchment, with each differing in LULC composition, slope, flow accumulation, and flow concentration. While surveys aimed to represent wetlands in equal distances relative to their lengths, the effects of individual sub-catchments may present themselves in different areas throughout the wetland. For instance, if an individual sub-catchment contains the majority of agricultural or urban land uses in a watershed, it's plausible that all other sub-catchments provide adequate groundwater seepage to maintain highly functioning hydrology.

5. Conclusion

The impact of any LULC class on wetland resources may not be equally detectable across areas with variable timespans in which those classes have been present. A lack of significant correlation between LULC and all field measurements may be attributable to this unaccounted variable, as agricultural LULC has been present throughout the region historically and urban LULC are largely new features on the landscape. Land use legacies may additionally contribute

to mixed results where forested and urban areas occupy former agricultural lands and vice versa. Furthermore, spatial configurations of LULC are complex and may not be best represented by NLCD alone. Landscape metrics could better explain high vs low impact areas where distances to wetlands and forested buffers are considered. Additionally, recent advancements in LULC datasets include spatial resolutions that may better represent minimum mapping units of headwater wetlands, such as 10 m products of the Coastal Change Analysis Program (CCAP). Upon exploring the use of NLCD as a simplistic predictor of headwater wetland conditions, we conclude that a considerable amount of variation is left unexplained. The addition of metrics that would better characterize hydrologic alterations present in headwater catchments, documentation of recent land use practices, and coupled hydrologic models that indicate drainage patterns independent of LULC would be highly valuable in future models. Strengths present in our model are demonstrated by ease of use, efficiency, and reproducibility in data collection efforts. Limitations of these rapid assessment methods may be bridged where additional data can support them.

6. Literature Cited

Aloui S, Mazzoni S, Elomri A, Aouissi J, Boufekane A, Zghibi A. 2023. A review of Soil and Water Assessment Tool (SWAT) studies of Mediterranean catchments: Applications, feasibility, and future directions. Journal of Environmental Management. 326: 116799. https://doi.org/10.1016/j.jenvman.2022.116799

Armstrong A, Stedman RC, Bishop JA, Sullivan PJ. 2012. What's a Stream Without Water? Disproportionality in Headwater Regions Impacting Water Quality. Environmental Management. 50(5): 849–860. https://doi.org/10.1007/s00267-012-9928-0

Avcioglu B, Anderson CJ, Kalin L. 2017. Evaluating the Slope-Area Method to Accurately Identify Stream Channel Heads in Three Physiographic Regions. Journal of the American Water Resources Association. 53(3): 562-575. https://doi.org/10.1111/1752-1688.12512

Barksdale FW and Anderson CJ. 2014. The influence of land use on forest structure, species composition, and soil conditions in headwater-slope wetlands of coastal Alabama, USA. International Journal of Biodiversity Science, Ecosystem Services & Management. 11(1): 61-70. https://doi.org/10.1080/21513732.2013.876449

Barksdale FW, Anderson CJ, Kalin L. 2014. The influence of watershed run-off on the hydrology, forest floor litter and soil carbon of headwater wetlands. Ecohydrology. 7(2): 803–814. https://doi.org/10.1002/eco.1404

Barnes BV, Zak DR, Denton SR, Spurr SH. 1997. Forest Ecology. 4th Edition. Hoboken, NJ. John Wiley & Sons, Inc.

Brinson MM. 1993. A Hydrogeomorphic Classification for Wetlands. U.S. Army Corps of Engineers, Waterways Experiment Station, Vicksburg, MS, USA. Technical Report WRP-DE-4, U.S. Army Engineer Waterways Experiment Station, Vicksburg, MS.

Colvin ARS, Sullivan SMP, Shirey PD, Colvin RW, Winemiller KO, Hughes RM, Fausch KD, Infanta DM, Olden JD, Bestgen KR, Danehy RJ, Eby L. 2019. Headwater streams and wetlands are critical for sustaining fish, fisheries, and ecosystem services. American Fisheries Society. 44(2): 49-108. https://doi.org/10.1002/fsh.10237

Dewitz J and U.S. Geological Survey. 2021. National Land Cover Database (NLCD) 2019 Products (ver. 2.0, June 2021): U.S. Geological Survey data release. https://doi.org/10.5066/P9KZCM54

Ebersole SE, Guthrie GM, VanDervoort DS. 2019. An update to the physiographic districts of Alabama: Alabama Geological Survey Open-File Report 1901, 20p + plate.

Foley JA, Defries R, Asner GP, Barford C, Bonan G, Carpenter SR, Chapin FS, Coe MT, Daily GC, Gibbs HK, Helkowski JH, Holloway T, Howard EA, Kucharik CJ, Monfreda C, Patz JA, Prentice IC, Ramankutty N, Snyder PK. 2005. Global consequences of land use. Science. 309(5734): 570-574. https://doi.org/10.1126/science.1111772

Gomi T, Sidle RC, Richardson JS. 2002. Understanding Processes and Downstream Linkages of Headwater Systems: Headwaters differ from downstream reaches by their close coupling to hillslope processes, more temporal and spatial variation, and their need for different means of protection from land use. BioScience. 52(10): 905–916. https://doi.org/10.1641/0006-3568(2002)052[0905:UPADLO]2.0.CO;2

Groffman PM, Boulware NJ, Zipperer WC, Pouyat RV, Band LE, Colosimo MF. 2002. Soil Nitrogen Cycle Processes in Urban Riparian Zones. Environmental Science & Technology. 36(21): 4547-4552. DOI: 10.1021/es020649z

Groffman P, Bain DJ, Band LE, Belt KT, Brush GS, Grove M, Pouyat R, Yesilonis I, Zipperer W. 2003. Down by the Riverside: Urban Riparian Ecology. Frontiers in Ecology and The Environment. 1(6): 315-321. http://dx.doi.org/10.2307/3868092

Halabisky M, Miller D, Stewart AJ, Yahnke A, Lorigan D, Brasel T, Moskal LM. 2023. The Wetland Intrinsic Potential tool: mapping wetland intrinsic potential through machine learning of multi-scale remote sensing proxies of wetland indicators. Hydrology and Earth System Sciences. 27(20): 3687–3699. https://doi.org/10.5194/hess-27-3687-2023

Hardison EC, O'Driscoll MA, DeLoatch JP, Howard RJ, Brinson MM. 2009. Urban Land Use, Channel Incision, and Water Table Decline Along Coastal Plain Streams, North Carolina. Journal of the American Water Resources Association. 45(4): 1032-1046. https://doi.org/10.1111/j.1752-1688.2009.00345.x

King RS, Baker ME, Whigham DF, Weller DE, Jordan TE, Kazyak PF, Hurd MK. 2005. Spatial Considerations for Linking Watershed Land Cover to Ecological Indicators in Streams. Ecological Applications. 15(1): 137-153. https://doi.org/10.1890/04-0481

Knight RR, Murphy JC, Wolfe WJ, Saylor CF, Wales AK. 2014. Ecological limit functions relating fish community response to hydrologic departures of the ecological flow regime in the Tennessee River basin, United States. Ecohydrology. 7(5): 1260–1280. https://doi.org/10.1002/eco.1460

Mitsch WJ and Gosselink JG. 2015. Wetlands. 5th Edition. Hoboken, NJ. John Wiley & Sons, Inc.

Monk CD. 1968. Successional and Environmental Relationships of the Forest Vegetation of North Central Florida. The American Midland Naturalist. 79(2): 441–57. https://doi.org/10.2307/2423190

Neary DG, Ice GG, Jackson CR. 2009. Linkages Between Forest Soils and Water Quality and Quantity. Forest Ecology and Management. 258(10): 2269-2281. https://doi.org/10.1016/j.foreco.2009.05.027

Noble CV, Wakeley JS, Robert TH, Henderson C. 2007. Regional Guidebook for Applying the Hydrogeomorphic Approach to Assessing the Functions of Headwater Slope Wetlands on the Mississippi and Alabama Coastal Plains. ERDC/EL TR-07-2, U.S. Army Corps of Engineers. Vicksburg, MS.

Noble CV, Murray EO, Klimas CV, Ainslie W. 2011. Regional Guidebook for Applying the Hydrogeomorphic Approach to Assessing the Functions of Headwater Slope Wetlands on the South Carolina Coastal Plain. ERDC/EL TR-11-11, U.S. Army Engineer Research and Development Center. Vicksburg, MS.

Ramesh R, Kalin L, Hantush M, Anderson CJ. 2020. Challenges Calibrating Hydrology for Groundwater-Fed Wetlands: a Headwater Wetland Case Study. Environmental Modeling & Assessment. 25(6): 355–371. https://doi.org/10.1007/s10666-019-09684-8

Rheinhardt RD, Rheinhardt MC, Brinson MM, Faser KE. 1999. Application of Reference Data for Assessing and Restoring Headwater Ecosystems. Restoration Ecology. 7(3): 241-251. https://doi.org/10.1046/j.1526-100X.1999.72017.x

Rheinhardt R, Wilder T, Williams H. 2013. Variation in Forest Canopy Composition of Riparian Networks from Headwaters to Large River Floodplains in the Southeast Coastal Plain, USA. Wetlands. 33(6): 1117–1126. https://doi.org/10.1007/s13157-013-0467-0

Schiff R and Benoit G. 2007. Effects of Impervious Cover at Multiple Spatial Scales on Coastal Watershed Streams. Journal of the American Water Resources Association. 43(3): 712-730. https://doi.org/10.1111/j.1752-1688.2007.00057.x

Soil Science Division Staff. 2017. Soil Survey Manual. Ditzler C, Scheffe K, Monger HD. USDA Handbook 18. Government Printing Office, Washington, D.C. https://www.nrcs.usda.gov/sites/default/files/2022-09/The-Soil-Survey-Manual.pdf

Soil Survey Staff. Natural Resources Conservation Service, United States Department of Agriculture. 2022. Web Soil Survey. Available online. Accessed [02/15/2022]. https://websoilsurvey.nrcs.usda.gov/app/

U.S. Census Bureau. 2021. County Population Totals: 2010-2020. (Baldwin and Mobile County, AL).

U.S. Census Bureau. 2022. County Population Totals: 2020-2021. (Baldwin and Mobile County, AL).

[NGCE] USDA/NRCS - National Geospatial Center of Excellence. 2022. LiDAR Elevation Dataset - Bare Earth Hillshade - 1 Meter. Baldwin County, AL Accessed [05/12/2022]. https://datagateway.nrcs.usda.gov/

[NGCE] USDA/NRCS - National Geospatial Center of Excellence. 2023. USDA-NAIP NRCS County Mosaic. Accessed [03/23/2023]. https://datagateway.nrcs.usda.gov/

U.S. Fish and Wildlife Service. 2022. National Wetlands Inventory - Version 2 - Surface Waters and Wetlands Inventory. Alabama. U.S. Department of the Interior, Fish and Wildlife Service, Washington, D.C. Available online. Accessed [02/15/2022]. https://www.fws.gov/program/national-wetlands-inventory/download-state-wetlands-data

U.S. Geological Survey. 2022$_a$. National Hydrography Dataset Plus High Resolution (NHDPlus HR) - USGS National Map Downloadable Data Collection. Available online. Accessed [04/23/2022]. https://apps.nationalmap.gov/downloader/

U.S. Geological Survey. 2022$_b$. Historical Topographic Maps 7.5 x 7.5 Minute Map Series. Available online. Accessed [04/23/2022]. https://ngmdb.usgs.gov/topoview/

U.S. Geological Survey. 2023. USGS 3D Elevation Program: 1 meter Digital Elevation Model. Accessed [03/23/2023]. https://apps.nationalmap.gov/downloader/

Walsh CJ, Roy AH, Feminella JW, Cottingham PD, Groffman PM, Morgan RP. 2005. The urban stream syndrome: current knowledge and the search for a cure. Journal of the North American Benthological Society. 24(3): 706-723. https://www.journals.uchicago.edu/doi/full/10.1899/04-028.1

Wardrop DH and Brooks RP. 1998. The Occurrence and Impact of Sedimentation in Central Pennsylvania Wetlands. Environmental Monitoring and Assessment. 51(1-2): 119–130. https://doi.org/10.1023/A:1005958429834

Zedler JB. 2003. Wetlands at your service: reducing impacts of agriculture at the watershed scale. Frontiers in Ecological Environments. 1(2): 65–72. https://doi.org/10.1890/1540-9295(2003)001[0065:WAYSRI]2.0.CO;2

Zedler JB and Kercher S. 2005. Wetland Resources: Status, Trends, Ecosystem Services, and Restorability. Annual Review of Environmental Resources. 30(1): 39-74. https://doi.org/10.1146/annurev.eg.30.102405.100001

Chapter III. Modeling Wetland Presence, Absence, and Extent in Coastal Alabama with Wetland Intrinsic Potential.

Abstract

Headwater wetlands along the northern Gulf of Mexico coast are a ubiquitous landscape feature but are difficult to map because of their transitional nature. Upwelling of groundwater through hillslope drainage exerts a strong control on slope wetland hydrology, where soils can remain saturated continuously via shallow water tables. These are important elements for regional drainage and there is a need for local and regional managers to better document their occurrence on the landscape. Due to various limitations on headwater wetland detection, we utilized the Wetland Intrinsic Potential (WIP) tool for its use of multi-scale topographic indices, hydrologic proxies, and random forest procedures that contribute to 'cryptic' wetland detection. Our resulting WIP model identified metrics which most accurately depicted the wetland-upland matrix within the Bushy Creek – Dyas Creek watershed, located near Bay Minette, Alabama. An initial model was trained and validated with an out of bag (OOB) accuracy assessment on a spatial subset of the watershed to predict wetland presence, absence, and extent. Our model resulted in an OOB accuracy rate of 96.0%, with wetland omission and commission errors of 7.0% and 2.5%, respectively. The model was then applied to the remaining spatial extent of the watershed for a secondary validation assessment. Overall accuracy for the secondary validation dataset was 92.3%, with wetland omission and commission errors of 14.0% and 4.5%, respectively. Early indications suggest the WIP tool reliably discerned wetlands from uplands, with an AUC of 0.98 and kappa coefficient of 0.83. Further analyses resulted in considerations for practitioners to address in model building, such as thresholds below 0.5 to better detect slope

wetlands. Wetland presence, absence, and extent maps shared 89.1% of agreement with National Wetland Inventory (NWI) classifications, and increased wetland area by as much as 8.7%. Our findings can be used to infer the applicability and limitations of this method for wetland mapping along the northern Gulf of Mexico and support future models which explore land use/cover and hydrogeomorphic relationships with wetlands.

1. Introduction

1.1. Wetland Mapping: Definitions and Conventional Techniques

Wetlands are critical components of the landscape because of the ecosystem services they provide, including water quality, flood attenuation and important habitats (MEAB 2005). Although many of these ecosystem services are well known, the extent to which they exist on the landscape is not always clear. Where disjunct landforms, geology, and areas of flow concentration result in distinct ecologic and hydrologic zones, delineating wetland boundaries can be fairly straightforward. This is not always the case though, as environmental gradients can be spatially variable. Gradual changes between uplands and wetlands can result in extended environmental gradients, so that some areas may fit the status of a wetland despite lacking strong contrasts with the surrounding upland (Stewart et al. 2024). These 'cryptic wetlands' can be difficult to map in order to support wetland inventories and to guide policies, such as the 'No Net Loss' executive order (U.S. EPA 2006). While these wetlands can still be delineated accurately through field reconnaissance, they present a challenge for remote wetland mapping.

In the United States, the National Wetland Inventory (NWI) is currently the most comprehensive inventory of mapped wetland extent, which among several objectives, serves as a

long term wetland monitoring program. Wetlands are not field delineated, but have been historically mapped using image interpretation methods with aerial imagery, soil surveys, topographic maps, etc. (FGDC 2009). NWI maps are largely snapshots of the imagery acquisition date used for photo interpretation, and mapped wetlands may not be reflected in the present day. Ideally, maps would be periodically updated to identify gains, losses, and trends in wetland areal coverage, but a lack of funds and manpower within the program have led to shortcomings for this purpose (U.S. EPA 2006). Thus, the NWI is generally a patchwork of mapping efforts over a 42-year time span, with many regions still reflecting wetland boundaries determined in the 1970s and 1980s. Additionally, the sole method of image interpretation for wetland mapping is subject to human error and underestimates discreet, 'cryptic' wetlands, that are difficult to detect (Tiner 1990).

1.2. Wetland Mapping: Remote Sensing & Machine Learning

A significant drawback of image interpretation as a sole method for wetland mapping is its lack of automation. The combination of deep learning methods and remotely sensed datasets provide an automated alternative that can greatly improve LULC classification and wetland detection, in terms of efficiency and accuracy (Felton et al. 2019). Imagery products are conventional variables used in such models, though digital terrain models (DTM) and DTM derivatives offer alternative and supplementary information. While imagery products reflect spectral information captured by remote sensing platforms, DTMs reflect elevation. Recent advancements in light detection and ranging (LiDAR) sensors have resulted in high-resolution elevation products in recent years, from which DTMs are produced. The availability of these products in the U.S. has also grown through initiatives like the National Digital Elevation

Program (NDEP) as publicly available datasets. The use of DTM derivatives to map wetlands have shown substantial improvements in recent years (Huang et al. 2014; Lang et al. 2013), and the combination of these products with machine learning frameworks have demonstrated increased potential to improve wetland prediction accuracy (O'Neill et al. 2020; Christensen et al. 2022).

Of the many machine learning frameworks, random forest is one that builds an ensemble model with multiple decision trees to generate class-based predictions (Breiman 2001). Wetland mapping with random forest procedures has grown in popularity for its computational efficiency, predictive accuracy, and use of bootstrapping techniques that are especially useful when training data are limited (Felton et al. 2019). Predictor variables are user specified, but generally represent those which collectively indicate wetland hydrology, hydrophytic vegetation, hydric soils, and associated topography. The random forest algorithm creates decision trees with randomly selected subsets of both training data and predictor variables, so that each tree represents a potentially unique classification scheme. To prevent model overfitting, a subset of all trees is randomly selected, from which a majority voting rule determines the final classification scheme based on out of bag (OOB) accuracy (Breiman 2001).

OOB accuracy assessments are a bootstrapped technique which validate the model's classification schema through a held out portion of training data. Although the randomization introduced throughout this process bolsters predictive power and accuracy, held out validation data represent areas consistent with those by which the model was developed from. An additional step that researchers often implement is a secondary validation assessment in a novel area to determine how well the model performs outside of the areas in which those models were designed. Validation techniques used in secondary validation vary based on research objectives,

data types, and data availability. Additionally, the randomization incorporated into each step of random forest models introduce significant data variation so that wetland-like uplands and upland-like wetlands are better differentiated, for improved 'cryptic' wetland detection and mapping (O'Neill et al. 2020).

1.3. Challenges and Innovations: Headwater Wetlands of the Eastern Gulf Coastal Plain

Headwater slope wetlands are associated with a variety of wetland and upland features that can be difficult to discern. Forested canopies share visual and spectral characteristics with those in surrounding uplands (Lang et al. 2013) and can be misleading to both aerial imagery interpreters and pixel-based classifiers (Huang et al. 2014). Publicly available imagery datasets currently lack adequate balances of spatial, spectral, and temporal resolutions necessary for mapping applications in small, forested, and rarely flooded wetlands (Christensen et al. 2022). Spatial configurations of headwater wetlands are often linear and narrow and limit the use of many datasets which have minimum mapping units that exceed wetland widths. High spatial resolution imagery (< 10 m) datasets are still limited in use for surface water detection of forested wetlands, where open water remains largely indetectable through dense canopies and where its presence is temporally variable (Barksdale and Anderson 2014; Christensen et al. 2022).

Landform associations with wetlands can be made evident through DTM derivatives and have shown to be consistent predictors of wetland status (Miller 2003; Halabisky et al. 2023). Gradient raster products characterize differences in relief between DTM cells and are expected to occur within a limited range for slope wetlands, with slope values below this range associated

with depressions and flats, and slopes values above this range with hillsides and channel banks. Planform curvature describes slope direction between adjacent cells in the horizontal plane, with negative values indicating slope convergence, positive values indicating divergence, and a value of 0 indicating uniform slope direction for all cells considered. Profile curvature describes slope shape in the vertical plane, with negative values indicating convexity, positive values indicating concavity, and a value of 0 indicating a linear slope. Both curvature metrics describe slope dimensions that exert various levels of control on flow direction and accumulation and may be associated with wetland vs. upland status. (Miller 2003; Halabisky et al. 2023_a). Elevation deviation is another topographic index which identifies the standard deviation of DTM cell elevations within a focal neighborhood. This metric shows promise for mapping areas with consistent elevational patterns relative to surrounding wetland and upland areas (Miller 2003).

Hydrologic proxies are also examples of DTM derivatives, such as topographic wetness index (TWI), which is a measure of inundation via landform influences on flow patterns (Beven and Kirkby 1978). Cartographic depth to water (DTW) is another example of a hydrologic proxy which models water table depth based on elevations of nearby waterbodies (Murphy et al. 2011). DTW and TWI may also be important predictor variables of headwater wetlands, as they are based on shallow subsurface flows, characteristic of headwater catchment hydrology. Additionally, the spatial resolution of aerial imagery datasets via the National Agricultural Imagery Program (NAIP) have substantially improved in recent years, with resolutions up to 0.91 m. Despite limitations in surface water detection, these datasets may be useful for calculation of the Normalized Difference Vegetation Index (NDVI) to depict vegetated vs. non-vegetated areas at relevant scales for headwater slope wetlands.

1.4. The Wetland Intrinsic Potential Tool: Applications in Coastal AL

The ability of random forest to present significant data variations in gradational landcovers provides the basis for our research. For this purpose, we utilized the Wetland Intrinsic Potential (WIP) Tool, as a random forest model tailored to forested and cryptic wetland prediction (Halabisky et al. 2023_a). A headwater dense area was identified in coastal Alabama in which to apply the WIP Tool for an assessment of predicted wetland probability and extent, using various imagery and DTM derivatives as model covariates. The WIP tool has demonstrated high levels of accurate predictions in the pacific northwest region, with an overall accuracy of 91.8% in secondary validation datasets (Halabisky et al. 2023_a). When compared to NWI, errors of omission were reduced by 33.4% and errors of commission increased by 8.6% (Halabisky et al. 2023_a). Our model was expected to behave similarly in coastal Alabama, provided that accurate and representative training data were used. Although some differences arise from local geology, the hydrologic and geomorphic profiles in headwater wetlands of coastal Alabama are consistent with others throughout the coastal plain region of the gulf and Atlantic coasts (Rheinhardt et al. 2000, 2013; Noble et al. 2007, 2011; Tufford 2011). The objectives of this research study were to 1) identify metrics which accurately depict the wetland-upland matrix within coastal Alabama and 2) produce wetland probability maps and accuracy metrics in which to contextualize the best use of such models for wetland prediction in the eastern gulf coastal plain region.

2. Methods

2.1. Characterization of Alluvial Wetlands Within the Study Area

Forested wetlands of the eastern gulf coastal plain occur extensively throughout headwater networks. Additionally, the dense network of headwater streams in the region result in a disproportionate influence on water quality regulation in mainstem streams (Nadeau and Rains 2007; Armstrong et al. 2012). Extending from eastern Louisiana to the Florida panhandle, the region experiences a subtropical climate with abundant precipitation, high humidity, hot summers, mild winters, and an extensive growing season. Headwater wetlands exhibit varying degrees of slope and floodplain wetland hydrology, dependent on geomorphic position, contributing drainage area, flow accumulation, and stream order. Headwater wetlands are described hereon after as wetlands occurring within or in association with 1st-3rd order streams, while Mainstem wetlands are those associated with mainstem streams, being 4th order and above.

Headwater wetland hydrology is characterized by groundwater seepage, with surface hydrology represented to a lesser degree. Headwater wetlands associated with 1st order streams occur in low sloping drainages, typically at toe slopes below flatwood pine forests. This geomorphic position (Fig. 3.1) ensures important connections with the hydrologic cycle and surrounding landscape, acting as a biogeochemical and physical buffer between upland drainage areas and headwater streams (Nadeau and Rains 2007; Ramesh et al. 2020). Headwater wetlands associated with 2nd-3rd order streams are more representative of surface water hydrology, though groundwater seepage in these gently sloped wetlands still remains a dominant component of water budgets. The link between mainstem wetlands and groundwater seepage lessen as the role of surface water hydrology increases with drainage area and flooding frequency. Mainstem streams have wider and more visible channels as a result, with wider wetland perimeters.

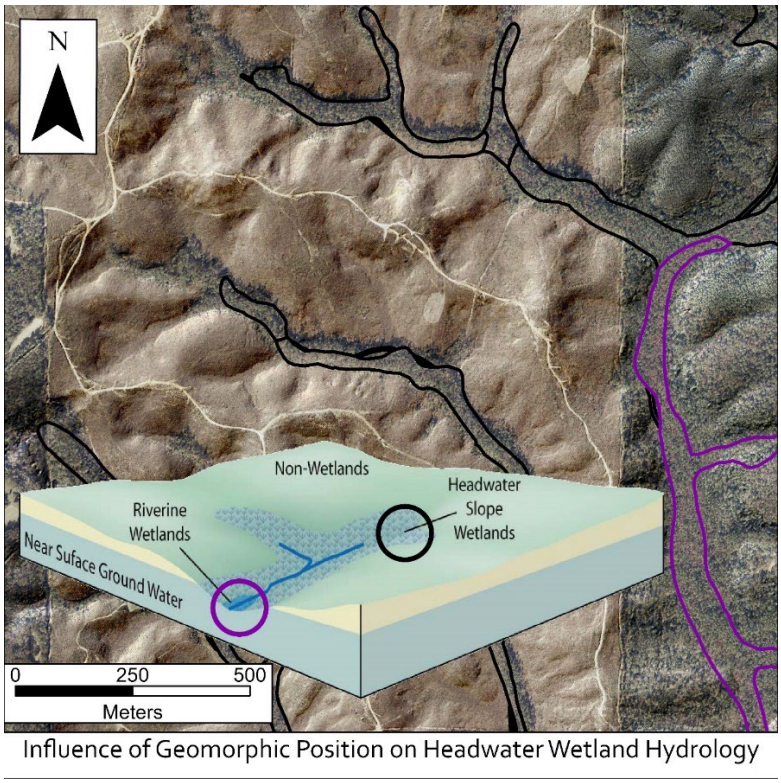

Figure 3.1. *Geomorphic position plays a large role in headwater wetland hydrology. As headwater slope wetlands converge along a downslope gradient, flows concentrate into perennial streams where surface water processes become more representative.*

Headwater wetlands in this region are associated with bay-tupelo forests which contain an array of facultative and obligate wetland species. Canopy tree strata are characterized by relatively low densities (250 – 425 stems/ha) of moderate to high basal area (≥ 30 cm) trees, for characteristic species such as sweet bay (*M. virginiana*), slash pine (*P. elliottii*), swamp tupelo (*N. biflora*), black gum (*N. sylvatica*), sweet gum (*L. styraciflua*), and tulip poplar (*L. tulipifera*) (Noble et al. 2007; Barksdale and Anderson 2014). Canopy trees associated with frequent flooding such as bald cypress (*T. distichum*) and water tupelo (*N. aquatica*), or with stream channel banks such as black willow (S. nigra) and American sycamore (P. occidentalis) are rare to nonexistent. These species occur primarily in mainstem wetlands instead (Reinhardt et al. 2013). Midstories of headwater wetlands consist of variably dense subcanopy trees and saplings,

shrubs, and vines. Common species include red bay (*P. borbonia*), red maple (*A. rubrum*), yaupon (*I. vomitoria*), coastal doghobble (L. axillaris), titi (*C. racemiflora*), and greenbrier (*Smilax spp.*) (Noble et al. 2007; Barksdale and Anderson 2014). Herbaceous vegetation is typically sparse for grasses, forbs, and rushes, though cinnamon fern (*O. cinnamomea*) and chain fern (*Woodwardia spp.*) can occur in relatively high densities (Noble et al. 2007; Barksdale and Anderson 2014).

All soil hydrologic groups (A, B, C, D) are represented in headwater wetlands soils throughout the region, reflecting their gradational nature between uplands and streams. Seasonal variation is also reflected in soil hydrologic groups, with many wetland soils characterized by both wet and dry ratings dependent on season (A/B, A/C, A/D, B/C, B/D) (Noble et al. 2007). Within the upper 15.25 cm of soil horizons, the accumulation of organic material results from infrequent flooding in these low slope environments. In-situ decomposition of detritus and plant materials is further prolonged by hummocky microtopography, the influence of fine root mass dynamics, and continuously saturated soils that contribute to considerable rates of carbon and nitrogen sequestration and cycling (Jones et al. 1996; Ramesh et al. 2020; Stewart et al. 2024). Soil textures beneath organic layers are variable, with some wetland soils containing sandy textures greater than 2 meters below the soil surface and others with sandy clay loams at 40 cm from the soil surface (Noble et al. 2007). Porosity and drainage characteristics are enhanced by sandy textures, though holding capacities are often exceeded by excess saturation (Noble et al. 2007; Tufford 2011).

Within this region, our model was applied to the ‘Bushy Creek – Dyas Creek’ located in central Baldwin County, AL. This watershed is described as a hydrologic unit code 10 watershed (HUC10) and is hereon referred to as BcDc10, referring to the total spatial extent of our study

area (Fig. 3.2). Topography throughout the region is relatively flat with steeper areas associated with alluvial valleys and terraces (Ebersole et al. 2019).

A challenge in wetland prediction using the WIP tool or similar models is reduced accuracy where hydrology has been modified through agricultural and urban LULC and land use practices (Halabisky et al., 2023_a). The selection of our study watershed reflects its relatively undeveloped and highly forested LULC to provide a basis for wetland prediction throughout coastal Alabama. BcDc10 also contains a dense network of headwater streams, with 92% of stream miles being 1^{st}-3^{rd} order (Table 3.1). BcDc10 is comprised of three individual hydrologic unit code 12 (HUC12) watersheds. The HUC12 watershed, 'Bushy Creek – Dyas Creek' (BcDc12), represents roughly half of the study area and was the extent for model training and building. 'McCurtin Creek' and 'Dyas Creek' HUC12s represent the remaining spatial extent of the study area, and were combined into a new boundary, 'McCurtin Creek- Dyas Creek' (McDc12), which was used for model validation. All watershed boundaries and their locations within Baldwin County, AL are depicted in Fig. 3.2.

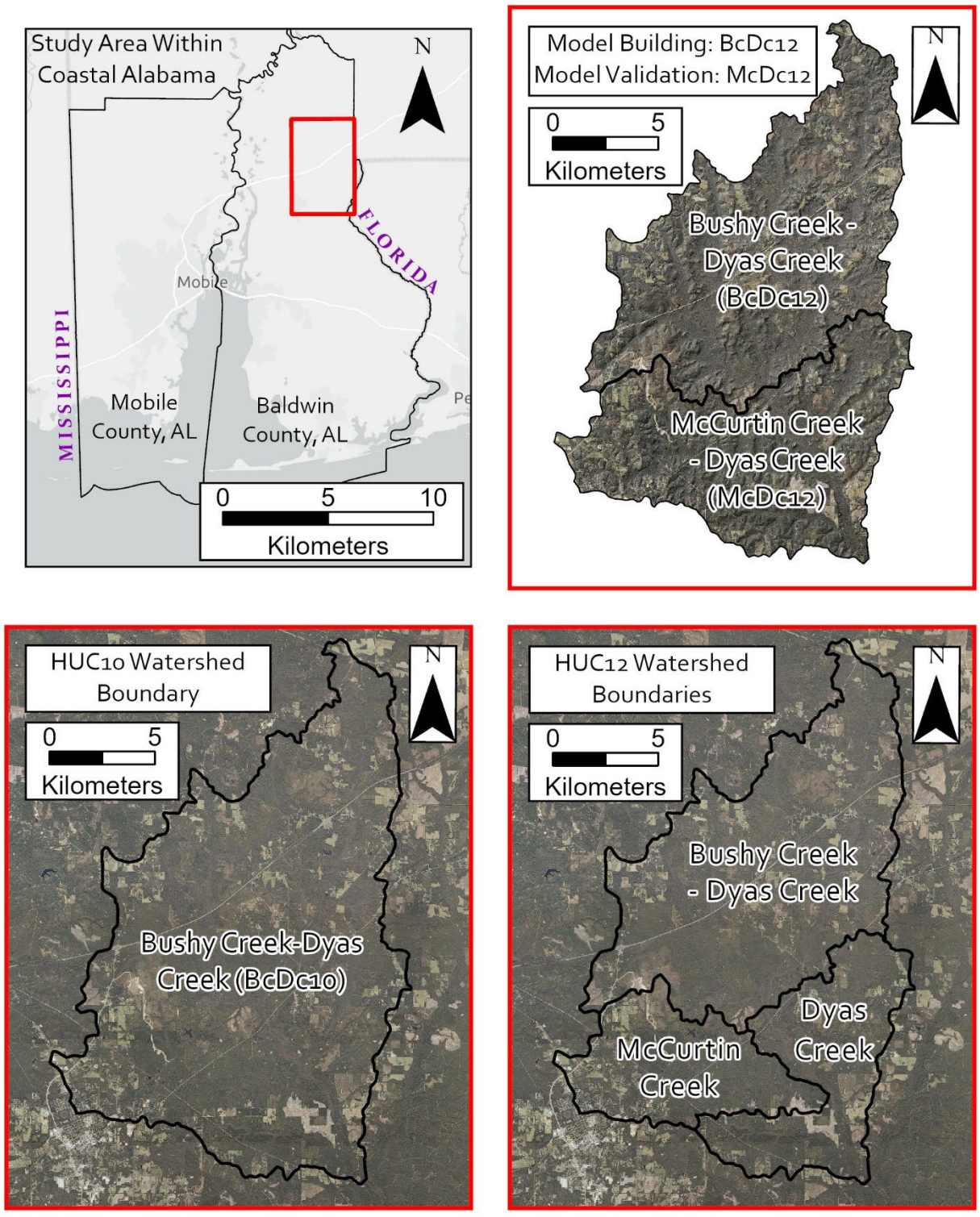

Figure 3.2. *The HUC10 watershed, 'Bushy Creek - Dyas Creek', encompasses the study area and is comprised of 3 separate HUC12 watersheds. The HUC12 watershed of the same name was used for the model training extent (BcDc12), while the other HUC12 watersheds were combined to create the extent for model validation (McDc12).*

Table 3.1. *Stream order and length attributes for BcDc10. Wetland training and validation data locations followed a stratified random sampling design based on stream order length per total watershed stream length. Wetlands associated with headwater streams represent 92% of training and validation data.*

BcDc10	Stahler Stream Order	Stream Length (km)	Proportion of Total Length	Wetlands Sites Per Stream Order
	1	177.8	0.61	61
Headwater	2	55.0	0.19	19
	3	36.4	0.12	12
Mainstem	≥ 4	24.6	0.08	8
	Total	293.9		

2.2. Data Sources, Transformations, & Definitions

Spatial datasets were acquired for various objectives related to image interpretation and model building/validation. The high-resolution national release of the National Hydrography Dataset (NHDPlus HR) was accessed via the National Map database (U.S. Geological Survey 2022). Select streamlines, water bodies, HUC10, and HUC12 watershed boundaries were extracted from NHDPlus HR. Streamline segments contained within the study area were manually assigned Stahler stream orders for use in stratified sampling methods. NHD streamlines and water bodies were additionally combined into a raster depicting total surface water extent for use in calculating cartographic depth to water (DTW). Mapped wetland boundary features were obtained through The National Wetland Inventory (NWI) (U.S. Fish and Wildlife Service 2022).

One-meter DTM tiles which encompassed the study were accessed through the National Map database (U.S. Geological Survey 2015). DTM tiles were mosaicked into a single raster and subsequently resampled with bilinear interpolation to 3 m resolution. The DTM was extracted to the boundaries of BcDc12 and McDc12, resulting in a 3 m DTM for each spatial extent.

Additionally, a 1 m DTM hill shade derivative was obtained through the geospatial data gateway (NGCE 2022), for the extent of Baldwin County, AL for use in image interpretation. The WIP tool was downloaded from the 'Forested Wetlands' GitHub repository, published by TerrainWorks-Seattle (Halabisky et al. 2023$_b$). The tool functions as two ESRI toolboxes which allow for the production of model covariates with the DEM Utilities toolbox, and random forest model building/validation with the Wetland Tools toolbox. Multi-scale topographic indices used as model covariates were produced from the DEM utilities toolbox, while ArcHydro's, 'Wetland Identification Model' (WIM) was used to produce all hydrologic proxies used as model covariates.

Aerial imagery products included four-band natural color (NC) and color infrared (CIR) National Agricultural Imagery Program (NAIP) orthophoto mosaics, acquired from the geospatial data gateway for the extent of Baldwin County, AL (NGCE 2023a, 2023b). Both datasets reflect 2021 acquisition years with 0.3 m spatial resolutions. NC imagery was used exclusively for image interpretation, and CIR imagery was resampled to 3 m resolution using bilinear interpolation and extracted to the extent of both BcDc12 and McDc12 for use in Normalized Difference Vegetation Index (NDVI) calculations.

2.3. Training & Validation Datasets

Mapped wetland presence, absence, and extent are largely a function of training and validation data used in the WIP tool. To ensure accurate representations of wetlands and uplands, wetlands from both BcDc12 and McDc12 were field verified prior to building training and validation datasets (Fig. 3.3). Patterns observed in aerial imagery and hill shade rasters for field

verified wetlands were referenced to manually adjust upland vs. wetland training and validation data locations when necessary. NWI was chosen as a primary bounding extent between wetlands and uplands, so that 100 wetland points were placed within NWI boundaries and 200 upland points were randomly distributed outside of NWI wetland boundaries for both BcDc12 and McDc12.

Figure 3.3. *Thirteen wetlands were field verified throughout BcDc10 prior to modelling. These were referenced to determine if and where manual adjustments of wetland and upland training data locations were necessary, based on DTM and imagery based indicators of wetland status.*

A stratified sampling method was implemented for wetland points, based on the proportion of total stream km per stream order throughout BcDc10 (Fig. 3.4). This resulted in 61 points occurring along 1st order streams, 19 points along 2nd order streams, 12 points along 3rd order streams, and 8 points along streams being 4th order and above. Within each stream order

class, points were distributed randomly along NHDPlus HR streamlines. To avoid spatial biases by placing training and validation points directly on streamlines, the cross sectional width of NWI wetlands were measured at each points location. A random multiplier between 0 – 100 was then chosen to determine an adjusted distance of the total cross sectional width. Points were manually adjusted to this distance, measured from the left most (facing up flow) to the right most extent of the wetland cross section.

Of the 61 first order wetlands, 30 were manually adjusted to locations which were mapped by NWI but lacked a mapped stream within the wetland boundary, to avoid further biases with NHD streamline presence. The longitudinal length of the wetland was measured from crown to outlet, and a random multiplier from 0 – 100 was chosen to adjust this distance. Measured downflow from the wetland crown to outlet, each point was placed at the adjusted distance. From this location, the cross sectional width rule was once again applied to determine its latitudinal position. Validation points followed the same protocol in McDc12, with 200 random upland locations and 100 wetland locations which were randomly selected within a stratified sampling design (Fig. 3.4).

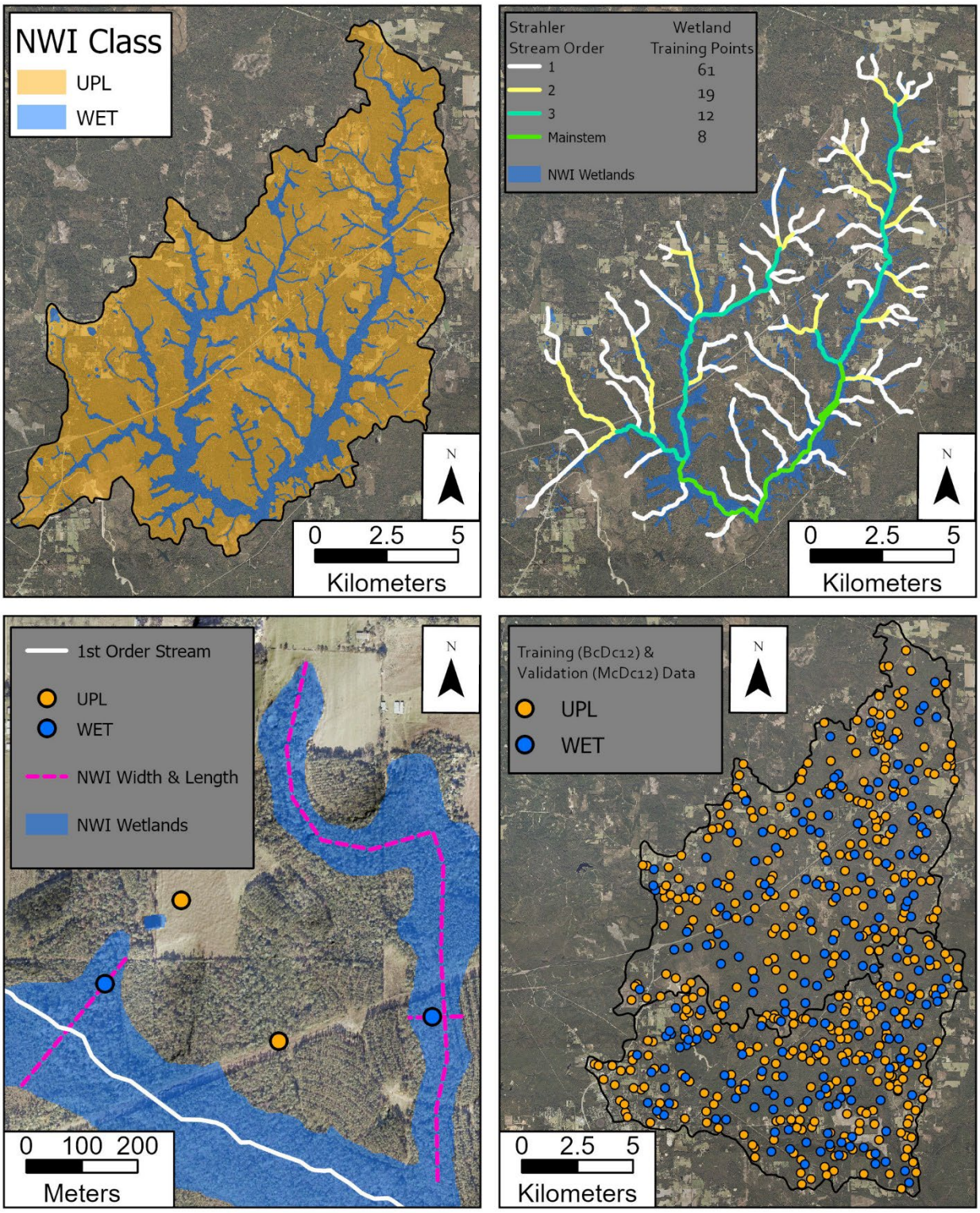

Figure 3.4. *Wetland training data points were placed at random locations along designated stream orders and adjusted to randomly selected positions perpendicular to the streamline. Half of the training points along 1st order streams were moved to the nearest wetland without a mapped stream and given a random longitudinal position as well. Upland locations were randomly distributed throughout non-NWI areas, points were manually adjusted where locations did not represent target classes, and the process was repeated for validation points as well.*

2.4. WIP Model Covariates

All WIP model covariates were 3m resolution rasters, as this provided a balance between excess variability that could lessen predictive relationships associated with high resolution datasets (Oruc et al. 2004) and a minimum mapping unit capable of headwater wetland detection (Christensen et al. 2022). DTW and TWI were generated using the 'calculate depth to water index (DTW) using surface parameters', and 'calculate topographic wetness index (DTW) using surface parameters' tools within Arc Hydro Pro tools for ArcGIS Pro. NDVI was additionally calculated with ArcGIS Pro's NDVI function using CIR imagery (Table 3.2). Along with hydrologic proxies (DTW, TWI) and a vegetative index (NDVI) (Fig. 3.5), multi-scale topographic indices were included as predictor variables in our model (Fig. 3.6). Multi-scale products were created for each topographic index relative to a specified length scale, similar to a focal neighborhood. The use of multi-scale topographic indices allows for landform associations to be contextualized so that metrics represent those at the wetland-upland interface at smaller length scales, and at the hillslope-valley complex at larger length scales.

Multi-scale topographic indices were produced within the WIP tool's DEM Utilities toolbox. Planform curvature, profile curvature, elevation deviation, and gradient were created at length scales of 50-, 150-, 300-, and 1000-m length scales, for a total of 16 multi-scale topographic indices (Table 3.2). Selected length scales reflect those used by Halabisky et al. (2023_a) and are expected to depict representative scales of landform associations with topographic indices but are also exploratory for the selected study area. Total model covariates used (n = 19) were limited to the extent of either BcDc12 for model building and training purposes or McDc12 for model validation purposes. Short form abbreviations of topographic indices used are defined as ElevDev (elevation deviation), gradient (gradient), ProfCurv (profile

curvature), and PlanCurv (planform curvature). Each index is further identified by an appended length scale, i.e., PlanCurv300.

Table 3.2. *Environmental variables used in random forest modeling (n = 19) and validation. NDVI was used as a singular vegetative index and the WIM tool was used to produced hydrologic proxies. All multi-scale (50 m, 150 m, 300 m, 1000 m) topographic indices were produced within the DEM Utilities toolbox housed within the WIP tool.*

Geoprocessing				Model Covaraites (n = 19)	
Tool	Source	Function	Additional Paramters	Name	Resolution (x, y)
NDVI Function	ArcGIS Pro 3.2.0; Analysis Tools	calculate normailzed difference vegetaion index (NDVI)	NA	NDVI	3.0 m
Wetland Identification Model (WIM)	ArcGIS Pro 3.2.0; Arc Hydro Tools Pro	calculate depth to water index (DTW) using surface parameters	slope neigborhood = 10 m	DTW	3.0 m
		calculate topographic wetness index (TWI) using surface parameters	slope neigborhood = 10 m hydrocondition = fill	TWI	3.0 m
Wetland Intrinsic Potential Tool (WIP): DEM Utilities	Halabisky et al. 2023[b]	create gradient raster using surface metrics	length scale = 50 m	Gradient_50	3.0 m
			length scale = 150 m	Gradient_150	3.0 m
			length scale = 300 m	Gradient_300	3.0 m
			length scale = 1000 m	Gradient_1000	3.0 m
		create elevation deviation (ElevDev) raster using surface metrics	length scale = 50 m	ElevDev_50	3.0 m
			length scale = 150 m	ElevDev_150	3.0 m
			length scale = 300 m	ElevDev_300	3.0 m
			length scale = 1000 m	ElevDev_1000	3.0 m
		create planfrom curvature (PlanCurv) raster using surface metrics	length scale = 50 m	PlanCurv_50	3.0 m
			length scale = 150 m	PlanCurv_150	3.0 m
			length scale = 300 m	PlanCurv_300	3.0 m
			length scale = 1000 m	PlanCurv_1000	3.0 m
		create planfrom curvature (ProfCurv) raster using surface metrics	length scale = 50 m	ProfCurv_50	3.0 m
			length scale = 150 m	ProfCurv_150	3.0 m
			length scale = 300 m	ProfCurv_300	3.0 m
			length scale = 1000 m	ProfCurv_1000	3.0 m

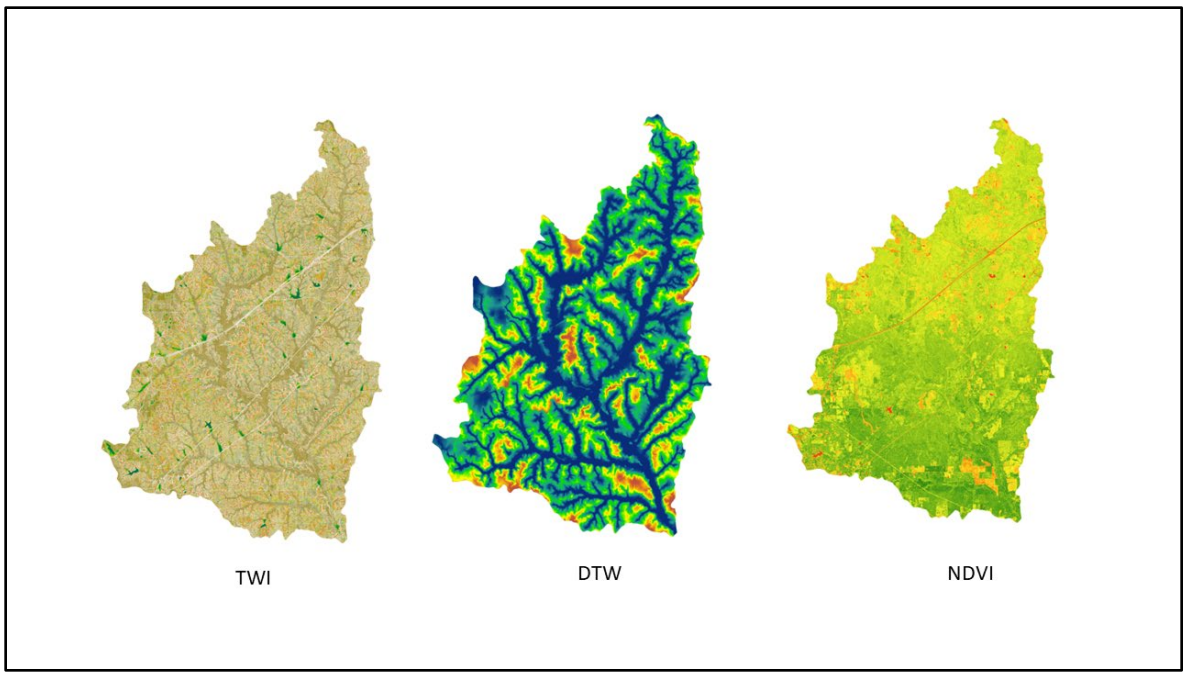

Figure 3.5. *Hydrologic variables were represented with TWI, representative of flow accumulation, and DTW, representative of areas with shallow depths to groundwater. NDVI was used as a sole vegetation variable, indicating vegetated areas.*

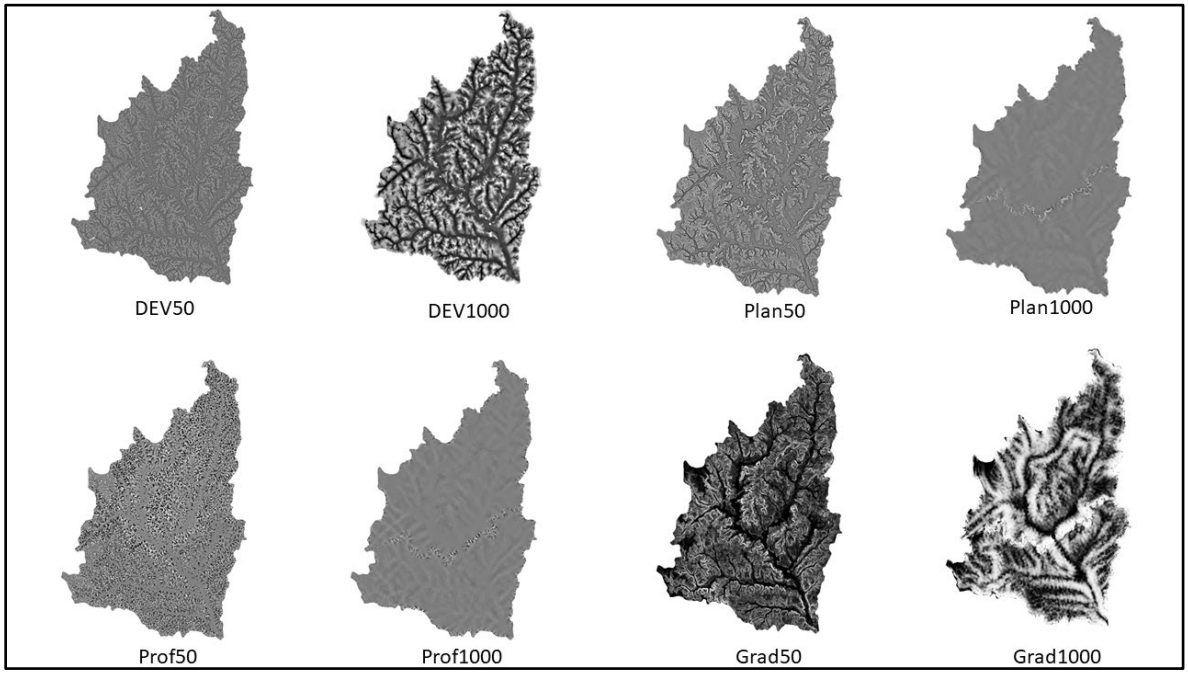

Figure 3.6. *Multi-scale topographic indices used in wetland prediction modeling. Examples show 50- and 1000-meter length scales for demonstration purposes, but each metric was additionally represented by 150- and 300-meter length scales as well. Gradient characterizes change in slope from one cell to the next, curvature metrics depict hillslope complexity and convergence, and elevation deviation describes how elevations deviate from those in nearby cells.*

2.5. Statistical Analysis

Model covariates and training data for BcDc12 were used to train and build a random forest model using 200 decision trees. From this model, a wetland probability map was produced for BcDc12, with raster cells containing values from 0 – 1, depicting low to high probabilities of wetland presence. Various statistical outputs were generated from the random forest model, all of which reflect a class threshold of 0.5, with raster cells above this threshold identified as wetlands and cells below as uplands. OOB error and OOB accuracy are reported for the model building procedure and spatial extent (BcDc12), which is further summarized with a confusion matrix to generate additional statistics. These include errors of omission (false negative rate) and commission (false positive rate), specificity (true negative rate), sensitivity (true positive rate), and a kappa coefficient (accuracy of results relative to random chance). Additionally, two charts depicting variable importance to model decisions were produced. A Gini coefficient output ranked variables in terms of contributions to majority voting by decision trees, while an additional plot ranked variables in terms of contributions to OOB accuracy. To determine how well our model performs in other areas of coastal Alabama, it was applied to the extent of McDc12 and assessed for accuracy with a novel validation dataset.

Running the model on McDc12 followed the same protocols as BcDc12 and produced a wetland probability map based on a threshold of 0.5 along with various statistical outputs. Model statistics for McDc12 included a confusion matrix to determine overall model error & accuracy, errors of omission and commission, sensitivity, specificity, and a kappa coefficient. To determine the model's efficacy to successfully distinguish classes, a receiving operator characteristic (ROC) curve was generated for McDc12s validation dataset from which area under the ROC (AUC) was calculated based on the specified threshold of 0.5.

Wetland presence, absence, and extent were mapped by reclassifying wetland probability maps for both BcDc12 and McDc12 by respective thresholds. Our initial assessment was based on a threshold of 0.5, as this was the default for model building. Raster cells with WIP values less than 0.5 were classified as uplands and cells with WIP values greater than or equal to 0.5 were classified as wetlands. Reclassified wetland probability maps are hereafter referred to as WIP wetland extent maps which are binary class-based rasters.

Cell values of McDc12s wetland probability map were extracted at each validation data point to further analyze accuracy metrics as model thresholds were adjusted. The wetland probability map was reclassified using alternative threshold values, resulting in alternative wetland extent maps for each iteration. Confusion matrices were built and analyzed from each wetland extent map until an ideal threshold was identified by optimal values of kappa, overall model accuracy, and class error rates. These data were then used to compare WIP wetland extent maps with NWI maps for differences in class area and coverage, and to contextualize model behaviors.

3. Results

3.1. Random Forest Model: Training, Validation, and Accuracy Metrics

The following section reflects model results with a class threshold of o.5, as our default model. Variables which demonstrated the greatest relative contributions towards model decisions were DTW, ElevDeV1000, and Gradient50 with Gini coefficients of 40.8, 19.9, and 13.9, respectively (Fig. 3.7). Gini coefficients for NDVI (1.67) and TWI (1.48) were low in terms of importance, though most other topographic indices were closely aligned near this range as well. AUC for McDc12 validation data was calculated to be 0.98, and WIP values for these validation

data were additionally plotted, showing bimodal distributions of wetlands and uplands, which were clustered at high and low ranges, respectively (Fig. 3.8). A mean WIP value for wetland validation data was calculated to be 0.79 ± 0.02, and 0.08 ± 0.01 for upland validation data. These results suggest that our model performed exceptionally well at distinguishing between upland and wetland classes for our validation dataset, though bimodal distributions of WIP values indicate that an adequate amount of variation may not captured in this data.

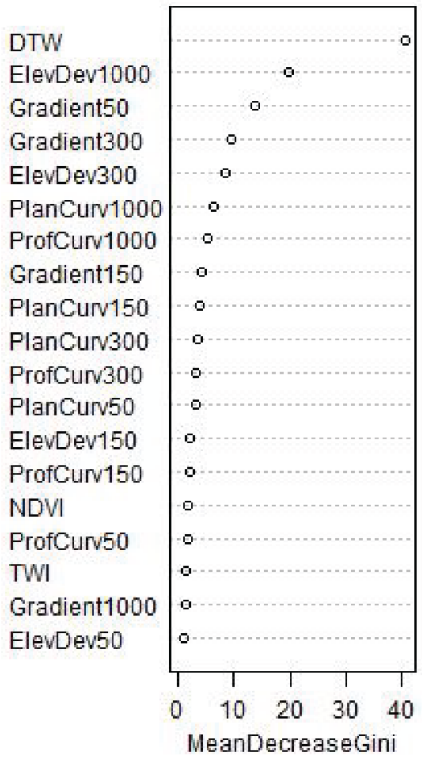

Figure 3.7. *Gini coefficients for all model covariates represent contributions to the BcDc12 random forest models' classification logic and are plotted by relative importance. DTW was substantially impactful for model decisions relative to other variables.*

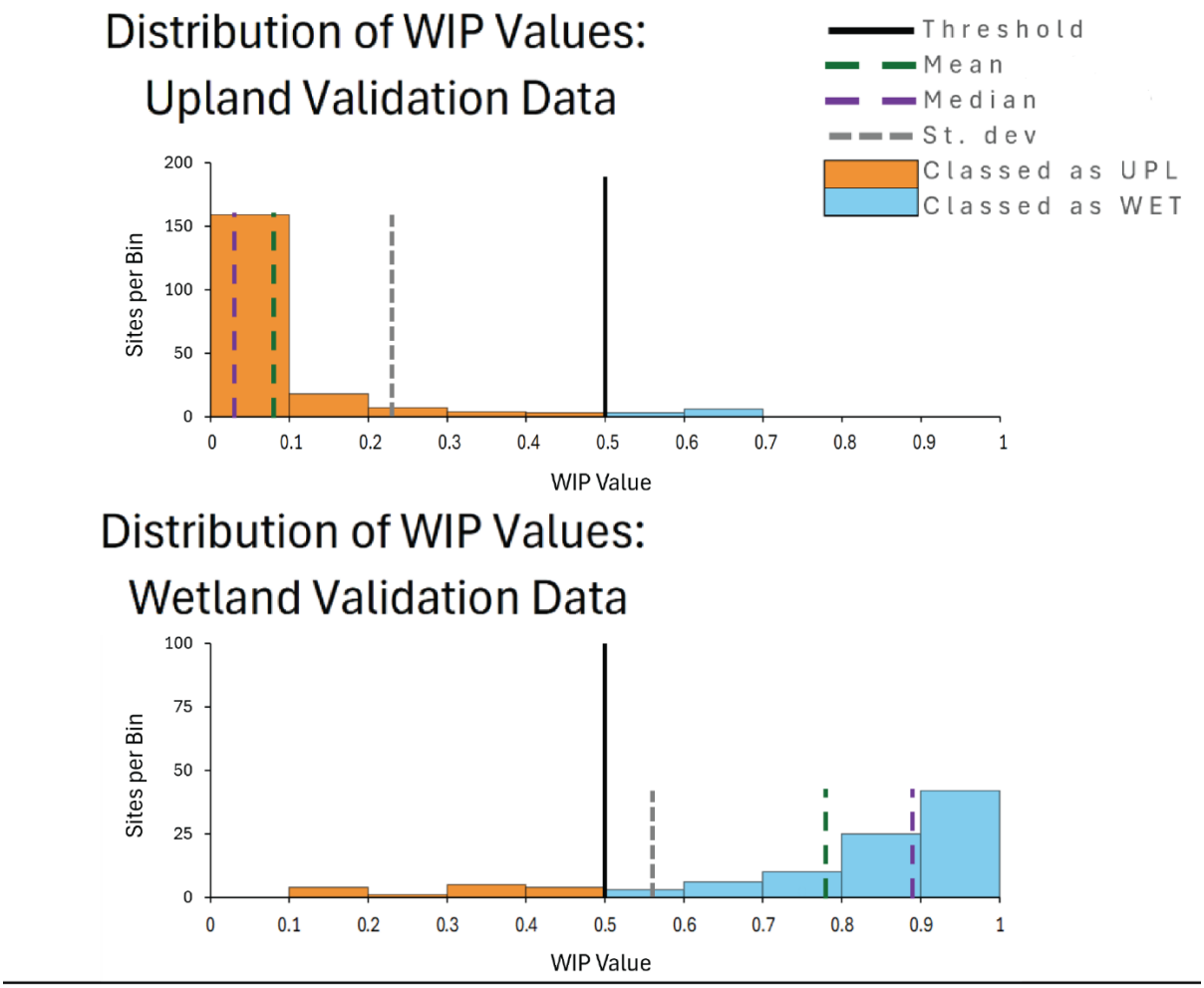

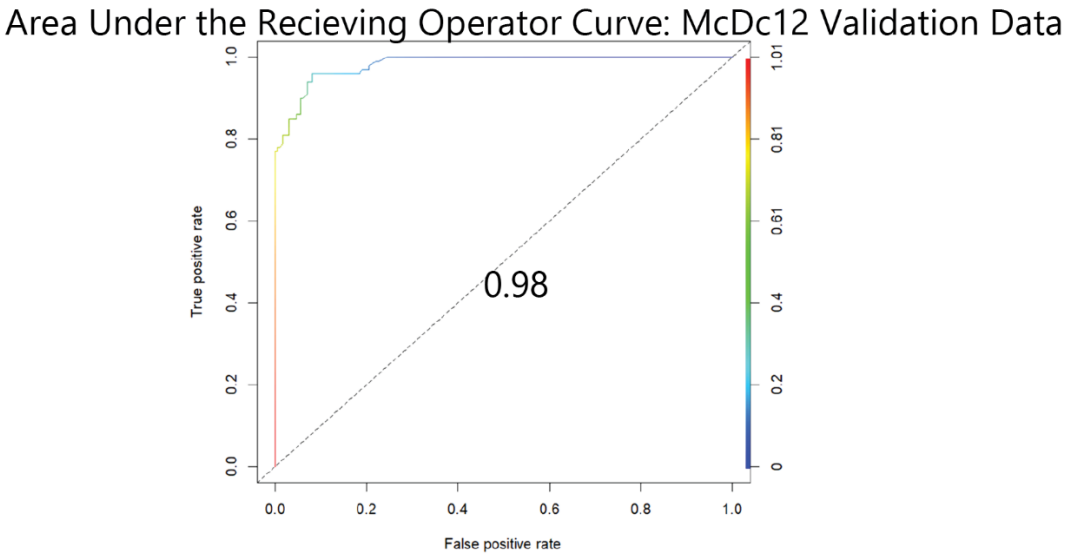

Figure 3.8. *Area under the receiving operator curve for the McDc12 validation dataset was 0.98, suggesting that the random forest model was especially effective at differentiating between upland and wetland classes. The distribution of WIP values for upland and wetland classes are additionally provided for context on the ranges present in validation data relative to the designated threshold of 0.5.*

Our random forest model, as it was applied to BcDc12, resulted in wetland omission and commission errors at 7.0% (false negative rate) and 2.5% (false positive rate), respectively. Sensitivity and specificity values were respectively, 0.93 (true positive rate) and 0.98 (true negative rate). This initial validation based on OOB procedures revealed that wetland sites in our training dataset were more frequently misclassified as uplands than upland sites were misclassified as wetlands. An OOB accuracy rate of 96.0% reflects highly accurate predictions when both metrics are considered, and a kappa coefficient of 0.91 indicate that our results are highly accurate compared with expected class agreement by chance. Upon running and validating the random forest model for the extent of McDc12, a confusion matrix resulted in overall model accuracy of 92.3%. Wetland omission errors were 14.0% (false negative rate) and wetland commission errors were 4.5% (false positive rate). Sensitivity and specificity values were respectively, 0.96 (true positive rate) and 0.86 (true negative rate), and a kappa coefficient was calculated to be 0.83. Although lower rates of accuracy are generally expected as models are applied to new areas, our random forest model remained highly accurate when validated on McDc12. Misclassification of wetlands as uplands continued to be the main source of error, though all metrics indicate a well performing model. Confusion matrices and model accuracy metrics relative to a class threshold of 0.5 are reported in Tables 3.3a and 3.3b for the random forest model (BcDc12) and the validation extent of the random forest model (McDc12).

3.2. Alternative Class Thresholds: Validation and Accuracy Metrics

The following section reports alternative threshold values and resulting statistics as they were applied to our model for the extent of McDc12. These findings are thus an exploratory analysis of alternative thresholds to guide future model building, rather than a validation of

distinct and separate models. In general, kappa coefficients increased as thresholds decreased from 0.5 (0.825) to 0.4 (0.836) to 0.3 (0.840) and decreased outside of this range. Overall model accuracy increased from 92.3% at a threshold of 0.5, to 92.7% at thresholds of both 0.3 and 0.4. Wetland omission (false negative rate) errors fell from a threshold of 0.5 (14.0%) to 0.4 (10.0%) while wetland commission errors (false positive rate) rose from 4.5% to 6.0%. Moving from a threshold of 0.4 to 0.3, wetland omission errors fell from 10.0% to 5.0% and wetland commission errors rose from 6.0% to 8.5%. These data are reported in Tables 3.3c and 3.3d and suggest an optimal threshold of 0.3 or 0.4, dependent on class-specific objectives.

Table 3.3. *Confusion Matrices and additional validation related statistics are reported for models with threshold values set at 0.5 for (a) BcDc12 and (b) McDc12. These statistics are also reported for alternate threshold values 0.4 (c) and 0.3 (d) for McDc12. BcDc12 statistics were based on an OOB assessment of training data and does not represent an equal method for comparisons for those in McDc12. With decreasing threshold values, Omission errors declined while commissions errors, overall accuracy, and kappa coefficients increased. Differences between (c) 0.4 and (d) 0.3 represent tradeoffs between class related errors.*

a.)

BcDc12*
Threshold = 0.5

Wetland Comission Error	2.51%
Wetland Omission Error	7.00%
OOB Error	4.01%
OOB Accuracy	95.99%

Predicted Class \ True Class	UPL	WET
UPL	194	7
WET	5	93
Total	199	100

Sensitivity	0.930
Specificity	0.975
Expected Agreement	0.557
Observed Agreement	0.960
Kappa	0.909

b.)

McDc12
Threshold = 0.5

Wetland Comission Error	4.50%
Wetland Omission Error	14.00%
Overall Model Error	7.67%
Overall Model Accuracy	92.33%

Predicted Class \ True Class	UPL	WET
UPL	191	14
WET	9	86
Total	200	100

Sensitivity	0.860
Specificity	0.955
Expected Agreement	0.561
Observed Agreement	0.923
Kappa	0.825

c.)

McDc12
Threshold = 0.4

Wetland Comission Error	6.00%
Wetland Omission Error	10.00%
Overall Model Error	7.33%
Overall Model Accuracy	92.67%

Predicted Class \ True Class	UPL	WET
UPL	188	10
WET	12	90
Total	200	100

Sensitivity	0.900
Specificity	0.940
Expected Agreement	0.553
Observed Agreement	0.927
Kappa	0.836

d.)

McDc12
Threshold = 0.3

Wetland Comission Error	8.50%
Wetland Omission Error	5.00%
Overall Model Error	7.33%
Overall Model Accuracy	92.67%

Predicted Class \ True Class	UPL	WET
UPL	183	5
WET	17	95
Total	200	100

Sensitivity	0.950
Specificity	0.915
Expected Agreement	0.542
Observed Agreement	0.927
Kappa	0.840

3.3. Mapped Wetland Presence, Absence, and Extent

Wetland probability, presence, absence, and extent are mapped in Fig. 3.9 for the extent of BcDc10. Our WIP model agreed with 89.1% of NWI classes, while 4.4% of NWI wetlands were recognized as uplands and 6.6% of NWI uplands were recognized as wetlands, for a cumulative difference of 2.2% in increased wetland coverage (Fig. 3.10). Land cover classes for BcDc10 were represented as 80.7% uplands and 19.3% wetlands, while our WIP model represented 78.4% of BcDc10 as uplands and 21.6% as wetlands. In terms of wetland area, this represents an 8.7% increase in total wetland area from that mapped by NWI.

Visual trends noted between NWI and WIP maps included considerable disagreement near wetland edges and headwater wetlands associated with 1st order streams. Rather than identifying newly mapped headwater wetlands which were undetected by NWI, areas around mapped NWI headwater wetlands often expanded, while the areas around unmapped NWI headwater wetlands were often omitted. Mapped NWI headwater wetlands were omitted as well and were often those which did not contain mapped streams within their boundaries.

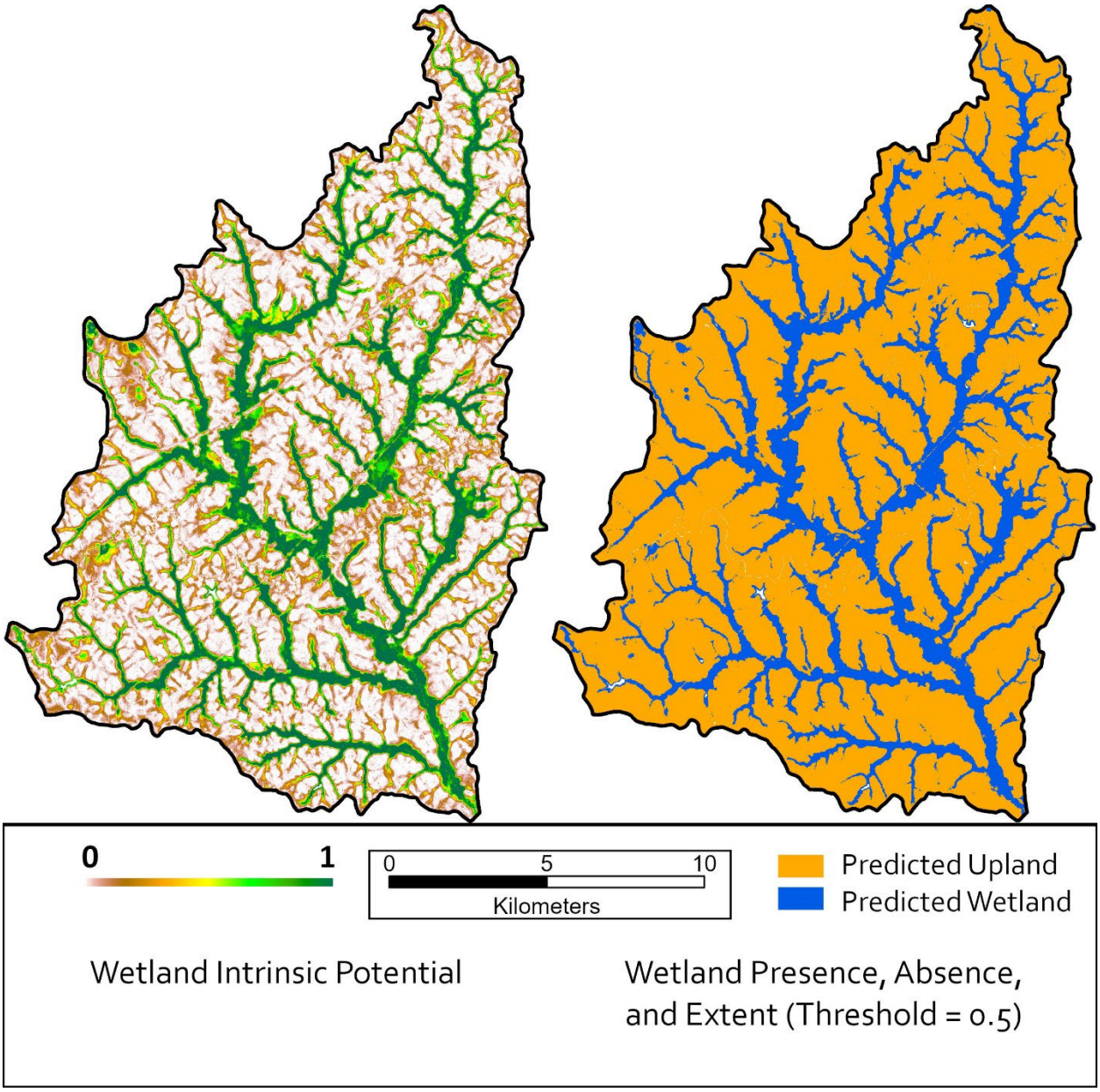

Figure 3.9. *Wetland probability (intrinsic potential) modeled for BcDc10, and a resulting wetland presence, absence, and extent map based on the model threshold of 0.5.*

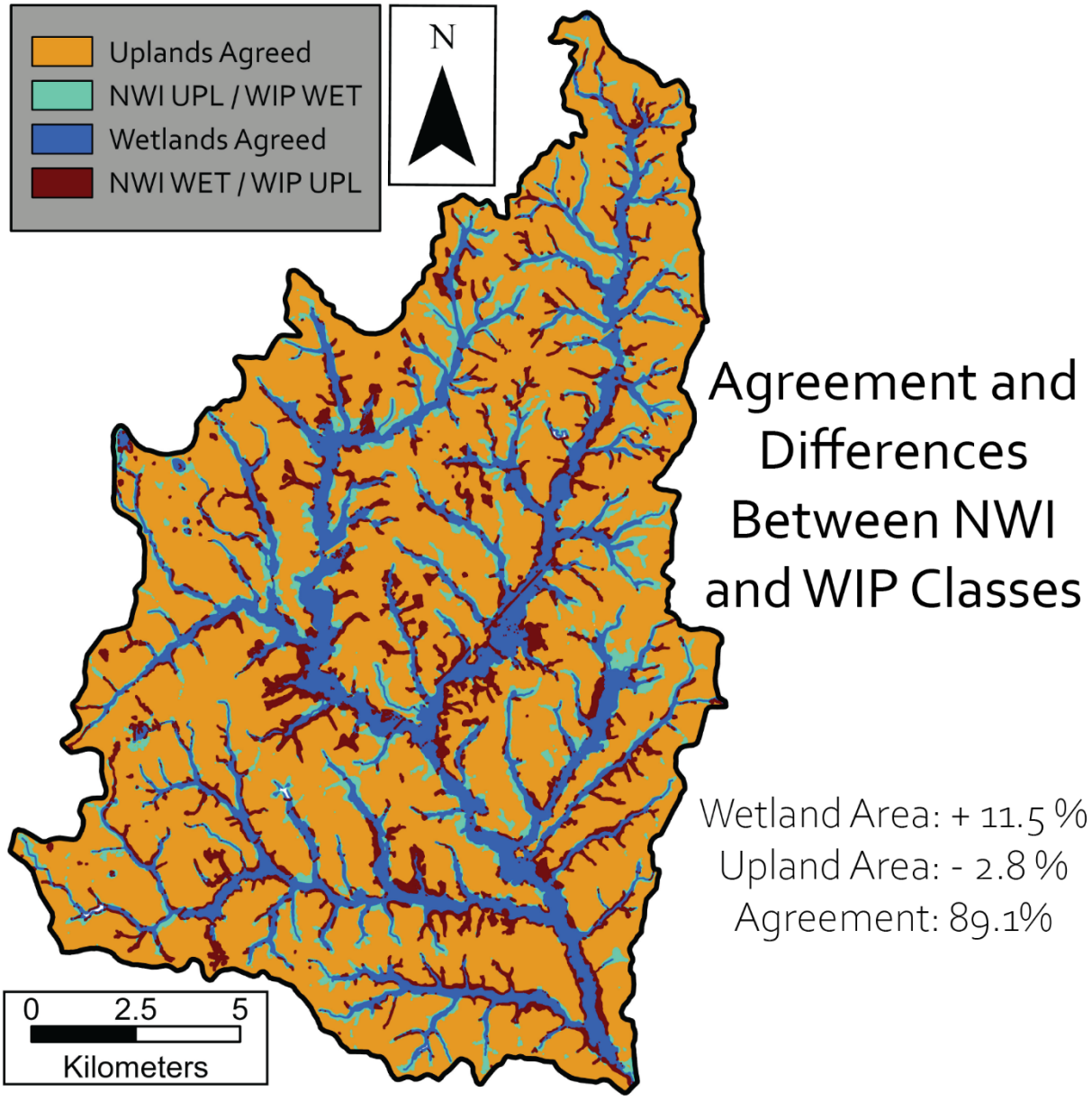

	Area			Cover		
Class	NWI (ha)	WIP (ha)	Change (%)	NWI (%)	WIP (%)	Difference (%)
WET	4,945.4	5,513.4	11.5	19.3	21.6	2.2
UPL	20,626.8	20,058.9	-2.8	80.7	78.4	-2.2

Figure 3.10. *WIP was highly representative of NWI wetland and upland classes (89.1% agreement). Of the classes which disagreed, the cumulative difference resulted in a 2.2% increase of wetland cover by the WIP model. This represented an 8.7% increase in total wetland area from the former extent mapped by NWI.*

4. Discussion

The WIP tool as it was applied to the total extent of the study area (BcDc10) resulted in highly accurate predictions of wetland presence and absence, indicated by validation metrics (omission rate, commission rate, sensitivity, specificity, overall accuracy, kappa). Through visual inspections of wetland extent maps, we observed potential model behaviors that tended towards the inclusion of wetland edges into total wetland cover for previously mapped headwater wetlands, while omitting entire headwater wetlands previously mapped by NWI. Though we expected increased coverage of previously unmapped wetlands, total wetland coverage increased nominally compared with NWI maps. This may have been the result of sampling designs and model covariates used, the spatial extent in which our analyses were constrained, or the unreliability of NWI boundaries. Alternatively, NWI may be an accurate representation of wetland presence, absence, and extent throughout BcDc10. While our methods sought to improve wetland mapping techniques, there was no immediate evidence to suggest that NWI had considerably under-mapped wetlands for this region in particular, and further efforts to field validate NWI wetlands are needed to fully address this possibility.

Bimodal distributions of wetland vs. upland WIP values resulted in an exceptionally high model AUC. These distributions indicate clear distinctions on the landscape between wetlands and uplands, which do not reflect the gradational nature of headwater wetlands. A possible explanation is that representation of headwater wetlands through stratified random sampling was an adequate approach to isolate landscape features associated with their occurrence relative to surrounding uplands. Alternatively, as these distributions are not indicative of the gradational nature of headwater wetlands, training/validation data may have been unrepresentative of wetlands with midrange WIP values, such as those near wetland edges. This may have

additionally resulted in overrepresentation of wetland extent for those which were most similar to training data locations, and underrepresentation for those which were dissimilar despite true wetland status. Optimal threshold values reported are thus relative to stratified random sampling designs and would likely be lower with greater representation of wetlands associated with mainstem wetlands. If differentiation between target wetlands and surrounding uplands is a primary mapping objective, stratified random sampling may be appropriate. Detection of all wetlands would be better guided by a completely randomized sampling design.

Another consideration for potential bias introduced by our sampling design was the method to manually adjust half of the randomly placed points along 1st order streams to the nearest headwater wetland with an unmapped stream. As the model was trained on BcDc12, morphological differences with those in McDc12 may have influenced predictive abilities. In BcDc12, headwater wetlands were noted for higher rates of convergence with other headwater wetlands at farther distances upstream than observed in McDc12. In McDc12, headwater wetlands were noted for regular spacing at perpendicular angles from the streams which they drained directly to. In BcDc12, adjusted locations for headwater wetlands without mapped streams were still fairly close to mapped streams, though in McDc12, headwater wetlands were spaced further apart, and potentially undetected where DTW values did not reflect those in training data. This method may have additionally excluded headwater wetland extent for those which drain directly to mainstem streams, as these were rarely the closest wetlands to mapped random points placed along 1st order streams.

Based on visual assessments of WIP wetland probability and extent maps, headwater wetlands which did not contain mapped streams showed evidence of omission via DTW, which was the most impactful predictor of wetland presence or absence. Wetland extent maps were

compared for all thresholds which were noted for closer alignment to known wetland boundaries as thresholds decreased from 0.5 to 0.3 (Fig 3.11). Conversely, mainstem wetlands appeared to be unrepresented by training data, as the processes which characterize flooding were diminished in mapped wetland extent. TWI was relatively unimpactful as a predictor variable, though is likely a better predictor where surface water hydrology and periodic flooding determine wetland status. Low TWI values present in headwater training data locations likely diminished this predictive relationship for those in mainstem wetlands. Through visual assessments of wetland extent maps, we infer that sampling designs may have constrained covariate ranges used for prediction to those in similar locations. Thus, accuracy metrics do not represent the totality of wetland conditions throughout BcDc10. Extended wetland boundaries around NWI wetland edges were noted as unlikely in many cases, especially where these areas were associated with agricultural ditches, ponds, and dams. The function of DTW assumes these areas to have shallow depths to groundwater, despite dissimilarity in these landscape modifications with reference wetland topography that induces groundwater upwelling.

Wetland extent maps with lowered thresholds resulted in fewer wetland omission errors and better captured portions of those omitted by a threshold of 0.5. While wetland commission errors remained low at thresholds of 0.3 (8.5%) - 0.4 (6.0%), the mapped extent of wetlands occurring in indisputable upland areas provides further evidence that validation data are not wholly representative of upland conditions. This issue was addressed by Halabisky et al. (2023_a) through the use of a preliminary model, trained on 2000 upland points and 1000 wetlands. The training data used in the final model were stratified by areas of low to high wetland probability, amongst four classes of WIP value bins (0-0.24, 0.25-0.49, 0.50-0.74, 0.75-1.0). Although AUC was exceptionally high in our validation dataset, bimodal distributions of probability near

minimum and maximum values further supports the merit provided by this additional step. We suggest this method to be prioritized in future modeling efforts to better represent areas of uncertainty.

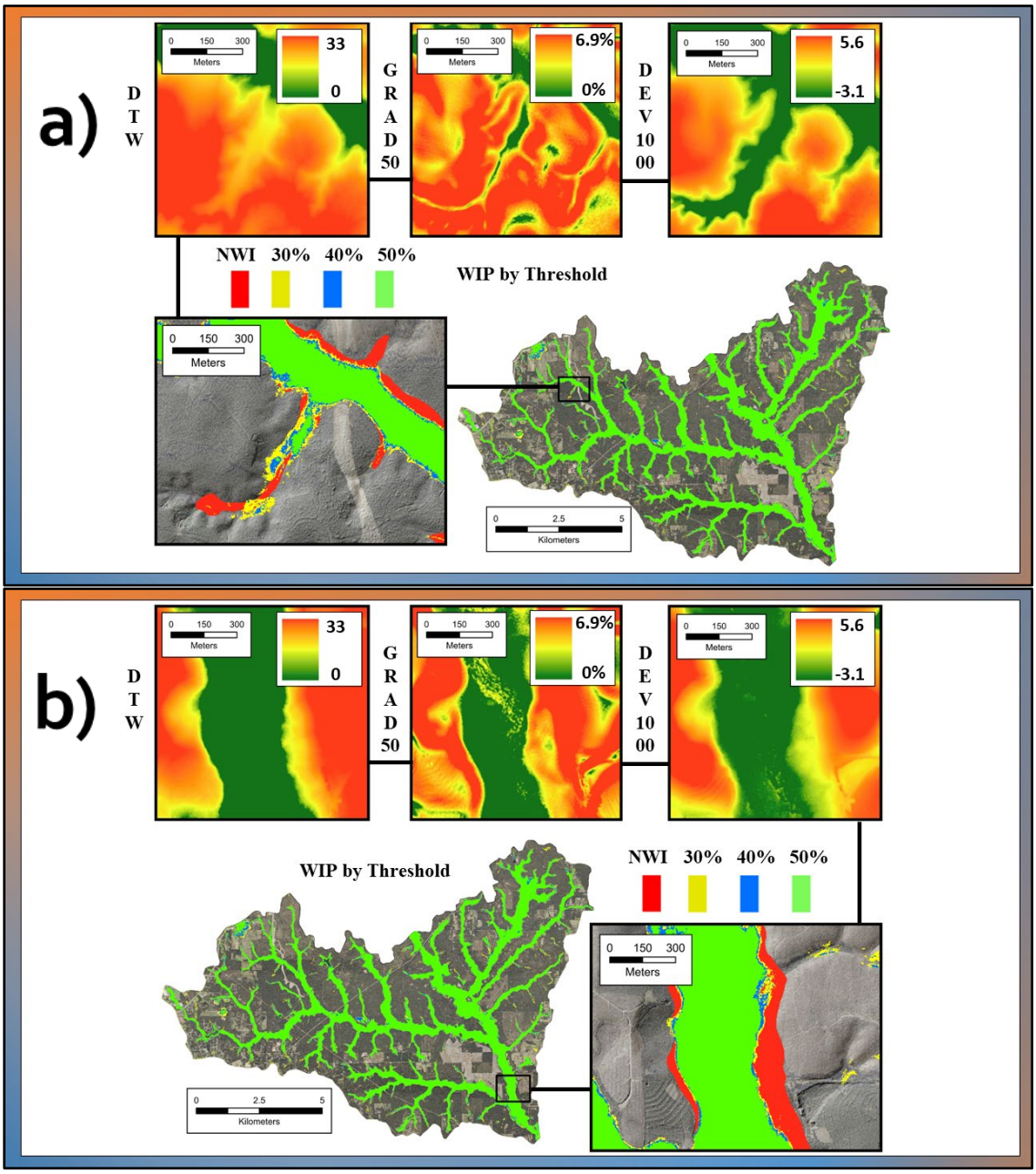

Figure 3.11. *Headwater wetlands present in NWI were often omitted in WIP models where (a) variables such as DTW may have disproportionately affected those lacking mapped streams. Core areas of floodplain wetlands associated with mainstem rivers were (b) largely agreed on between NWI and WIP models, though floodplain width was reduced considerably in all variations of model thresholds.*

5. Conclusion

The objectives which guide the use of wetland predictive models vary, as do the results which support those objectives. If headwater wetland detection is a primary objective, a stratified sampling design by stream order may be useful despite inaccuracies in wetlands that are not of interest. If the accurate detection of all wetlands is desired, alternative sampling designs such as equally stratified groups or complete randomization may be more appropriate. Our work explores a single design, focused on headwater wetland detection. The use of NWI as a restraining feature additionally presents biases towards wetlands associated with NWI wetland detection, such as areas associated with or closely aligned to mapped streams. For detection of previously unmapped wetlands, training and validation data are most robust where they include areas which are not mapped by NWI.

Results from this study are meant to introduce valuable perspectives to wetland mappers of the coastal plain region on potential tradeoffs between detection, accuracy, and target wetlands. Such models should be treated as tools to better guide wetland resource managers towards accurate and representative wetland inventories, rather than a single step from which to produce them. The need for field validated wetlands and data unrepresentative of NWI is critical for improved wetland mapping. The availability of standardized, georeferenced, and open source wetland delineations could greatly improve models that rely on training data for wetland mapping applications. Field validated boundaries like these could help address uncertainties regarding optimal thresholds near wetland edges and in slope wetlands. With improved sampling designs and model building processes, our exploratory analysis may be furthered throughout the region to identify metrics which are highly predictive and representative of wetlands across the landscape.

6. Literature Cited

Armstrong A, Stedman RC, Bishop JA, Sullivan PJ. 2012. What's a Stream Without Water? Disproportionality in Headwater Regions Impacting Water Quality. Environmental Management. 50(5): 849–860. https://doi.org/10.1007/s00267-012-9928-0

Barksdale FW and Anderson CJ. 2014. The influence of land use on forest structure, species composition, and soil conditions in headwater-slope wetlands of coastal Alabama, USA. International Journal of Biodiversity Science, Ecosystem Services & Management. 11(1): 61-70. https://doi.org/10.1080/21513732.2013.876449

Beven KJ and Kirkby MJ. 1979. A physically based, variable con-tributing area model of basin hydrology. Hydrological Sciences Bulletin. 24(1): 43–69. https://doi.org/10.1080/02626667909491834

Breiman L. 2001. Random Forests. Machine Learning. 45(1): 5–32. https://doi.org/10.1023/A:1010933404324

Brinson MM. 1993. A Hydrogeomorphic Classification for Wetlands. Technical Report WRP-DE-4, U.S. Army Engineer Waterways Experiment Station, Vicksburg, MS.

Christensen JR, Golden HE, Alexander LC, Pickard BR, Fritz KM, Lane CR, Weber MH, Kwok RM, Keefer MN. 2022. Headwater streams and inland wetlands: Status and advancements of geospatial datasets and maps across the United States. Earth-Science Reviews. 235(1): 104230. https://doi.org/10.1016/j.earscirev.2022.104230.

Ebersole SE, Guthrie GM, VanDervoort DS. 2019. An update to the physiographic districts of Alabama: Alabama Geological Survey Open-File Report 1901, 20p + plate.

[FGDC] Federal Geographic Data Committee. 2009. FGDC Document Number FGDC-STD-015-2009 Wetlands Mapping Standard. Reston, Va., Federal Geographic Data Committee.

Felton BR, O'Neil GL, Robertson MM, Fitch GM, Goodall JL. 2019. Using Random Forest Classification and Nationally Available Geospatial Data to Screen for Wetlands over Large Geographic Regions. Water. 11(6): 1158. https://doi.org/10.3390/w11061158

Halabisky M, Miller D, Stewart AJ, Yahnke A, Lorigan D, Brasel T, Moskal LM. 2023$_a$. The Wetland Intrinsic Potential tool: mapping wetland intrinsic potential through machine learning of multi-scale remote sensing proxies of wetland indicators. Hydrology and Earth System Sciences. 27(20): 3687–3699. https://doi.org/10.5194/hess-27-3687-2023

Halabisky M, Miller D, Lorigan D, Brasel T. 2023$_b$. Wetland Intrinsic Potential (WIP) Tool, version: 1.0.0. https://github.com/TerrainWorks-Seattle/ForestedWetlands

Huang C, Peng Y, Lang M, Yeo IY, McCarty G. 2014. Wetland inundation mapping and change monitoring using Landsat and airborne LiDAR data. Remote Sensing of Environment. 141(5): 231-242. https://doi.org/10.1016/j.rse.2013.10.020.

Jones RH, Lockaby BG, Somers GL. 1996. Effects of Microtopography and Disturbance on Fine-Root Dynamics in Wetland Forests of Low-Order Stream Floodplains. American Midland Naturalist. 136(1): 57-71. https://doi.org/10.2307/2426631

Lang M, McCarty G, Oesterling R, Yeo IY. 2013. Topographic Metrics for Improved Mapping of Forested Wetlands. Wetlands. 33(1): 141–155. https://doi.org/10.1007/s13157-012-0359-8

[MEAB] Millennium Ecosystem Assessment Board. 2005. Ecosystems and Human Well-Being: Wetlands and Water Synthesis. World Resources Institute, Washington, DC.

Miller DJ. 2003. Programs for DEM Analysis. Landscape Dynamics and Forest Management, General Technical Report RMRS-GTR-101CD, USDA Forest Service, Rocky Mountain Research Station, Fort Collins, CO, USA.

Murphy PNC, Ogilvie J, Meng FR, White B, Bhatti JS, Arp PA. 2011. Modelling and mapping topographic variations in forest soils at high resolution: A case study. Ecological Modeling. 222(14) 2314 – 2332. https://doi.org/10.1016/j.ecolmodel.2011.01.003

Nadeau TL and Rains MC. 2007. Hydrological Connectivity Between Headwater Streams and Downstream Waters: How Science Can Inform Policy. Journal of the American Water Resources Association. 43(1): 118-133. https://doi.org/10.1111/j.1752-1688.2007.00010.x

Noble CV, Wakeley JS, Robert TH, Henderson C. 2007. Regional Guidebook for Applying the Hydrogeomorphic Approach to Assessing the Functions of Headwater Slope Wetlands on the Mississippi and Alabama Coastal Plains. U.S. Army Corps of Engineers: Vicksburg, MS.

Noble CV, Murray EO, Klimas CV, Ainslie W. 2011. Regional Guidebook for Applying the Hydrogeomorphic Approach to Assessing the Functions of Headwater Slope Wetlands on the South Carolina Coastal Plain. ERDC/EL TR-11-11, U.S. Army Engineer Research and Development Center. Vicksburg, MS.

O'Neill GL, Goodall JL, Behl M, Saby L. 2020. Deep learning Using Physically-Informed Input Data for Wetland Identification. Environmental Modelling and Software. 126(1): 104665. https://doi.org/10.1016/j.envsoft.2020.104665

Oruc M, Marangoz AM, Buyuksalih G. 2004. Comparison of pixel based and object oriented classification approaches using Landsat 7 ETM spectral bands. In: Orhan Altan, Editor. 20th ISPRS Congress Technical Commission IV. Proceedings of the 20th International Society for Photogrammetry and Remote Sensing Congress; July 12-23, 2004; Istanbul, Turkey. ISPRS Archives: 35(B4) p. 1118–1122.

Ramesh R, Anderson CJ, Kalin L. 2020. Characterizing nitrogen attenuation by headwater slope wetlands across different land uses. Ecological Engineering. 149(1): 105833. https://doi.org/10.1016/j.ecoleng.2020.105833.

Rheinhardt R, Whigham D, Khan H, Brinson M. 2000. Vegetation of Headwater Wetlands in the Inner Coastal Plain of Virginia and Maryland. Castanea: The Journal of the Southern Appalachian Botanical Society. 65(1): 21–35.

Rheinhardt R, Wilder T, Williams H. 2013. Variation in Forest Canopy Composition of Riparian Networks from Headwaters to Large River Floodplains in the Southeast Coastal Plain, USA. Wetlands. 33(6): 1117–1126. https://doi.org/10.1007/s13157-013-0467-0

Stewart AJ, Halabisky M, Babcock C. 2024. Revealing the hidden carbon in forested wetland soils. Nature Communications. 15(1):726. https://doi.org/10.1038/s41467-024-44888-x

Tiner RW. 1990. Use of high-altitude aerial-photography for inventorying forested wetlands in the United States. Forest Ecology and Management. 33-34(10): 593–604. https://doi.org/10.1016/0378-1127(90)90221-V

Tufford D. 2011. Shallow Water Table Response to Seasonal and Interannual Climate Variability. Transactions of the ASABE: American Society of Agricultural and Biological Engineers. 54(6): 2079-2086. https://doi.org/10.13031/2013.40663

[NGCE] USDA/NRCS - National Geospatial Center of Excellence. 2022. LiDAR Elevation Dataset - Bare Earth Hillshade - 1 Meter. Baldwin County, AL *Accessed 05/12/2022.*

[NGCE] USDA/NRCS - National Geospatial Center of Excellence. 2023_a. USDA-NAIP NRCS County Mosaic. Baldwin County, AL. *Accessed 03/23/2023.*

[NGCE] USDA/NRCS - National Geospatial Center of Excellence. 2023_b. USDA-NAIP NRCS Alternate County Mosaic. Baldwin County, AL *Accessed 03/23/2023.*

[U.S. EPA] U.S. Environmental Protection Agency. 2006. 2006–2011 EPA strategic plan: charting our course. EPA-190-R-06-001. U.S. Environmental Protection Agency, Office of Planning, Analysis, and Accountability, Washington, DC.

U.S. Fish and Wildlife Service. 2022. National Wetlands Inventory - Version 2 - Surface Waters and Wetlands Inventory. Alabama. U.S. Department of the Interior, Fish and Wildlife Service, Washington, D.C. Available online. Accessed [02/15/2022]. https://www.fws.gov/program/national-wetlands-inventory/download-state-wetlands-data

U.S. Geological Survey. 2015. 1/9th Arc-second Digital Elevation Models (DEMs) - USGS National Map 3DEP Downloadable Data Collection: U.S. Geological Survey. *Accessed 03/17/2023*. https://www.sciencebase.gov/catalog/item/4f70aac4e4b058caae3f8de7

U.S. Geological Survey. 2022. USGS National Hydrography Dataset Plus High Resolution National Release 1 FileGDB: U.S. Geological Survey. *Accessed 07/07/2022*. https://doi.org/10.5066/P9WFOBQI

Appendix

Table 1. *Locations of study sites per dataset. Coordinates reflect Locations within wetland boundaries*.

		Location (UTM 16N)			
Dataset	Site	Easting	Northing	State	County
2010	Bark_4	3371302	435590	AL	Baldwin
2010	Bark_9	3364875	440948	AL	Baldwin
2010	Bark_11	3359898	441733	AL	Baldwin
2010	Bark_14	3371367	433756	AL	Baldwin
2010	Bark_17	3368210	418788	AL	Baldwin
2010	Bark_20	3370704	422239	AL	Baldwin
2010	Bark_23	3362378	427593	AL	Baldwin
2010	Bark_25	3361361	423899	AL	Baldwin
2010	Bark_26	3365731	421442	AL	Baldwin
2010	Bark_27	3364974	416420	AL	Baldwin
2010	Bark_28	3373476	412034	AL	Baldwin
2010	Bark_32	3361336	455592	AL	Baldwin
2010	Bark_36	3361471	442471	AL	Baldwin
2010	Bark_37	3366498	435561	AL	Baldwin
2010	Bark_39	3358564	450336	AL	Baldwin
2010	Bark_40	3359940	450405	AL	Baldwin
2010	Bark_41N	3357456	439043	AL	Baldwin
2010	Bark_41S	3362213	455777	AL	Baldwin
2010	Bark_43	3368401	434267	AL	Baldwin
2010	Bark_52	3363620	429530	AL	Baldwin
2010	Bark_53	3364590	430219	AL	Baldwin
2010	Bark_56	3371342	447141	AL	Baldwin
2022 - 2023	BayM_ACC	3413799	425490	AL	Baldwin
2022 - 2023	BayM_BAMS_N	3421344	428677	AL	Baldwin
2022 - 2023	BayM_BAMS_S	3419967	428781	AL	Baldwin
2022 - 2023	BayM_UlmP	3414128	425070	AL	Baldwin
2022 - 2023	Citr_OC	3433369	385734	AL	Mobile
2022 - 2023	Citr_PRC	3437197	382749	AL	Mobile
2022 - 2023	Dap_BS	3389959	418420	AL	Baldwin
2022 - 2023	Dap_JB	3389135	413104	AL	Baldwin
2022 - 2023	Dap_SP	3388393	413775	AL	Baldwin
2022 - 2023	Elb_BC	3358302	443029	AL	Baldwin
2022 - 2023	Elb_LF_NW	3368517	451519	AL	Baldwin
2022 - 2023	Elb_LF_SE	3367541	452804	AL	Baldwin
2022 - 2023	Elb_WolfNolf	3356599	448749	AL	Baldwin
2022 - 2023	Fol_BS	3356420	431719	AL	Baldwin

Table. 1. *Continued.*

Dataset	Site	Location (UTM 16N) Easting	Northing	State	County
2022 - 2023	Fol_MkF	3368466	429912	AL	Baldwin
2022 - 2023	Gbay_Drisk_BB	3382164	369216	AL	Mobile
2022 - 2023	Gbay_Drisk_CC	3382947	367138	AL	Mobile
2022 - 2023	Gbay_Drisk_SL	3384586	365645	AL	Mobile
2022 - 2023	Irv_Drisk_NE	3368317	375057	AL	Mobile
2022 - 2023	Irv_Drisk_SW	3368127	374900	AL	Mobile
2022 - 2023	Mob_BMS	3387807	385951	AL	Mobile
2022 - 2023	Mob_MemG	3385736	386002	AL	Mobile
2022 - 2023	Mob_MIMS	3388551	388070	AL	Mobile
2022 - 2023	Mob_UM	3407525	392220	AL	Mobile
2022 - 2023	Mob_USA_01	3397477	387049	AL	Mobile
2022 - 2023	Mob_USA_02	3396734	386579	AL	Mobile
2022 - 2023	Per_WMA_N	3399060	450778	AL	Baldwin
2022 - 2023	Per_WMA_S	3393506	457538	AL	Baldwin
2022 - 2023	Prd_MTEP	3406547	387914	AL	Mobile
2022 - 2023	RobD_BeHP	3378944	436847	AL	Baldwin
2022 - 2023	RobD_BFA	3381180	430664	AL	Baldwin
2022 - 2023	RobD_DB	3385206	437185	AL	Baldwin
2022 - 2023	RobD_MHP	3384796	436440	AL	Baldwin
2022 - 2023	RobD_RC	3381383	432184	AL	Baldwin
2022 - 2023	Sem_EdAd	3399361	383119	AL	Mobile
2022 - 2023	SF_GW	3395892	422051	AL	Baldwin
2022 - 2023	SF_SFHS	3395481	417494	AL	Baldwin
2022 - 2023	SF_SR	3395114	421591	AL	Baldwin
2022 - 2023	SumD_BeAP	3373142	438360	AL	Baldwin
2022 - 2023	SumD_LFF	3374231	435992	AL	Baldwin
2003 - 2004	Nob_WMS	3401311	411849	MS	Harrison
2003 - 2004	Nob_Tar	3401511	411880	AL	Mobile
2003 - 2004	Nob_SHB	3400684	413406	AL	Baldwin
2003 - 2004	Nob_PC	3400953	382577	AL	Mobile
2003 - 2004	Nob_LDM	3363597	328122	MS	Jackson
2003 - 2004	Nob_GVC	3389966	322104	MS	Jackson
2003 - 2004	Nob_GC	3431197	372630	AL	Mobile
2003 - 2004	Nob_BSP_SB	3434242	435775	AL	Baldwin
2003 - 2004	Nob_BSP_JS	3393884	382446	AL	Baldwin
2003 - 2004	Nob_BSP_5	3377793	308784	AL	Baldwin

Table 2. *Slope and area metrics for each site's watershed, inititial contributing area, and wetland. The proportion of wetland area vs. initial contribting area coverage is additionally reported as coverage per watershed.*

Site	Watershed		Initial Contributing Area			Headwater Wetland		
	Area (ha)	Mean Slope (%)	Area (ha)	Mean Slope (%)	Coverage (%)	Area (ha)	Mean Slope (%)	Coverage (%)
Bark_4	224.9	2.2	220.2	2.2	97.9	4.7	1.7	2.1
Bark_9	170.6	3.3	151.1	3.3	88.6	19.5	3.7	11.4
Bark_11	98.1	2.6	93.2	2.6	95.0	4.9	2.3	5.0
Bark_14	315.7	1.5	309.3	1.5	98.0	6.4	2.1	2.0
Bark_17	102.1	5.0	96.1	4.9	94.2	6.0	6.3	5.8
Bark_20	83.8	3.4	73.9	3.5	88.2	9.9	3.1	11.8
Bark_23	143.6	3.2	131.1	3.2	91.3	12.5	4.0	8.7
Bark_25	170.1	2.4	167.0	2.3	98.2	3.1	4.8	1.8
Bark_26	158.8	3.8	146.6	3.8	92.3	12.3	3.7	7.7
Bark_27	531.2	2.7	477.9	2.7	90.0	53.3	2.7	10.0
Bark_28	123.3	4.5	120.9	4.4	98.1	2.4	6.2	1.9
Bark_32	216.1	3.5	200.4	3.4	92.7	15.7	4.2	7.3
Bark_36	107.2	3.1	102.2	3.1	95.3	5.0	4.4	4.7
Bark_37	59.7	2.5	54.7	2.6	91.7	5.0	1.9	8.3
Bark_39	31.8	5.6	29.3	5.6	92.1	2.5	5.1	7.9
Bark_40	160.9	3.1	156.1	3.0	97.0	4.9	7.2	3.0
Bark_41N	183.1	2.6	168.3	2.6	91.9	14.8	2.7	8.1
Bark_41S	39.2	4.6	37.1	4.5	94.6	2.1	5.9	5.4
Bark_43	268.1	2.1	260.4	2.1	97.1	7.7	2.2	2.9
Bark_52	183.4	2.6	179.6	2.6	97.9	3.8	3.0	2.1
Bark_53	264.6	3.1	259.2	3.1	98.0	5.4	5.1	2.0
Bark_56	30.7	3.8	28.5	3.9	92.8	2.2	2.7	7.2
BayM_ACC	73.5	3.6	71.9	3.6	97.8	1.6	5.4	2.2
BayM_BAMS_N	33.6	8.2	29.1	8.7	86.8	4.4	5.0	13.2
BayM_BAMS_S	73.9	6.3	61.1	6.8	82.6	12.9	3.7	17.4
BayM_UlmP	37.6	4.7	36.8	4.7	97.9	0.8	5.4	2.1
Citr_OC	53.7	9.2	48.4	9.5	90.3	5.2	6.0	9.7
Citr_PRC	47.7	9.6	43.2	10.0	90.6	4.5	6.0	9.4
Dap_BS	69.3	4.9	65.7	4.8	94.8	3.6	5.2	5.2
Dap_JB	76.1	7.6	71.2	7.3	93.5	4.9	11.3	6.5
Dap_SP	143.6	6.8	138.6	6.8	96.6	4.9	7.6	3.4
Elb_BC	74.0	2.6	72.0	2.5	97.3	2.0	5.0	2.7
Elb_LF_NW	714.6	1.8	697.3	1.7	97.6	17.3	2.5	2.4
Elb_LF_SE	237.7	2.0	214.4	2.0	90.2	23.3	2.2	9.8
Elb_WolfNolf	146.8	3.6	138.8	3.6	94.6	8.0	3.5	5.4
Fol_BS	76.2	2.6	73.1	2.6	96.0	3.0	2.9	4.0

Table 2. *Continued.*

Site	Watershed		Initial Contributing Area			Headwater Wetland		
	Area (ha)	Mean Slope (%)	Area (ha)	Mean Slope (%)	Coverage (%)	Area (ha)	Mean Slope (%)	Coverage (%)
Fol_MkF	292.7	1.8	285.0	1.7	97.4	7.6	6.0	2.6
Gbay_Drisk_BB	324.8	2.1	295.9	2.1	91.1	28.9	2.2	8.9
Gbay_Drisk_CC	247.8	1.6	237.6	1.5	95.9	10.2	4.7	4.1
Gbay_Drisk_SL	279.2	3.2	271.9	3.1	97.4	7.3	5.0	2.6
Irv_Drisk_NE	388.0	1.4	384.4	1.4	99.1	3.7	3.1	0.9
Irv_Drisk_SW	48.7	2.2	47.5	2.1	97.5	1.2	5.1	2.5
Mob_BMS	166.6	6.6	153.0	6.9	91.8	13.6	3.9	8.2
Mob_MemG	200.0	7.1	182.4	7.2	91.2	17.6	6.0	8.8
Mob_MIMS	52.4	9.2	46.4	9.0	88.4	6.1	10.5	11.6
Mob_UM	149.1	5.7	134.1	5.9	90.0	15.0	4.3	10.0
Mob_USA_01	146.0	4.5	140.8	4.3	96.5	5.1	10.5	3.5
Mob_USA_02	46.5	6.5	44.5	6.4	95.8	1.9	8.5	4.2
Per_WMA_N	56.7	5.7	46.4	6.4	81.8	10.3	2.7	18.2
Per_WMA_S	92.9	4.9	86.5	4.6	93.2	6.4	9.6	6.8
Prd_MTEP	42.2	7.1	40.0	7.0	94.8	2.2	9.1	5.2
RobD_BeHP	104.2	3.7	96.6	3.8	92.7	7.6	3.2	7.3
RobD_BFA	162.1	2.6	153.5	2.7	94.7	8.5	1.4	5.3
RobD_DB	309.0	3.0	283.9	3.1	91.9	25.1	1.5	8.1
RobD_MHP	133.7	3.9	121.3	4.0	90.7	12.4	2.9	9.3
RobD_RC	1566.5	1.7	1539.5	1.7	98.3	27.0	3.1	1.7
Sem_EdAd	163.3	4.9	153.9	4.6	94.2	9.4	8.9	5.8
SF_GW	58.3	9.3	55.2	8.8	94.6	3.1	18.5	5.4
SF_SFHS	13.0	7.6	12.3	6.9	94.5	0.7	19.0	5.5
SF_SR	81.9	7.0	74.3	6.0	90.8	7.6	15.9	9.2
SumD_BeAP	325.7	1.7	320.3	1.7	98.3	5.5	2.3	1.7
SumD_LFF	160.4	2.6	147.6	2.5	92.0	12.8	4.0	8.0
Nob_WMS	27.9	6.4	24.7	5.6	88.8	3.1	13.0	11.2
Nob_Tar	217.0	6.2	207.7	6.1	95.7	9.3	10.3	4.3
Nob_SHB	56.0	5.4	51.1	4.5	91.2	4.9	14.3	8.8
Nob_PC	118.7	7.5	106.1	7.5	89.4	12.6	7.8	10.6
Nob_LDM	9.9	6.7	8.7	6.6	88.2	1.2	7.6	11.8
Nob_GVC	1.2	8.7	1.0	9.1	82.0	0.2	6.5	18.0
Nob_GC	173.3	5.5	164.3	5.5	94.8	8.9	6.0	5.2
Nob_BSP_SB	62.8	8.5	52.7	9.8	83.9	10.1	1.5	16.1
Nob_BSP_JS	45.2	8.1	35.9	8.5	79.5	9.3	6.6	20.5
Nob_BSP_5	32.2	9.3	29.7	9.8	92.3	2.5	4.4	7.7

Table 3. *LULC proportions and Comp. loading scores for each initial contributing area that drains to a wetland site. Open water is provided as supplementary data but was not used in PCA to create Comps. 1, 2, and 3.*

	Initial Contributing Area: LULC (%)				PCA Loading Scores		
Site	Water	Urban	Forest	Agriculture	Comp. 1	Comp. 2	Comp. 3
Bark_4	1.03	6.69	18.04	74.24	-50.48	-20.04	-0.07
Bark_9	2.80	10.88	19.90	66.42	-43.58	-14.27	-1.12
Bark_11	0.00	18.50	21.55	59.96	-37.75	-6.14	0.46
Bark_14	0.07	23.33	4.51	72.08	-58.30	0.04	0.43
Bark_17	2.19	8.81	54.55	34.45	3.50	-17.56	-0.85
Bark_20	0.35	10.71	54.93	34.01	4.10	-15.99	0.20
Bark_23	0.21	7.83	24.34	67.63	-41.34	-19.08	0.39
Bark_25	0.38	8.39	35.51	55.72	-25.01	-18.50	0.25
Bark_26	0.31	10.90	70.10	18.69	25.66	-16.01	0.18
Bark_27	1.17	12.48	32.97	53.39	-25.10	-13.17	-0.22
Bark_28	5.90	28.40	58.93	6.78	26.43	7.69	-3.12
Bark_32	0.58	41.96	36.08	21.38	0.12	22.42	-0.06
Bark_36	2.09	26.92	46.30	24.70	4.80	4.56	-0.87
Bark_37	0.00	15.71	45.31	38.98	-6.15	-9.90	0.40
Bark_39	1.37	5.28	84.33	9.03	42.48	-22.65	-0.44
Bark_40	0.06	7.78	73.41	18.75	27.92	-19.95	0.34
Bark_41N	3.23	4.52	54.70	37.55	1.36	-22.37	-1.43
Bark_41S	0.00	98.52	1.48	0.00	-8.48	91.56	0.05
Bark_43	0.21	22.42	20.25	57.12	-36.61	-1.26	0.31
Bark_52	0.50	16.63	23.18	59.68	-36.42	-8.23	0.16
Bark_53	0.56	22.24	30.43	46.78	-22.10	-1.50	0.09
Bark_56	0.00	11.68	53.94	34.38	3.15	-14.93	0.40
BayM_ACC	0.00	81.55	15.97	0.28	1.35	71.56	-1.17
BayM_BAMS_N	0.00	0.00	100.00	0.00	59.87	-29.86	0.34
BayM_BAMS_S	0.23	3.49	96.04	0.24	56.95	-25.46	0.20
BayM_UlmP	0.00	71.39	27.69	0.91	9.05	58.14	0.13
Citr_OC	0.17	3.08	49.21	47.54	-9.61	-25.26	0.37
Citr_PRC	0.00	11.32	73.01	15.67	29.86	-15.66	0.35
Dap_BS	0.27	35.44	33.20	31.08	-8.86	14.41	0.16
Dap_JB	0.00	33.43	62.96	3.62	31.57	11.39	0.26
Dap_SP	0.00	65.14	24.77	10.09	0.41	50.58	0.18
Elb_BC	0.13	6.59	30.60	62.69	-33.44	-20.72	0.43
Elb_LF_NW	0.18	4.88	17.49	77.45	-53.17	-22.58	0.44
Elb_LF_SE	0.30	3.91	18.06	77.73	-52.97	-23.72	0.37
Elb_WolfNolf	0.79	22.87	64.12	12.21	26.17	-1.15	-0.15
Fol_BS	0.25	9.57	34.43	55.76	-25.79	-17.10	0.33
Fol_GCNP_E	0.00	0.00	83.32	16.68	36.28	-29.60	0.39
Fol_GCNP_W	0.00	0.77	96.82	2.40	55.93	-28.87	0.34

Table 3. *continued.*

	Initial Contributing Area: LULC (%)				PCA Loading Scores		
Site	Water	Urban	Forest	Agriculture	Comp. 1	Comp. 2	Comp. 3
Fol_MkF	0.22	5.59	4.93	89.26	-70.39	-21.50	0.45
Gbay_Drisk_BB	4.14	5.16	29.17	61.53	-33.63	-20.84	-1.89
Gbay_Drisk_CC	0.68	4.21	8.67	86.44	-65.77	-23.06	0.18
Gbay_Drisk_SL	2.82	1.39	16.71	79.08	-54.91	-25.76	-1.07
Irv_Drisk_NE	1.71	7.16	16.47	74.66	-51.88	-19.18	-0.46
Irv_Drisk_SW	1.47	5.17	27.16	66.20	-38.37	-21.86	-0.34
Mob_BMS	0.00	74.33	25.21	0.46	7.65	61.75	0.12
Mob_MemG	0.00	18.23	76.12	5.65	39.23	-7.30	0.30
Mob_MIMS	0.00	73.67	26.14	0.19	8.49	60.93	0.13
Mob_UM	0.00	49.18	49.35	1.47	23.67	30.77	0.20
Mob_USA_01	0.00	88.21	11.74	0.06	-1.40	78.85	0.09
Mob_USA_02	0.04	85.35	12.42	2.19	-2.47	75.38	0.07
Per_WMA_N	0.00	8.32	90.91	0.78	53.00	-19.59	0.32
Per_WMA_S	0.10	4.33	93.59	1.98	54.00	-24.45	0.28
Prd_MTEP	0.00	34.68	56.66	8.66	23.56	13.02	0.26
RobD_BeHP	0.00	3.58	34.56	61.86	-30.09	-24.49	0.50
RobD_BFA	0.00	53.78	7.93	38.29	-31.59	37.01	0.29
RobD_DB	1.58	6.78	29.13	62.51	-34.34	-19.88	-0.42
RobD_MHP	0.00	7.19	64.05	28.76	14.21	-20.55	0.40
RobD_RC	0.27	24.06	10.85	64.82	-48.68	0.90	0.30
Sem_EdAd	0.23	63.12	31.59	5.06	8.76	48.10	0.04
SF_GW	0.00	54.59	42.89	2.52	18.43	37.46	0.19
SF_SFHS	0.16	44.20	55.64	0.00	29.09	24.68	0.12
SF_SR	0.00	52.06	38.44	9.51	10.31	34.44	0.22
SumD_BeAP	0.08	25.16	6.62	68.13	-53.99	2.24	0.41
SumD_LFF	0.24	15.91	6.01	77.84	-61.41	-8.95	0.37
Nob_WMS	0.00	1.37	98.63	0.00	58.92	-28.17	0.34
Nob_Tar	0.00	8.04	91.96	0.00	54.29	-19.95	0.32
Nob_SHB	0.00	13.03	86.82	0.14	50.63	-13.79	0.30
Nob_PC	0.14	23.89	48.99	26.98	5.04	0.06	0.27
Nob_LDM	0.00	34.27	65.73	0.00	36.10	12.38	0.24
Nob_GVC	0.00	9.96	89.46	0.58	52.14	-17.57	0.31
Nob_GC	1.09	0.74	94.23	3.94	53.02	-28.43	-0.28
Nob_BSP_SB	3.09	0.00	96.91	0.00	57.70	-28.58	-1.44
Nob_BSP_JS	0.14	61.02	26.37	12.47	-0.20	45.59	0.12
Nob_BSP_5	0.00	7.57	88.50	3.93	49.06	-20.47	0.33

Table. 4. *Wetland Field Measurements for all study sites.*

	Canopy Tree Structure		Cover (%)				Munsell Soil Color	
Site	Mean DBH (cm)	Stems/ha	Canopy Tree	Shrub/ Sapling	Herbacious	Detritus	Value	Chroma
Bark_4	48.77	1350	72.50	40.00	15.00	80.00	3.00	2.00
Bark_9	49.28	625	52.50	55.00	71.25	82.50	2.70	1.40
Bark_11	50.80	1475	67.50	43.75	28.13	100.00	2.00	2.00
Bark_14	61.47	900	46.25	30.00	62.50	92.50	2.50	2.30
Bark_17	61.47	825	83.75	15.00	26.25	73.80	3.00	1.80
Bark_20	53.09	375	57.50	58.75	52.50	88.80	2.60	1.40
Bark_23	52.58	1550	85.00	38.75	2.00	25.00	3.00	2.30
Bark_25	40.64	1125	81.25	18.75	41.25	42.50	3.00	2.40
Bark_26	49.28	750	52.50	66.25	9.50	80.00	2.80	1.30
Bark_27	57.91	700	85.00	57.50	16.25	38.80	3.00	2.20
Bark_28	55.63	1025	71.25	55.00	81.25	83.80	3.00	2.50
Bark_32	34.80	1100	66.25	22.50	50.00	50.00	3.00	1.60
Bark_36	46.23	975	71.25	40.00	60.00	82.50	2.60	1.40
Bark_37	45.72	1175	75.00	32.50	60.00	91.30	3.10	1.10
Bark_39	43.43	1000	67.50	43.75	28.13	92.50	2.90	2.30
Bark_40	58.67	1050	71.25	65.00	41.25	52.50	3.00	1.50
Bark_41N	43.18	750	43.75	57.25	77.50	91.50	2.40	1.20
Bark_41S	62.48	1100	--	47.50	73.75	100.00	2.20	1.00
Bark_43	44.20	875	88.75	12.50	16.25	100.00	2.90	2.00
Bark_52	68.07	725	40.00	66.25	27.50	100.00	2.90	2.30
Bark_53	61.21	425	40.00	73.75	11.25	88.80	3.40	2.30
Bark_56	55.88	1050	76.25	40.00	36.25	37.50	2.50	1.20
BayM_ACC	32.21	225	--	--	--	73.75	3.19	3.19
BayM_BAMS_N	22.85	575	54.00	4.38	14.38	74.75	2.84	1.69
BayM_BAMS_S	19.84	800	58.00	2.50	5.13	60.00	2.16	1.31
BayM_UlmP	24.49	600	NA	NA	NA	30.00	3.84	4.00
Citr_OC	23.54	900	66.25	42.50	7.38	76.25	3.66	2.38
Citr_PRC	23.09	875	61.88	26.25	6.88	46.88	3.41	2.81
Dap_BS	19.18	975	59.63	38.75	21.25	56.88	3.94	3.81
Dap_JB	24.38	725	50.88	25.00	6.38	51.25	3.44	1.94
Dap_SP	15.49	1750	60.00	36.25	5.63	64.38	4.56	2.50
Elb_BC	25.35	500	--	32.50	--	70.00	3.81	2.63
Elb_LF_NW	20.83	575	26.88	51.25	21.25	48.75	4.69	3.69
Elb_LF_SE	24.38	825	70.00	19.38	36.25	81.88	2.56	1.50
Elb_WolfNolf	21.40	1475	60.25	3.13	1.25	32.50	4.31	1.69
Fol_BS	25.12	700	62.50	41.25	12.50	58.75	2.31	1.88
Fol_GCNP_E	21.34	1300	65.50	4.25	4.88	86.25	2.63	1.06

Table. 4. *Continued.*

Site	Canopy Tree Structure		Cover (%)				Munsell Soil Color	
	Mean DBH (cm)	Stems/ha	Canopy Tree	Shrub/ Sapling	Herbacious	Detritus	Value	Chroma
Fol_GCNP_W	22.50	775	59.50	8.75	26.25	87.50	2.19	1.38
Fol_MkF	28.09	925	47.50	51.25	17.50	74.38	3.06	1.50
Gbay_Drisk_BB	34.49	225	38.75	30.00	18.13	29.25	2.00	1.56
Gbay_Drisk_CC	26.62	800	46.88	37.50	11.88	69.38	3.56	3.25
Gbay_Drisk_SL	28.13	750	46.25	13.75	77.50	38.38	2.19	1.81
Irv_Drisk_NE	28.85	525	29.38	30.00	0.75	57.50	3.06	1.56
Irv_Drisk_SW	23.37	275	25.00	43.75	1.75	63.75	3.75	3.06
Mob_BMS	54.00	575	--	--	--	96.25	3.69	3.38
Mob_MemG	16.13	1200	--	--	--	87.50	4.25	2.19
Mob_MIMS	53.95	450	--	--	--	77.50	4.19	2.33
Mob_UM	49.68	725	--	--	--	55.00	2.63	--
Mob_USA_01	54.74	675	--	--	--	51.25	3.75	2.38
Mob_USA_02	28.85	525	--	--	--	88.75	3.03	1.63
Per_WMA_N	20.14	975	--	12.75	--	51.25	2.38	1.00
Per_WMA_S	41.50	525	--	NA	--	0.00	2.75	1.06
Prd_MTEP	17.70	1650	--	NA	--	71.25	4.03	2.66
RobD_BeHP	45.25	700	48.75	25.63	50.63	35.50	3.69	2.50
RobD_BFA	36.73	1250	--	78.75	--	34.25	4.25	1.69
RobD_DB	58.48	800	66.80	32.50	--	36.25	2.63	1.75
RobD_MHP	80.04	325	--	--	--	60.00	3.00	1.81
RobD_RC	28.27	700	--	52.50	28.13	67.50	4.00	2.50
Sem_EdAd	44.45	550	--	--	--	100.00	3.44	2.75
SF_GW	33.78	450	60.00	55.00	11.25	45.63	3.72	2.13
SF_SFHS	23.37	800	--	25.00	--	78.13	3.78	2.34
SF_SR	34.21	1075	--	12.50	--	25.00	4.88	4.31
SumD_BeAP	30.18	925	51.25	28.75	26.25	42.50	2.34	1.38
SumD_LFF	59.82	500	--	45.00	--	62.50	2.69	1.88
Nob_WMS	53.34	350	--	15.00	10.00	98.00	3.50	--
Nob_Tar	99.06	300	--	19.00	27.50	99.38	3.50	--
Nob_SHB	52.07	663	--	11.00	6.50	82.88	4.25	--
Nob_PC	76.20	300	--	34.00	34.00	98.25	4.00	--
Nob_LDM	86.36	550	--	10.00	26.00	100.00	3.50	--
Nob_GVC	73.66	638	--	NA	25.00	91.25	3.63	--
Nob_GC	80.01	300	--	48.50	4.00	100.00	2.00	--
Nob_BSP_SB	66.04	250	--	9.00	14.00	99.50	4.00	--
Nob_BSP_JS	92.29	200	--	61.33	61.67	10.83	5.33	--
Nob_BSP_5	76.20	400	--	25.00	18.00	98.25	3.25	--

Table. 5. *HGM Variable scores for average canopy tree diamter (Vctd), canopy tree density (Vctden), shrub/sapling cover (Vssc), ground vegetation cover (Vgvc), and vegetative compositon (Vcomp) for our 2022-23 dataset. Scores were generated with vegetative field measurements for each site per HGM protocol specified by Noble et al. 2007.*

	HGM Variable Score				
SITE	**Vctd**	**Vctden**	**Vssc**	**Vgvc**	**Vcomp**
BayM_ACC	0.22	0.90	--	--	--
BayM_BAMS_N	0.22	0.75	0.02	0.21	0.57
BayM_BAMS_S	0.00	0.39	0.00	0.07	0.35
BayM_UlmP	0.08	0.71	--	--	--
Citr_OC	0.07	0.22	0.59	0.11	0.43
Citr_PRC	0.06	0.26	0.34	0.10	0.37
Dap_BS	0.00	0.10	0.53	0.30	0.17
Dap_JB	0.08	0.51	0.33	0.09	0.33
Dap_SP	0.00	0.10	0.49	0.08	0.29
Elb_BC	0.10	0.88	0.44	--	0.36
Elb_LF_NW	0.02	0.75	0.72	0.30	0.19
Elb_LF_SE	0.08	0.35	0.24	0.52	0.22
Elb_WolfNolf	0.03	0.10	0.00	0.02	0.21
Fol_BS	0.00	0.55	0.57	0.18	0.84
Fol_GCNP_E	0.03	0.10	0.01	0.07	0.26
Fol_GCNP_W	0.05	0.43	0.10	0.38	0.37
Fol_MkF	0.15	0.18	0.72	0.25	0.19
Gbay_Drisk_BB	0.26	0.90	0.40	0.26	0.29
Gbay_Drisk_CC	0.12	0.39	0.51	0.17	0.33
Gbay_Drisk_SL	0.15	0.47	0.16	1.00	0.26
Irv_Drisk_NE	0.00	0.67	0.40	0.01	0.17
Irv_Drisk_SW	0.06	1.00	0.61	0.03	0.27
Mob_BMS	0.61	0.75	--	--	--
Mob_MemG	0.00	0.10	--	--	--
Mob_MIMS	0.61	0.96	--	--	--
Mob_UM	0.53	0.51	--	--	--
Mob_USA_01	0.62	0.59	--	--	--
Mob_USA_02	0.16	0.84	--	--	--
Per_WMA_N	0.01	0.10	--	--	--
Per_WMA_S	0.39	0.84	--	--	--
Prd_MTEP	0.00	0.10	--	--	--
RobD_BeHP	0.45	0.55	0.33	0.72	0.35
RobD_BFA	0.30	0.10	--	--	--
RobD_DB	0.69	0.39	0.44	--	0.49
RobD_MHP	1.00	1.00	--	--	--
RobD_RC	0.15	0.55	0.74	0.40	0.28
Sem_EdAd	0.44	0.80	--	--	--
SF_GW	0.25	0.96	0.78	0.16	0.76
SF_SFHS	0.06	0.39	--	--	--
SF_SR	0.26	0.10	--	--	--
SumD_BeAP	0.18	0.18	0.38	0.38	0.20
SumD_LFF	0.71	1.00	0.61	1.00	0.54

Table. 6. *HGM Variable scores for hydrologic alterations (Vhalt), detritus cover (Vdetritus), soil organic matter content (Vssom), upland land use (Vupuse), change in catchment size (Vcatch), and habitat connections (Vconnect) for our 2022-23 dataset. Scores were generated with for each site per HGM protocol specified by Noble et al. 2007.*

	HGM Variable Score					
SITE	**Vhalt**	**Vdetritus**	**Vssom**	**Vupuse**	**Vcatch**	**Vconnect**
BayM_ACC	0.00	0.76	0.80	0.41	0.10	0.68
BayM_BAMS_N	1.00	0.77	0.80	0.41	1.00	0.68
BayM_BAMS_S	0.00	0.62	1.00	1.00	0.91	1.00
BayM_UlmP	0.00	0.31	0.60	0.47	0.35	0.64
Citr_OC	0.52	0.79	0.60	0.94	1.00	0.28
Citr_PRC	1.00	0.48	0.80	0.63	1.00	1.00
Dap_BS	1.00	0.59	0.60	0.88	1.00	0.28
Dap_JB	1.00	0.53	0.8	1.00	1.00	0.37
Dap_SP	1.00	0.66	0.4	0.92	1.00	0.33
Elb_BC	0.000	0.72	0.60	0.90	1.00	0.47
Elb_LF_NW	0.00	0.50	0.40	0.81	1.00	0.34
Elb_LF_SE	1.00	0.84	0.80	0.87	1.00	0.18
Elb_WolfNolf	0.00	0.34	0.60	0.97	1.00	1.00
Fol_BS	1.00	0.61	1.00	0.71	1.00	0.62
Fol_GCNP_E	1.00	0.89	0.80	1.00	1.00	1.00
Fol_GCNP_W	1.00	0.90	1.00	1.00	1.00	1.00
Fol_MkF	1.00	0.77	0.80	0.48	0.58	0.22
Gbay_Drisk_BB	0.00	0.30	1.00	0.92	1.00	0.18
Gbay_Drisk_CC	0.00	0.72	0.60	0.58	0.65	0.13
Gbay_Drisk_SL	0.00	0.40	1.00	0.87	0.79	0.17
Irv_Drisk_NE	0.04	0.59	0.80	0.43	0.10	0.00
Irv_Drisk_SW	0.00	0.66	0.60	0.53	1.00	0.00
Mob_BMS	1.00	0.99	0.60	0.90	1.00	0.51
Mob_MemG	1.00	0.90	0.60	1.00	1.00	0.82
Mob_MIMS	1.00	0.80	0.60	1.00	1.00	0.22
Mob_UM	1.00	0.57	0.80	1.00	1.00	0.43
Mob_USA_01	0.00	0.53	0.60	0.96	1.00	0.23
Mob_USA_02	0.00	0.91	0.80	1.00	1.00	0.13
Per_WMA_N	0.47	0.53	1.00	1.00	1.00	1.00
Per_WMA_S	0.00	0.00	0.80	0.97	1.00	1.00
Prd_MTEP	1.00	0.73	0.60	0.92	1.00	1.00
RobD_BeHP	0.00	0.37	0.60	0.87	0.76	0.25
RobD_BFA	0.00	0.35	0.60	0.52	1.00	0.33
RobD_DB	0.00	0.37	0.80	0.72	0.89	0.30
RobD_MHP	1.00	0.62	0.80	0.77	0.93	0.37
RobD_RC	0.00	0.70	0.60	0.61	0.71	0.34
Sem_EdAd	1.00	1.00	0.80	1.00	1.00	0.50
SF_GW	1.00	0.47	0.60	0.68	1.00	0.24
SF_SFHS	1.00	0.81	0.60	1.00	1.00	0.43
SF_SR	0.00	0.26	0.40	0.95	1.00	0.31
SumD_BeAP	0.00	0.44	1.00	0.54	1.00	0.39
SumD_LFF	0.00	0.64	0.80	0.65	0.99	0.17

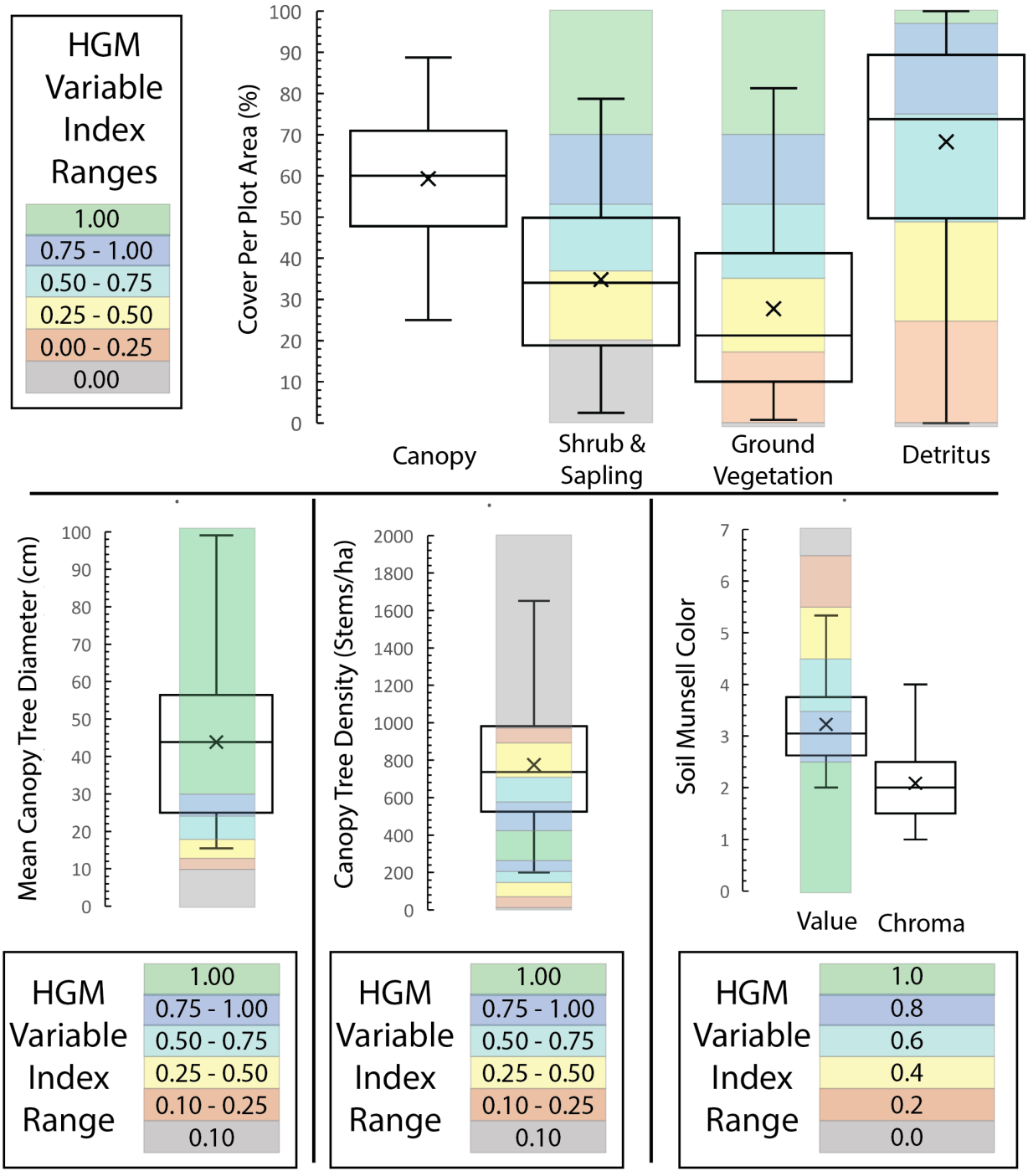

Figure 1. *Distributions for all field measurements relative to HGM variable index score ranges. Shrub/sapling index scores reflect wetland sites with < 20% canopy tree cover and are thus not indicative of true wetland conditions observed in any sites. The same applies to ground vegetation index scores for sites with < 20% canopy tree and shrub/sapling cover. Munsell chroma and canopy tree cover are not HGM variables but were included as response variables in linear regression.*